U.S. Department of Energy
Office of Advanced Automotive Technologies
1000 Independence Avenue S.W.
Washington, D.C. 20585-0121

FY 2000

Progress Report for the Advanced Technology Development Program

Energy Efficiency and Renewable Energy
Office of Transportation Technologies
Office of Advanced Automotive Technologies
Energy Management Team

Raymond A. Sutula **Energy Management Team Leader**

December 2000

CONTENTS

CONTENTS (CONTINUED)

ACKNOWLEDGEMENT

We would like to express our sincere appreciation to Computer Systems Management, Inc. (CSMI) for their artistic and technical contributions in preparing and publishing this report.

In addition, we would like to thank all of our program participants for their contributions to the program and the authors who prepared project abstracts that make up this report.

1. INTRODUCTION

Advanced Technology Development Program

On behalf of the Department of Energy's Office of Advanced Automotive Technologies (OAAT), I am pleased to introduce the Fiscal Year (FY) 2000 Accomplishments Report for the Advanced Technology Development (ATD) Program. OAAT funds high-risk research and development to provide enabling technologies for fuel efficient and environmentally-friendly light duty vehicles. The ATD Program focuses on high-power battery development in support of the Partnership for a New Generation of Vehicles (PNGV), a government-industry partnership striving to develop, by 2004, a mid-sized passenger vehicle capable of achieving up to three times the fuel economy of today's vehicles, while adhering to future emissions standards, and maintaining such attributes as affordability, performance, safety, and comfort.

Initiated in late 1998, the ATD program focuses on finding solutions to barriers that are impeding U.S. battery manufacturers in their efforts to produce and market high-power batteries for use in hybrid electric vehicles. Hybrid electric vehicles - which combine the heat engine and fuel tank of a conventional vehicle with the battery and electric motor of an electric vehicle - offer an attractive alternative to conventional vehicles because they can deliver the extended range and rapid refueling that consumers expect from a conventional vehicle while achieving increased fuel economy and reduced greenhouse gases and criteria pollutants. By providing strong technical direction, management and financial support, OAAT is a leader in supporting the development of high-power battery technology for hybrid electric vehicle applications.

High-power battery technology is a key element to the ultimate success of hybrid electric vehicles in the commercial marketplace. The primary challenges facing the commercialization of high-power battery technology include abuse tolerance, cost, and calendar life. The ATD Program addresses these technical challenges through five major program areas, including: baseline cell development (Gen 1); diagnostic evaluations; electrochemical improvement (Gen 2); advanced materials for Gen 3 cells; and, low-cost packaging. The organization of the program requires that five national laboratories (ANL, BNL, LBNL, INEEL, SNL) work in close coordination to achieve the objectives of the program. Additional information on the purpose, focus, organization and direction of the ATD program can be found in *Section 1. Background/Overview*.

This report highlights the activities and progress achieved during FY 2000 under the ATD Program. The report is comprised of twelve (12) technical project summaries, submitted by five national laboratories and two universities, that provide an overview of the exciting work being conducted to tackle tough technical challenges associated with high power batteries. We are encouraged by the technical progress realized under this dynamic program in FY 2000, and look forward to continued program success in FY 2001.

Raymond A. Sutula
ATD Program Manager
Office of Advanced Automotive Technologies
Office of Transportation Technologies
Department of Energy

2. ATD PROGRAM OVERVIEW AND FY 2000 HIGHLIGHTS

A. Advanced Technology Development (ATD) Program: Purpose, Focus, Organization and Direction

Vincent Battaglia and Gary Henriksen
Argonne National Laboratory, Argonne IL 60439-4837
(202) 488-2461; fax (202) 488-2413; e-mail: batman@anl.gov

The Advanced Technology Development (ATD) Program was established to help solve the key technical barriers limiting the development of high-power lithium-ion battery technology for hybrid electric vehicles (HEVs). The program was initiated in late 1998 through the Partnership for a New Generation of Vehicles (PNGV) to focus on solutions to barriers that are impeding US battery manufacturers in their efforts to produce and market high-power lithium-ion HEV batteries. PNGV is a government-industry partnership striving to develop by 2004 a mid-sized passenger vehicle capable of achieving 80 miles per gallon while adhering to future emissions standards and maintaining such attributes as affordability, performance, safety, and comfort. Close collaboration with battery developers is considered essential to the program's success.

The objectives of the ATD Program are:

1) to determine the root cause of power fade as a function of calendar time;
2) to determine the chemical mechanisms associated with thermal abuse intolerance;
3) to narrow the field and refine the diagnostic tools that provide the greatest insight into the degradation and safety-related mechanisms;
4) to pursue low-cost alternatives in cell packaging and battery materials' processing; and,
5) to facilitate cooperation between battery developers and the laboratories in order to efficiently utilize resources and accelerate the pace to commercialization.

ATD Program Organization

The ATD Program was created to assist in the development of an affordable, high-power battery having a ten-year life. The program is managed by the Energy Management Team of the Office of Advanced Automotive Technologies (OAAT). Technical guidance to the program is provided through semi-quarterly meetings with the PNGV Electrochemical Energy Storage Technical Team. Five national laboratories work in a collaborative manner to carry out the research and report their results through monthly reports and quarterly reviews. The PNGV industrial battery contractors attend the review meetings and provide feedback to the labs.

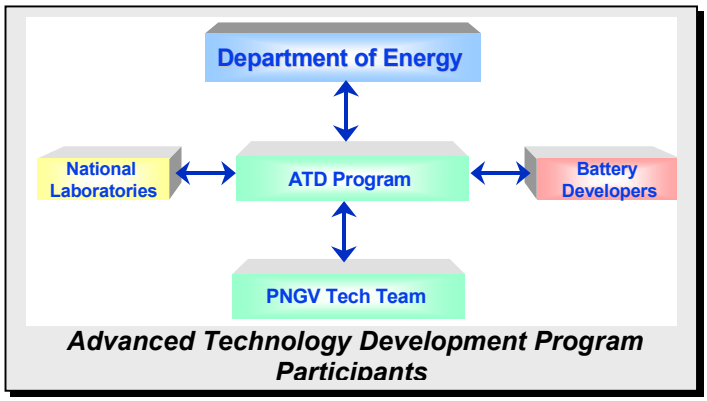

Addressing Three Major Technical Barriers

The ATD Program is focused on three major technical barriers confronting high-power battery technology, as follows:

A. Calendar Life

Calendar life of high-power batteries is presently between 5 to 7 years. A 10-year calendar life is required to reduce overall system costs. To address issues associated with the calendar life of high-power batteries, the ATD Program is:

- Developing and validating accelerated life test methods.
- Identifying life-limiting mechanisms.
- Identifying advanced cell components that address these life-limiting mechanisms and extend cell life.

B. Abuse Tolerance

The behavior of the candidate cell technologies in high-power battery applications is circumspect. Multiple strings of cells pose a challenge for some of the technologies, especially when exposed to overcharge or thermally harsh conditions. The systems do not presently maintain inherent overcharge or thermal runaway protection. Electronic control and mechanical safety devices are being developed and implemented by the battery developers.

The PNGV program approach to safety issues includes:

- Specify relevant abuse conditions and desired responses to those conditions, along with standards for abuse testing.
- Test, evaluate, and redesign cell and chemistry (developer proprietary information) to ensure abuse tolerance.
- Develop detection and management controls for battery state-of-charge, battery temperatures, and electrical faults. Controls at the cell level will include devices for relief of internal pressure buildup and for internal circuit interruption.
- Develop *in situ* overcharge protection.

The ATD Program is assisting in this overall effort by investigating the thermal failure modes through comprehensive cell testing and diagnostic efforts. It is anticipated that the detailed thermal runaway mechanisms will be understood and addressed with more optimal materials. This information will be shared with the developers and used to develop cells that are more inherently safe.

C. Cost

The current cost of high-power lithium-based cells is prohibitively high. The ATD program is addressing cell cost issues through the following activities:

- Developing lower cost cell components: electrolytes, anodes, and cathodes.
- Developing low-cost processing methods for producing advanced cell materials.
- Working with potential US suppliers to implement low-cost material production.
- Developing low-cost cell packaging alternatives.

ATD Program Participants

The ATD program requires the close coordination of research and diagnostic efforts of five national laboratories: Argonne National Laboratory, Brookhaven National Laboratory, Idaho National Engineering and Environmental Laboratory, Lawrence Berkeley National Laboratory, and Sandia National Laboratory

(BNL, INEEL, LBNL, and SNL). Close communication is maintained with battery developers and the PNGV Electrochemical Energy Storage Technical Team to ensure that the issues being investigated within the program will be of direct benefit to the U.S. battery manufacturing community. To make an impact on the cost barriers, the ATD Program has established over a dozen relationships with present and potential battery component vendors. In addition, the ATD Program maintains close ties with other governmental organizations involved in advanced battery research through the Interagency Power Working Group. This ensures that relevant technical issues being addressed and timely solutions being developed are disseminated amongst the other government agencies.

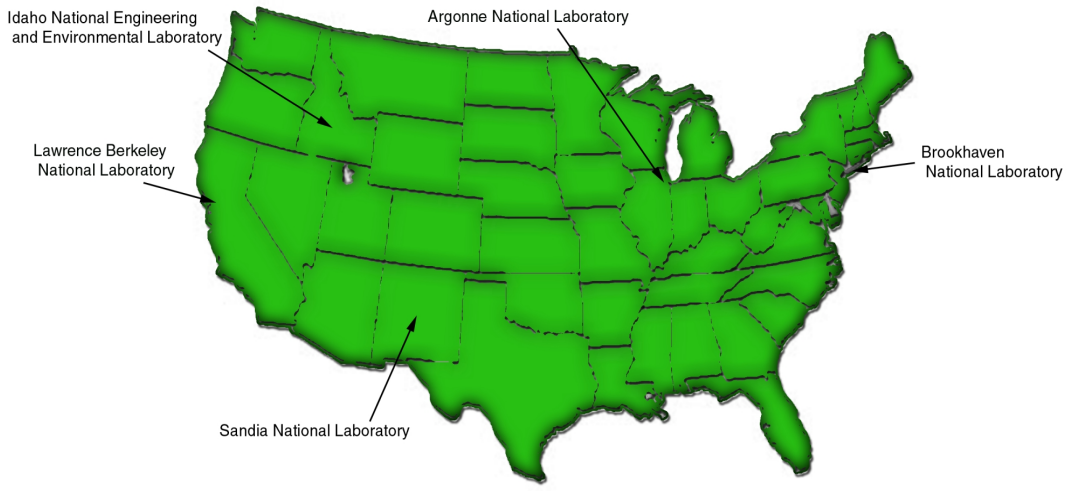

Advanced Technology Development Program Participants

Accomplishments in FY 2000

The major accomplishments for the Advanced Technology Development Program in FY 2000 are presented below, organized by program area:

Gen 1 Cell Development & Evaluation

- A viable high-power Gen 1 cell chemistry was characterized and conditioned to various levels of calendar and cycled aging by accelerated methods.
- The three testing laboratories established a standard analysis methodology.
- Correlation of aged cell data indicates a square-root of time dependence of cell impedance rise and a thermal activation of approximately 10 kJ/mol.
- ARC tests show the onset of adiabatic thermal runaway at approximately 80°C, initated at the anode/electrolyte interface. Thermal runaway accelerates at approximately 160°C due to a rapid reaction of electrolyte with the cathode active material.

Gen 1 Cell Diagnostic Evaluations

- A variety of sophisticated and specialty diagnostic tools were put to use in studying cycle and calendar life degradation mechanisms. The initial sweep of diagnostics has been narrowed to those tools most capable of identifying the source of cell failure.

- Electrolyte decomposition products found in aged cells are similar to those found when PF_5 is reacted with the electrolyte and when the electrolyte is heated to 70°C.
- CO_2 and CO are the main constituents of gas generation during cell aging.
- Cell impedance rises rapidly within the first 30 days of testing, even at room temperature.
- The major source of cell impedance rise can be attributed to the positive electrode.
- It apears that structural changes occur at the surface of the active material leading to a less conductive material.

Electrochemistry Improvement: Gen 2 and Gen 3

- After evaluating as many as 30 metal oxide cathodes, 14 carbon anodes, four binders, and several electrolytes and additives, a Gen 2 cell chemistry was selected.
- The Gen 2 cell chemistry has a lower impedance and a smaller themal response than the Gen 1 chemistry.
- A new electrolyte was optimized for conductivity and low-temperature performance for use in Gen 2 cells.
- The Gen 2 cell consists of 40% lower materials cost than Gen 1 cells.
- Mg doped $LiNiCoAlO_2$ showed increases in electrical conductivity by as much as a factor of 5.
- Identified low-cost processes for synthesizing multi-doped cathode material for Gen 3 cells and produced lab-scale quantities for evaluation.
- Identified approaches for developing pre-passivated and PC-compatible anode materials; and identified industrial collaborators.
- Developed additives for enhancing electrolyte stability and identified collaborators.

Low Cost Packaging

- Evaluated several combinations of candidate barrier layer materials for use in making laminated flexible cell containers that a have 10 year life.
- Identified several packaging companies willing to assist in the development of advanced packaging efforts.

Future Directions

The ATD program will continue to focus on overcoming the main barriers to the successful development and commercialization of high-power lithium-ion batteries. The following modifications to the program are being implemented in FY 2001 to enhance its effectiveness:

- An advanced chemistry will be studied in a welded cell construction on an 18650 size battery cell level.
- Three additional chemistries will also be evaluated at the 18650 size level in FY 01.
- Diagnostics will be focused on understanding power fade as identified at the cathode/electrolyte interface.
- The abuse tolerance efforts are being shifted from characterization toward chemical identification of thermal events.
- The low-cost cell packaging effort will move toward technology transfer and proof-of-concept with established packaging compainies.
- An advanced process research effort is being enhanced to ensure that low-cost industrial-scale processes are transferred to commercially viable battery material suppliers.

3. GEN 1: CELL DEVELOPMENT AND TESTING

A. Overview of ATD Gen 1 Cell Performance and Life Evaluations

Chet Motloch
Idaho National Engineering and Environmental Laboratory, Idaho Falls, ID 83415-3830
(208)-526-0643; fax: (208)-526-0969; e-mail: motlcg@inel.gov

Ira Bloom
Argonne National Laboratory, Argonne, IL 60439-4837
(630)-252-4516; fax: (630)-252-4176; e-mail: bloom@cmt.anl.gov

Terry Unkelhaeuser and David Ingersoll
Sandia National Laboratory, Albuquerque, NM 87185-0613
(505)-845-8801; fax: (505)-844-6972; e-mail: dingers@snl.gov

Objectives

- Perform coordinated ATD Gen 1 testing at INEEL, SNL, and ANL.
- Measure and report baseline performance, and subsequent calendar life improvements, in high-power lithium-ion batteries.
- Develop methodologies for predicting calendar and cycle life.

Approach

- Testing protocols developed using Sony 18650 lithium-ion cells.
- Testing includes both standard PNGV characterization tests, and special calendar life and life cycle tests to help identify factors that limit calendar life.
- Life test matrix has 135 Gen 1 lithium-ion cells:
  - Three States of Charge (80%, 60%, and 40%)
  - Four temperatures (40°C, 50°C, 60°C, and 70°C)
  - Four life-cycle profiles (0%, 3%, 6%, and 9% ΔSOC pulse-profiles)
- Concurrent testing at INEEL (74 cells), SNL (43 cells), and ANL (31 cells).
- Selected cells sent to diagnostics labs after 4 weeks of life testing, and the remainder at the end-of-testing or end-of-life.

Accomplishments

- ATD 18650 Gen 1 Lithium-Ion Cells test plans issued for use (Rev. 1, July 16, 1999; Rev. 2, July 30, 1999; Rev. 3, August 16, 1999; Rev. 4, December 8, 1999).
- Round-robin data exchanges between INEEL, SNL, and ANL completed.
- Standard analysis methodologies between INEEL, SNL, and ANL implemented.

- New pulse-per-day calendar life test successfully implemented.
- All cells completed testing and sent to diagnostics labs.
- Preliminary data analysis completed.
- Innovative calendar-life modeling methodologies developed.

Future Directions

- Inventory all data and check data consistency.
- Establish data review team and continue data analysis at the three testing laboratories.
- Develop list of phenomena to be explained.
- Develop phenomenological hypotheses to explain performance and power fade.
- Correlate testing results with diagnostic results.
- Continue to conduct and coordinate testing and resolve testing related issues.
- Prepare for ATD Gen 2 testing.

The intent of the ATD testing program is to characterize the performance, and determine the cycle life and calendar life behavior, of lithium-ion cells (nominal 0.9 Ah capacity). In general, these cells were subjected to the performance and life test procedures that have been defined for the Partnership for a New Generation of Vehicles (PNGV) Program. The cells covered by this test plan are 18650-size cells manufactured by PolyStor Corporation specifically for the PNGV ATD Program. These cells were built to ANL specifications.

Battery testing has been performed to measure baseline performance, and subsequent improvements, in high-power lithium-ion batteries that are being developed for the ATD Program. Testing included both standard PNGV characterization tests (Reference 1) and special life tests to help identify factors that limit calendar life. A key parameter related to calendar life for PNGV applications is power fade. Consequently, testing and associated data analysis is centered on this aspect.

During the previous reporting period, protocols were developed using Sony 18650 lithium-ion cells. Lessons learned from the Sony cell testing were then used to develop the ATD Gen 1 test plan. The test plan helped ensure coordinated testing between the three test laboratories, INEEL, ANL, and SNL. It defined the purpose for testing and identified the equipment requirements, prerequisites, cell rating and limitations, and safety concerns. It defined the tests to be performed, and the data acquisition requirements. It described the anticipated results, and prescribed the disposition of the cells at the completion of testing. Several revisions were made to the test plan as new information was learned. Table 1 summarizes the ATD Gen 1 cell ratings and limits.

Table 1 shows the nominal ratings and test limits for the Gen 1 cells. The rated capacity is 0.9 Ah at a $C_1/1$ discharge rate. The cell operating temperature range is –20°C to +60°C. The minimum discharge voltage is 3.0 V. The maximum charge voltage is 4.1 V continuous and 4.3 V for up to a 2-second pulse.

Ratings	
Cell rated capacity	0.9 Ah at a C_1/1 discharge rate
Cell operating temperature range	-20°C to +60°C
Cell nominal weight	41.4 g
Voltage Limits	
Minimum discharge voltage	3.0 V
Maximum charge voltage	4.1 V continuous; 4.3 V for up to a 2-second pulse
Current	
Maximum discharge current	2.0 A continuous; 7.2A (8C) for up to an 18-second pulse; 13 A for up to a 2-second pulse.
Maximum charge current	0.9 A continuous; 12 A for up to a 2-second pulse

Table 1. ATD Gen 1 Cell Ratings and Test Limits

The maximum discharge currents are 2.0 A continuous, 7.2 A for up to an 18-second pulse, and 13 A for up to a 2-second pulse. The maximum charge currents are 0.9 A continuous, and 12 A for up to a 2-second pulse.

Characterization tests were performed on all the cells. These tests included impedance measurements at 0% SOC and 100% SOC; C_1/1 Static Capacity; low- and medium-current Hybrid Pulse Power Characterization at 2.7 A and 7.2 A, respectively; and a 7-day self-discharge at 3.660 V, which corresponds to 50% SOC. Thermal Performance tests consisting of the static capacity and low-current HPPC tests were performed on four cells at ambient temperatures of +5°C and +40°C. Finally, Reference Performance Tests (RPTs) were conducted on all cells prior to commencing life testing. The RPTs consist of a single C_1/1 constant current discharge, one medium-current HPPC test, and impedance measurements at 100% SOC and 0% SOC. The RPTs are repeated every four weeks for the cells at 40°C, 50°C, and 60°C, and every two weeks for the cells at 70°C.

All of these are standard PNGV tests, and are described in detail in Reference 1. Figures 1 and 2 show the impedance at 100% SOC and 0% SOC for each of the 69 INEEL cells. The mean impedance at each condition is 23.81 $\pm$ 0.73 mΩ and 24.42 $\pm$ 0.76 mΩ, respectively.

Figure 1. INEEL ATD Gen 1 Li-Ion Cells 100% SOC Impedance (69 Cells)

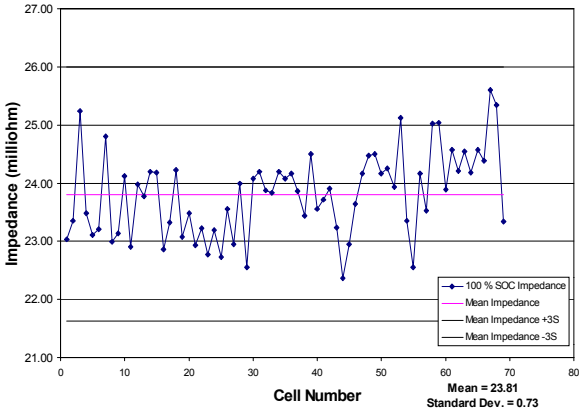

Figure 2. INEEL ATD Gen 1 Li-Ion Cells 0% SOC Impedance (69 Cells)

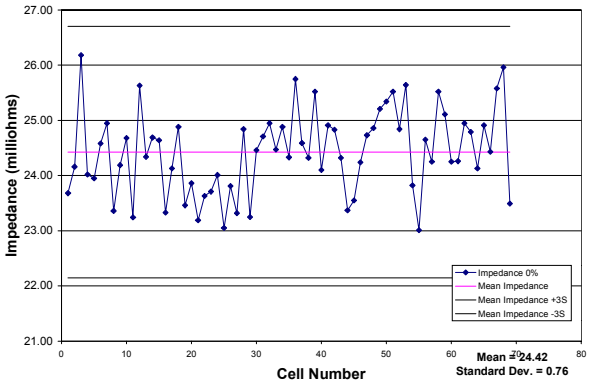

Figure 3 shows that the average C_1 capacity for these cells is 0.917 $\pm$ 0.02 Ah. Figure 4 shows that the average self-discharge is 0.0667 $\pm$ 0.0597. Results from all three testing laboratories have been reviewed. Some systemic differences have been observed. These differences are being investigated and are believed to be largely due to differences in test equipment and temperature control, and also to differences in storage time and temperature, and how the cells were fabricated.

SOC / ΔSOC	Test Temperatures (°C)											
	INEEL				SNL				ANL			
	40	50	60	70	40	50	60	70	40	50	60	70
80%												
zero (calendar life)	3	3	3	3	3	3	3	3				
3%			3		3	3		3				
6%			3		3	3		3				
9%			3		3	3		3				
60%												
zero (calendar life)	3	3	3	3					3	3	3	3
3%	3	3	3	3								
6%	3	3	3	3							3	
9%	3	3	3	3								
40%												
zero (calendar life)									3	3	3	3
3%												
6%												
9%												
TOTALS	15	15	24	15	12	12	3	12	6	6	9	6

Table 2. Calendar Life and Life Cycle Matrix for ATD Gen 1 Cells

Table 2 shows the calendar life and life cycle matrix for the 135 Gen 1 lithium-ion cells that were tested at INEEL, SNL, and ANL. The life test matrix distributes the 135 cells over three States-of-Charge (SOC) (80%, 60%, and 40%), four temperatures (40°C, 50°C, 60°C, and 70°C) and four life cycle profiles (0%, 3%, 6%, and 9% ΔSOC pulse-profiles). At 80% SOC and 60% SOC, all the test group locations are populated by either three or six cells. Only calendar life testing was done at the 40% SOC condition. For data comparison and data validation, some of the test groups overlapped between the labs. Similar testing will be performed on the Gen 2 and Gen 3 cells during those phases of the ATD program, although it is expected that the number of cells and conditions may be revised based upon what is learned from Gen 1 cells.

One out of every three cells in each test matrix group was removed from testing at the end of 4 weeks and shipped to the diagnostics labs for further investigations. These cells were those that exhibited the largest fade in capacity. The details of the diagnostic examinations are found elsewhere in this report. The remaining two cells in each test group continued testing until the end of testing (EOT)

Figure 3. INEEL ATD Gen 1 Li-Ion Mean Static Capacity

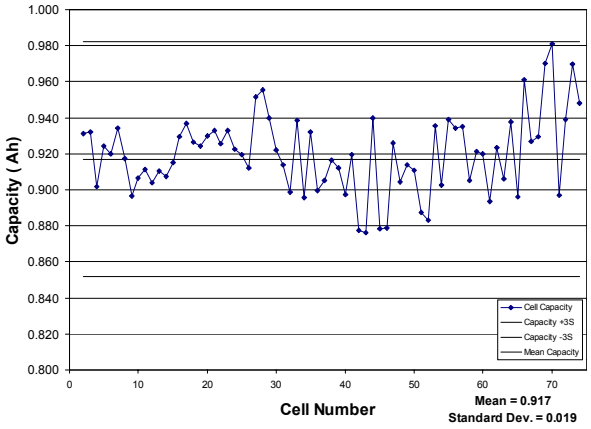

Figure 4. INEEL ATD Gen1 Li-Ion Cells % Daily Loss (69 Cells)

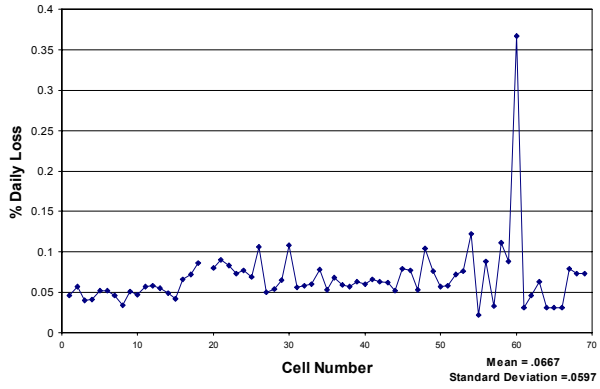

criterion was reached. For the life cycle cells, EOT was reached when a cell was unable to perform its life cycle test profile (within the voltage limits) at the target temperature and SOC conditions. For the calendar life cells, no PNGV EOT criterion is defined, although the inability to perform the PNGV Hybrid Pulse Profile Characterization (HPPC) reference test profile at any SOC at the medium current test value implicitly defines EOT. The EOT criterion has been further defined to occur when a cell is unable to perform the medium-HPPC at 60% Depth-of-Discharge (DOD)

Measurement and data acquisition requirements were specified to enable the three test laboratories to have consistent data logging methodologies. Also, a standardized methodology for analyzing HPPC results was developed as reported in Reference 2. This included a set of four standard plots for each cell for each set of RPTs. The first is the 18-second discharge and 2-second regen Area Specific Impedance (ASI) as a function of cell voltage as measured at the start of the discharge or regen pulse. The second is the cell power density as a function of the equilibrium OCV corresponding to the start of discharge of the regen pulse. The third is the cell power as a function of the cumulative energy removed. Lastly, the fourth is the available energy as a function of power. All of these curves were updated as testing progressed with overlays that show changes in performance as a function of time. As an example, Figure 5 shows the change in available energy as a function of power at four different times for a representative ATD Gen 1 cell. From this, one can observe how the performance of the cells degrades with testing. These data can also be used to develop aging models.

Two additional standardized bar charts are being used to show changes in cell performance as a function of test condition and time. Figure 6 shows the normalized change in static capacity with time for all the INEEL cells at 40°C. Cell identification numbers are shown below each set of bars, and the test condition is shown below each group of cell numbers. For example "60340" means 60% SOC, 3% pulse profile, and 40°C.

Figure 5. ATD Gen. 1 Available Energy Comparison through Life, INEEL Cell 70 (60640)

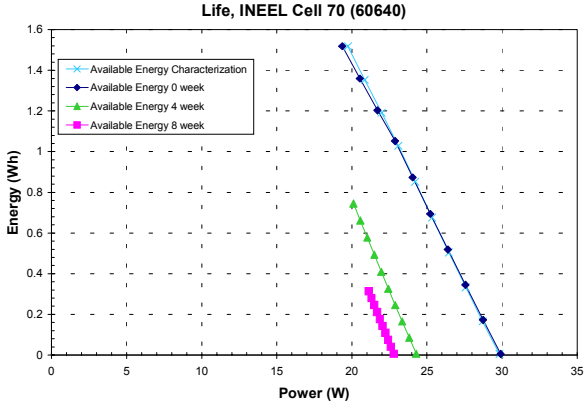

Figure 6. Normalized Gen 1 Static Capacity at 40 °C

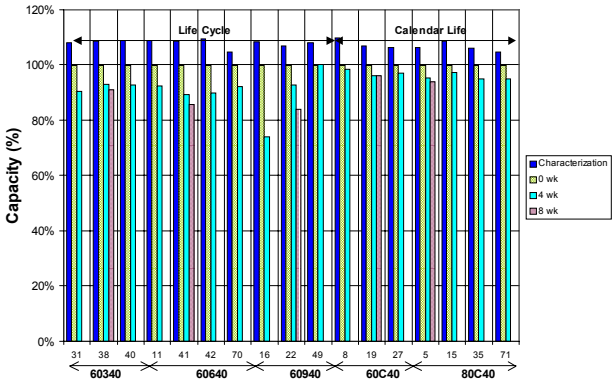

Figure 7. Normalized Gen 1 Pulse Power Limit at 40°C

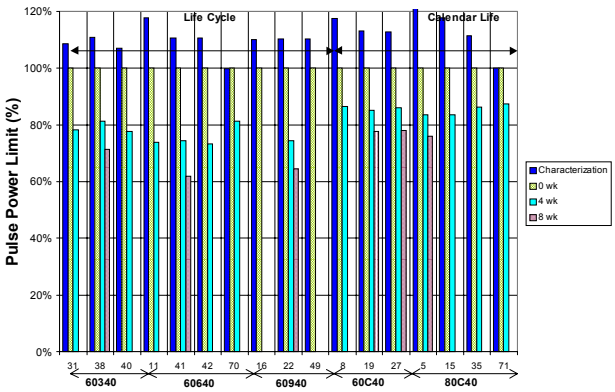

Table 3 shows the average capacity fade from the 0-week to the 4-week RPTs. From the information in Figure 6 and Table 3 several general observation are made regarding capacity fade. The average capacity fade for the characterization to the 0-week RPTs is about 10%. Capacity fade is greater for cycle life than calendar life. Capacity fade increases with temperature. Capacity fade is greater at 80% SOC than at 60% SOC. Capacity fade increases with increasing SOC.

Temperature (°C)	Life Cycle Capacity Fade (%)		Calendar Life Capacity Fade (%)	
	60% SOC	80% SOC	60% SOC	80% SOC
40	9.3		2.7	4.5
50	10.0		3.7	5.7
60	11.0	11.7	6.0	8.3
70 (2 weeks only)	13.3		8.0	7.3

Table 3. Average Capacity Fade from the 0-Week to the 4-Week RPTs.

Figure 7 shows an example of the second standard bar chart, which is the change in normalized pulse power limit with time, for all the INEEL cells at 40°C. Table 4 shows the average pulse power fade from the 0-week to the 4-week RPTs. From the information in Figure 7 and Table 4, several general observations are made regarding power fade. Pulse power fade is greater for cycle life than calendar life. Pulse power fade increases with temperature and time for both life cycle and calendar life. The average pulse power fade from the characterization to the 0-week RPTs is about 10%. Similar charts have been generated for the cells at 50°C, 60°C, and 70°C. All three testing laboratories are employing the same standardized methodologies to facilitate data comparison and analysis.

Tables 5 shows the ATD performance for a representative cell compared to the PNGV Dual Mode Hybrid Goals (Reference 1). The PNGV goals are specified at the level of an automobile, whereas the ATD results are shown at the cell level. To compare the two, one must calculate the number of ATD cells required to meet the PNGV system goals, from which one can then calculate specific values for direct comparison (e.g., specific power or specific energy). Table 5 shows that the Pulse Discharge Power, Peak Regen Pulse Power, Available Energy, and Available Specific Energy all decreased from 0 weeks to 4 weeks to 8 weeks. While at the same time, the Required Number of Cells and Maximum Weight increased. The drop in power with time is indicative of the calendar life problem.

These trends are as expected, but the rate of change is higher than initially anticipated. Notably, the 0-week results are close to meeting all the PNGV goals, but fall off rapidly thereafter. Also, the change in self-discharge is very large from the 0-week to the 4-week point. No data to calculate self-discharge were available for the selected cell at 8 weeks.

Characteristics for INEEL Cell 70 (90408.102):
Life test condition: 60% SOC, 6% ΔSOC, 40°C (replacement cell)
Weight as received: 39.72 g
Average self-discharge: 0.0667% /day
4 week power fade: 20% (group average is 24.3%)
4 week capacity fade: 7.5% (group average is 9.0%)

ATD Gen 1 analysis of the testing data is continuing. Data from all 135 ATD Gen 1 cells at the three testing laboratories have been reviewed and scrutinized. Some anomalies have been identified and are being resolved. Outliers are being culled from the data sets. The remaining "gold" cells will be utilized for calendar life modeling, life cycle modeling, and correlation to diagnostics results. Ultimately, a major goal is to use results from the testing to develop Arrhenius-like or other types of models that may be used to predict calendar life at standard automobile operating conditions. More discussion on life cycle results and calendar life results, and modeling efforts are presented elsewhere in this report.

At the completion of the life cycle and calendar life testing, the cells were shipped to diagnostics labs for post-test examination and analysis. The recipient of cells was determined in advance, based upon diagnostic capabilities, and mapped against the test matrix.

Each testing laboratory has posted results on individual ATD web sites. Results from the Gen 1 cell testing have formed the baseline against which the performance of Gen 2 and Gen 3 cells will be evaluated.

Temperature (°C)	Life Cycle Power Fade (%)		Calendar Life Power Fade (%)	
	60% SOC	80% SOC	60% SOC	80% SOC
40	**23.6**		**14.0**	**15.2**
50	**28.4**		**20.3**	**23.3**
60	**34.1**	**34.9**	**29.0**	**31.5**
70 (2 weeks only)	**36.4**		**33.3**	**33.5**

Table 4. Average Pulse Power Fade from the 0-Week to the 4-Week RPTs.

Characteristic	PNGV Target	ATD Units	0 Week	4 Week	8 Week (all values extrapolated)
Pulse Discharge Power	40,000 W	W/cell	24.0	20.2	19.2
Peak Regen Pulse Power	40,000 W	W/cell	24.0	20.2	19.2
Available Energy	1,500 Wh	Wh/cell	0.900	0.757	0.720
Required No. of Cells	N/A	cells	1,666.7	1,980.2	2,083.3
Max. Weight	65 kg	Kg/pack	66.2	78.6	82.7
Available Specific Power	615.4 W/kg	W/kg	604.2	508.6	483.4
Available Specific Energy	23.1 Wh/kg	Wh/kg	22.7	19.1	18.1
Max. Self Discharge	50 Wh/day	Wh/day/pack	37.3 (ATD Avg.)	89.9	**N/A**

Table 5. ATD Cell Performance vs. PNGV Dual Mode Hybrid Goals for INEEL Cell 70 (60640)

References

1. PNGV Battery Test Manual, Revision 2, DOE/ID-10597, August 1999.

2. C. G. Motloch et al., "Developing a Test Plan for the ATD Program," Advanced Technology Development, 1999 Annual Progress Report, Energy Management Team, U. S. Department of Energy, Office of Advanced Automotive Technologies, March 2000.

B. Life Cycle Testing of High-Power 18650 Lithium-Ion Cells

Terry Unkelhaeuser and David Ingersoll
Sandia National Laboratory, Mail Stop 0613, Albuquerque, NM 87185-0613

Chet Motloch
Idaho National Engineering and Environmental Laboratory

Vince Battaglia and Ira Bloom
Argonne National Laboratory

Harold Haskins
Ford Motor Company

Contact: T. Unkelhaeuser,(505) 845-8801; fax (505) 844-6972; e-mail: tmunkel@sandia.gov

Objectives

- Develop a life cycle test protocol for characterization of high-power 18650 lithium-ion cells.
- Demonstrate the adequacy of the test protocol using commercially available cells and prototype Gen 1 cells.
- Design an experimental test matrix that encompasses test parameters known to affect cell performance, such as state-of-charge and temperature.
- Specify a series of pre- and post-test electrical studies that will allow for characterization of cell degradation mechanisms.
- Identify the testing resources necessary for implementation the test plan.
- Develop a post-test diagnostic schedule for each cell in the test matrix.

Approach

- Modify existing PNGV test protocols for use for high-power characterization of 18650 cells.
- Perform an evaluation of the modified test protocols using commercially available cells and prototype Gen 1 cells by placing these cells on a limited test schedule.
- Identify critical cell test parameters, such as state-of-charge and temperature, based on previous experience or by performing limited experimental testing.
- Develop a complete test matrix encompassing this critical parameter space.
- Populate the matrix within the constraints of limited cell resources beginning with the high-value matrix elements.
- Identify test resources required for implementation of the test matrix.
- Identify a post-test diagnostic schedule for each cell in the matrix.

Accomplishments

- Developed a fully automated high-power life cycle test that allows for control of the state-of-charge of the cell on each cycle of the test, and which also obviates the need for performing the Operating Set Point Stability Test described in the PNGV test protocol. This was accomplished by using the cell voltage as a measure of the state-of-charge of the cell, and employing a controlled voltage step as the last element in the pulse profile. Enough flexibility of the test protocol has been attained such that this procedure has general applicability to a wide variety of cells.

- Developed and tested a prototype test fixture to ensure maintenance of a uniform and stable cell temperature during testing. Due to the high currents passed in the test, and the small but finite cell resistance, it was anticipated that the cell would exhibit significant i^2R heating, resulting in a significant deviation of cell temperature from the target value. This was experimentally verified, and a prototype cell fixture was designed and tested in order to eliminate this effect.

- Developed and published a test plan that identifies the test matrix, test conditions, handling procedures, and pre- and post-test electrical characterization procedures for each cell.

- Identified the requisite test facilities necessary for plan implementation. Due to the large number of cells and test conditions employed, it was clear that no single test facility could successfully implement the plan. Consequently, three sites were deemed necessary for full plan implementation. These sites are Argonne National Laboratory, Idaho National Engineering Laboratory, and Sandia National Laboratories.

- Completed testing of the 79 cycle life Gen 1 cells.

- Processed all of the cell test data. The complete analysis of all of the data is continuing and will be completed before the Gen 2 testing program begins.

Future Directions

- Complete the analysis of cell performance data.

- Develop the Gen 2 test plan.

- Implement the test protocol on Gen 2 cells.

It is well recognized that the conditions of use of a cell will affect its performance, as well as influence its eventual failure and mechanism of failure. Hence, in order to gain an understanding of the potential failure mechanisms of the cell, and to make predictive statements regarding cell performance under actual use conditions, it is necessary to subject the cell to a wide variety of test conditions within the expected performance envelope. A series of diagnostic tests aimed at exploring the fundamental characteristics of the cells, such as the structural changes of the cathode material for example, could then be performed. These tests would be performed either at the end-of-test in the case of destructive diagnostic methods of analysis, or interspersed during execution of the test in the case of non-destructive tests. Following this approach, a life cycle testing protocol was designed and developed which was applied to the Gen 1 cells. In order to gain a fundamental understanding of cell behavior, as well as to aid in future cell design, this protocol will continue with the Gen 2 cells.

The Gen 1 cycle life cells were tested under two state-of-charge conditions (60% and 80%), three delta state-of-charge conditions (3%, 6%, 9%), and four temperatures (40°C, 50°C, 60°C, 70°C). Control of the state-of-charge during each cycle of the test was accomplished by making a fundamental change in the way that the state-of-charge is recognized. Normally, this is accomplished strictly on the basis of capacity, and relative capacity added and/or removed from the cell. We initially adhered to this protocol and obtained voltage vs. capacity

data at a low rate (C/25). However, we then tied these capacity levels to the open circuit voltage (OCV) of the cell, and in essence generated a calibration curve of OCV vs. state-of-charge. During the course of the test we controlled to this value, and a reset was done as the last step in a complete pulse profile.

The basic pulse profile used consists of a series of controlled current steps. One of the profiles is shown in Figure 1. Also contained in the figure is a table that summarizes the various current levels and time duration for each pulse. The final pulse, and

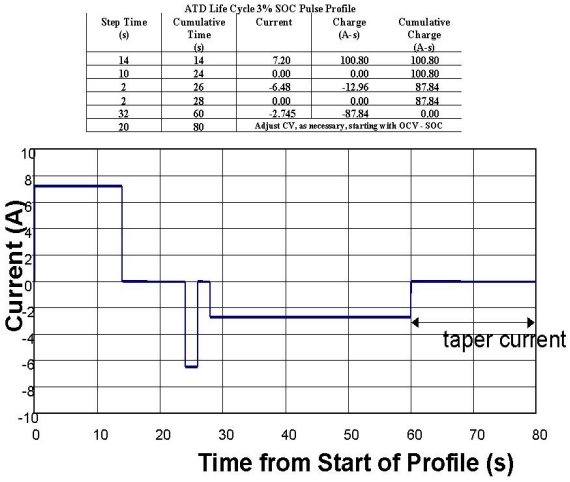

Figure 1. Life Cycle Test Profile for Gen 1 Cell

the key to maintaining the state-of-charge on each cycle, is a controlled voltage step. In this way, by bringing the cell back to the desired voltage, the state-of-charge can be maintained at the desired level.

The amount of charge added to or removed from the cell during the pulse profile (ΔSOC), can significantly affect cell performance. We recognized this as one of the critical test parameters in our program, and three ΔSOCs corresponding to 3%, 6%, and 9% were included in our test design. Each of the different levels was obtained by using one, two, or three repetitions, respectively, of the basic life cycle test profile shown in Figure 1. A comparison of the three different profiles is shown in Figure 2.

From the above discussion, it is evident that the critical parameters are state-of-charge, ΔSOC, and cell temperature. Based on these, three test matrices were developed that span the parameter space given the limited resources. Three matrices are used since three test sites, each with their own unique capabilities, are utilized to implement this program. Tables 1 – 3 show each of these matrices.

The testing of the 43 Gen 1 cells (39 + 4 replacements) assigned to SNL is complete. The test results were combined with the results from INEEL and ANL to present a unified testing result to the ATD and DOE program managers. Nineteen cells have been shipped to diagnostic labs and 20 cells are in cold storage (10°C). Three cells vented during testing and were replaced in the matrix.

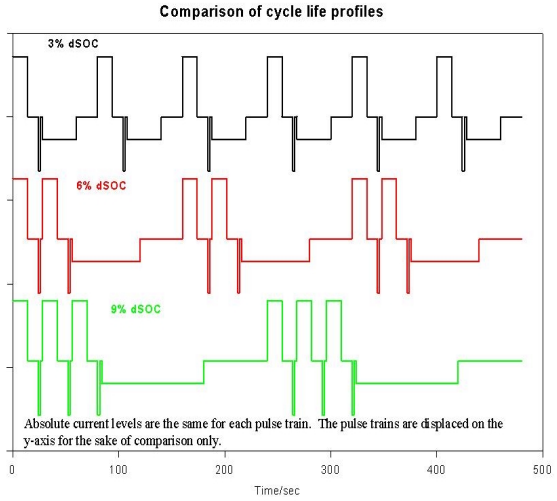

Figure 2. Life Cycle Test Profiles Corresponding to 3%, 6%, and 9% ΔSOC

Matrix for ATD GEN 1 Baseline Cells at INEEL				
SOC / ΔSOC	Test Temperature			
	40 ◦C	50 ◦C	60 ◦C	70 ◦C
80%				
zero (calendar life)	3	3	3	3
3%			3	
6%			3	
9%			3	
60%				
zero (calendar life)	3	3	3	3
3%	3	3	3	3
6%	3	3	3	3
9%	3	3	3	3
40%				
zero (calendar life)				
3%				
6%				
9%				
TOTALS	15	15	24	15

Table 1. Life Cycle Matrix Implemented at INEEL

Matrix for ATD GEN 1 Baseline Cells at Argonne National Laboratories				
SOC / ΔSOC	Temperature			
	40 °C	50 °C	60 °C	70 °C
80%				
zero (calendar life)				
3%				
6%				
9%				
60%				
zero (calendar life)	3	3	3	3
3%				
6%			3	
9%				
40%				
zero (calendar life)	3	3	3	3
3%				
6%				
9%				
Totals	6	6	9	6

Table 2. Life Cycle Matrix Implemented at ANL

Matrix for ATD GEN 1 Baseline Cells at Sandia National Laboratories				
SOC / ΔSOC	Temperature			
	40 °C	50 °C	60 °C	70 °C
80%				
zero (calendar life)	3	3	3	3
3%	3	3		3
6%	3	3		3
9%	3	3		3
60%				
zero (calendar life)				
3%				
6%				
9%				
40%				
zero (calendar life)				
3%				
6%				
9%				
Totals	12	12	3	12

Table 3. Life Cycle Matrix Implemented at SNL

The average capacity fade of the Gen 1 cells was higher at 80% SOC. Also, at 80% SOC, only the 40°C data have a steady increase in capacity fade with increasing ΔSOC. Capacity fade at other temperatures is somewhat insensitive to ΔSOC. At 60% SOC, a steady increase in fade is observed up to 70°C. These trends are shown in Figures 3 – 6.

	0%dsoc	3%dsoc	6%dsoc	9%dsoc
4 week 40°C	7.5	12.6	13.5	17.0
4 week 50°C	12.2	16.5	18.9	17.3
4 week 60°C	14.8	20.9*	21.0*	15.0*
2 week 70°C	16.0	19.9	19.9	20.1
Average	12.6	17.5	18.3	17.4

* = INEEL Data

Figure 3. Average % Capacity Fade at first RPT (80% SOC)

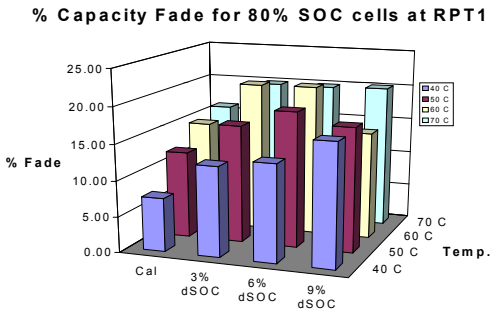

Figure 4. Higher Temperature and Higher ΔSOC Cause Higher Capacity Fade – 80% SOC Data

	3% dsoc	6% dsoc	9% dsoc
4 week 40 °C	7.9	9.0	11.0
4 week 50 °C	8.7	10.6	10.6
4 week 60 °C	9.9	10.5	12.5
2 week 70 °C	13.0	13.4	13.4
Average	9.9	10.9	11.9

All Data is from **INEEL**

Figure 5. Average % Capacity Fade at first RPT (60% SOC)

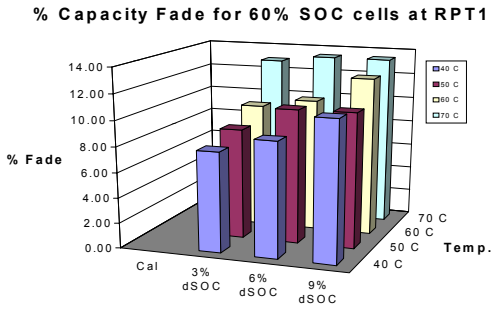

Figure 6. Higher Temperature and Higher ΔSOC Cause Higher Capacity Fade – 60% SOC Data

Pulse power fade was also observed for the Gen 1 test cells. For the INEEL test cells at 60% SOC, the average pulse power fade from characterization to the zero week RPTs was 10.6%. From zero week to the first RPT, the average pulse power fade ranged from 34% to 38% for the 70°C cells down to 21% to 26% for the 40°C cells.

The average pulse power fade from zero week to the first RPT for the 80% SOC cells tested at SNL ranged from 37% to 44% for the 70°C cells down to 24% to 34% for the 40°C cells. These results show that pulse power fade increases with higher SOC and higher ΔSOC. Figures 7 and 8 graphically illustrate the trend in increased pulse power fade.

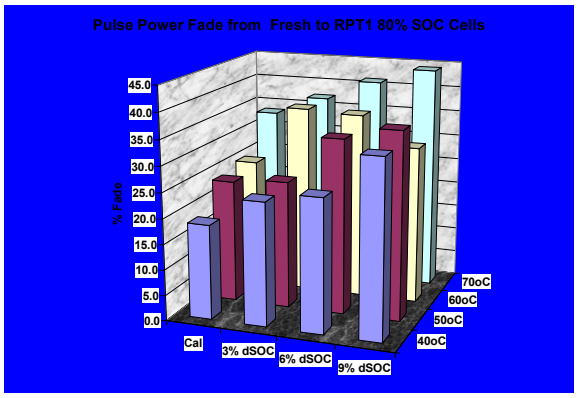

Figure 7. Pulse power fade, fresh to RPT 1 for 80% SOC cells

The mid-level Hybrid Pulse Power Characterization Tests (M-HPPC) show that the increased resistance of the Gen 1 cells is primarily due to charge transfer resistance with a secondary ohmic resistance effect. This can be seen by examining the first 7.2A, 18-second pulse of the M-HPPC test. The charge transfer resistance increases at a faster rate as the cell ages. Figure 9 illustrates the contribution of ohmic and charge transfer resistance to cell performance. Note, however, that Figure 9 is not corrected for the ohmic drop in the nickel tabs and test leads connected to the cell. We are in the process of making the appropriate measurements to correct the readings for the nickel tabs and test leads.

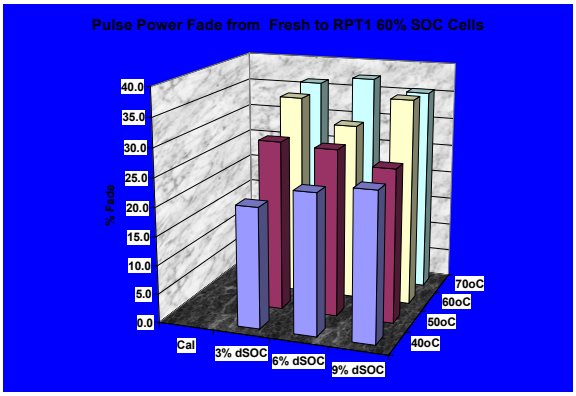

Figure 8. Pulse power fade, fresh to RPT 1 for 60% SOC cells.

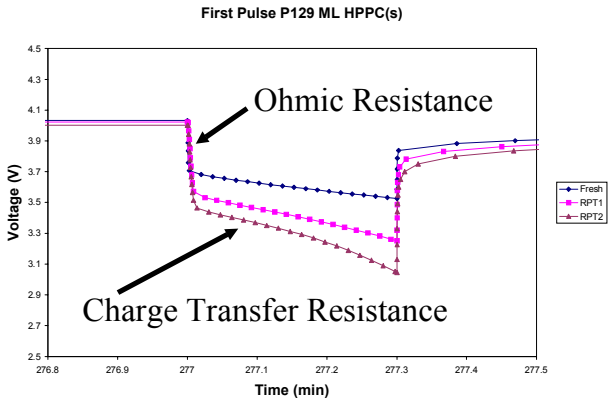

Figure 9. Typical first 7.2A, 18-second discharge pulse showing ohmic vs. charge transfer effects.

Acknowledgments

Sandia National Laboratories is a multiprogram laboratory operated by Sandia Corporation, a Lockheed Martin Company, for the United States Department of Energy under contract DE-AC04-94AL85000.

4. DIAGNOSTICS
Calendar/Cycle Life

A. Development of Diagnostic Techniques for Characterizing Electrode Surfaces and Electrode Processes

Frank McLarnon, Robert Kostecki, Fanping Kong, Philip Ross, Sherry Zhang, Elton Cairns, Kathryn Striebel, John Kerr, Steven Sloop, and James Pugh
90-1142, Lawrence Berkeley National Laboratory, Berkeley CA 94720
(510) 486-4636; fax (510) 486-4260; e-mail: frmclarnon@lbl.gov

Objectives

- Establish diagnostic protocols to determine electrode structural and morphological changes that lead to cell performance degradation as it is aged, cycled, and/or abused.
- Study solid electrolyte interphase (SEI) formation and dissolution as cells are cycled and aged.
- Identify electrolyte reactivity trends in lithium-ion cells with respect to cell history.

Approach

- Use atomic force microscopy, Raman spectroscopy, impedance, and other techniques to detect and characterize surface processes that contribute to cell deterioration.
- Use the IR microscope at the LBNL Advanced Light Source IR beam line to provide detailed vibrational spectra of SEIs.
- Use solvent extraction, gas chromatography, and thermal analysis to characterize lithium-ion cell components.

Accomplishments

- Detected significant changes in impedance, surface morphology, and composition of cathodes from aged and cycled Gen 1 (baseline) lithium-ion cells.
- Achieved good understanding of anode SEI chemical composition, and detected anode SEI dissolution in cells cycled at elevated temperatures.
- Found lithium-ion cell reaction products similar to those observed when PF_5 gas is reacted with the electrolyte and when the electrolyte is heated.

Future Directions

- Continue systematic spectroscopic and microscopic studies of aged and cycled cells to correlate changes of electrode surface and structural characteristics with cell performance degradation.
- Correlate SEI composition with cell performance.
- Use quantitative gas chromatography techniques to compare lithium-ion cell chemistries as a function of cell history.

Topographic AFM images of cathodes taken from an untested cell and a cell that was cycle-life tested at 70°C (Figure 1) revealed significant changes in surface morphology. The initial large and flat grains of cathode active material are still recognizable, but the entire surface of the cycled cathode is covered by nanocrystalline (50-200 nm) deposits. Considerable amounts of this deposit accumulated in the inter-granular spaces, however nanoparticles were scattered randomly across the crystal planes of the active material. We determined that the amount of deposit, and the extent of morphology change, increased with increased test temperature. Cathode surface morphology changes were more pronounced in calendar-life cells compared to cycle-life cells, which suggests a precipitation mechanism of deposit formation rather than an electrochemical dissolution-deposition process. These morphology changes were accompanied by a significant decrease of cathode surface electronic conductance. Current-sensing AFM measurements showed that the average conductance decreased significantly with increased cell test temperature, contributing to the impedance rise of the cathode. We confirmed that an SEI is formed on the anode surface during cell formation cycles. An epoxide-containing SEI material (RCHOCHR') was detected on the anode surface in most tested cells along with lithium alkyl carbonate. Cells in which this material was not detected were those cycled with large swings in state of charge (ΔSOC) and at high temperatures (Figure 2).

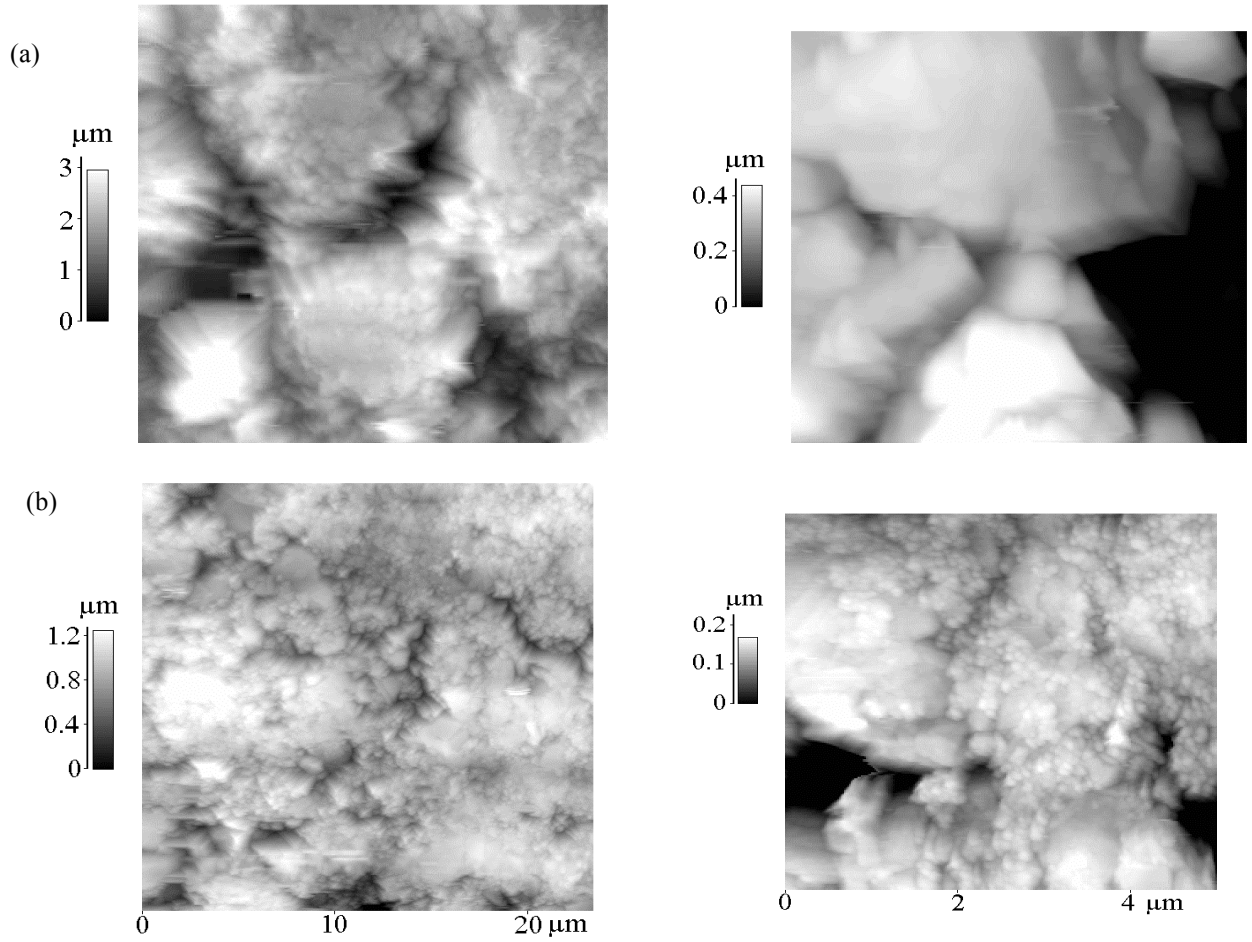

Figure 1. Topographic AFM images (23 x 23 μm and 5 x 5 μm areas) of cathodes extracted from an untested cell (a) and a cell which was cycled at 70°C, 60% SOC and 3% ΔSOC (b).

The anode SEI breaks down under cell test conditions of large ΔSOC and high temperature, presumably forming a more-resistive inorganic film, *e.g.* containing Li_2O and other Li salts. The exact function of this newfound epoxide material on cell performance is unclear at present. More cells will be examined to enable trend analysis of both charge and temperature effects on SEI layer composition.

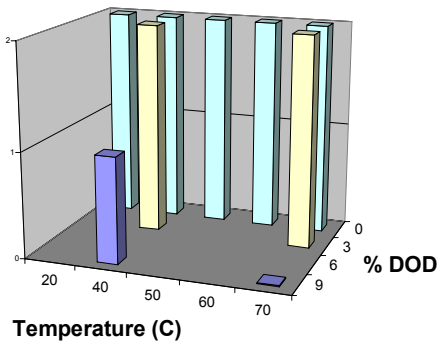

Figure 2. Relative intensities of IR vibrational peak at 832-838 cm^{-1} (characterized as strong, weak or absent) *vs*. cell test temperature and depth of discharge.

The SEI layer was distributed non-uniformly over the anode surface; an important result based on IR spectroscopic studies of samples collected from different locations on the anodes in tested cells. This phenomenon could potentially cause a decline in cell power. The exact cause for SEI non-uniformity is not known, however it may be a result of too-few current-collector strips, and will be investigated further.

The electrochemical behavior of small samples of anodes and cathodes, harvested from Gen 1 cells cycled at various temperatures, was analyzed with slow-sweep cyclic voltammetry (CV) and electrochemical impedance spectroscopy (EIS) as a function of state-of-charge. The capacity (as measured by CV) of the cathodes varied little, whereas the impedance of the cathode samples increased monotonically with Gen 1 cell test temperature. The low-frequency (100 mHz) specific impedance is shown in Figure 3 as a function of electrode potential *vs.* Li for several cells. The impedance increases at low states of charge and higher temperature, consistent with the results of other ATD Program diagnostic laboratories.

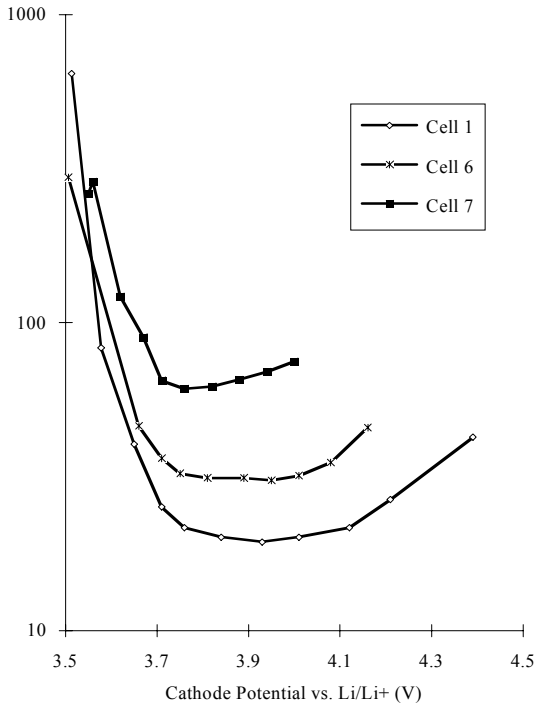

Figure 3. Low-frequency (100 mHz) impedance of cathode samples taken from cells tested/stored at three temperatures. Cell 1 (90319-132) was subjected only to formation cycles at 25°C. Cell 6 (90324-114) was cycled at 40°C. Cell 7 (90407-115) was cycled at 70°C.

The EIS and CV behavior of the anode samples was more complex. The initial anode-ample impedance was high, and increased with increasing Gen 1 cell test temperature. However, this impedance decreased to the expected low value after three or more constant-current cycles with a taper charge at 0.01 V *vs*. Li. This behavior is consistent with the formation (or precipitation) of a resistive film on the anode after removal of the volatile component of the electrolyte, *i.e.* diethyl carbonate (DEC). This layer is then reduced (or dissolved) in the relatively large amount of electrolyte used in the Swagelok test cells. A sample of the fresh (unformed) anode tested in the Gen 1 electrolyte showed the expected low impedance without the need for taper charging. This confirms that the high impedance recorded with samples taken from the cells is related to the history of the anode in the Gen 1 cell and is not only an artifact of the testing procedure.

We have demonstrated that our quantitative gas chromatography (GC) technique is useful in comparing the relative concentrations of products formed in Gen 1 lithium-ion cells. A new product with a GC retention time of 16.6 min was detected in all Gen 1 cells. Because this product and ethylene carbonate (EC) are relatively non-volatile, their absolute amounts change little while carrying out GC analyses; therefore their ratio is a reliable indicator of product concentration. Figure 4 shows the ratio of [new product]:EC in the electrolyte removed from Gen 1 lithium-ion cells, and that for a control experiment to monitor the reaction of EC-DEC-$LiPF_6$ electrolyte with PF_5. The [new product]:EC ratios for each cell and the control experiment are very similar, only the untested cell exhibits a low ratio, an expected result.

The similar product concentrations in tested cells and the control experiment demonstrate the reactivity of the electrolyte solvents with PF_5. Even though the cell testing protocol included a range of temperatures and ΔSOC, the product chemistry of each tested cell was similar. Our results suggest that cell thermal or electrochemical reactions produce PF_5, which then reacts with the solvents in a very consistent manner.

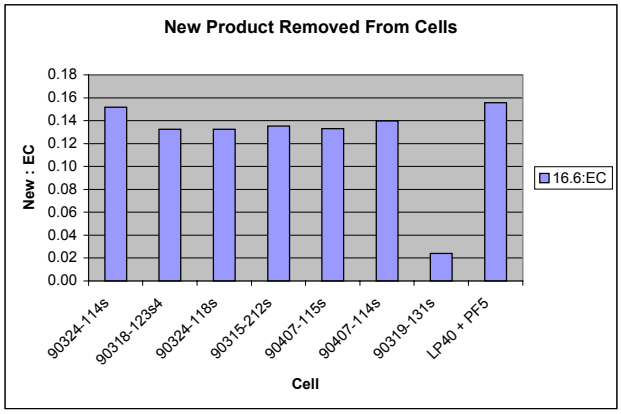

Figure 4. Amount of new product (relative to EC = unity) in the electrolyte removed from Gen 1 lithium-ion cell separators. The untested cell 90319-131 shows the lowest concentration of new product; whereas the tested cells and the control experiment exhibit similar new product concentrations.

B. The Development of Diagnostic Techniques for Examining Cathode and Anode Structural Degradation

James McBreen
Brookhaven National Laboratory, DAS-Bldg. 480, P.O. Box 5000, Upton, NY 11973-5000
(631) 344-4513; fax (631) 344-4071; email: jmcbreen@bnl.gov

Objective

- Determine the nature of the degradation processes that occur in cathodes and anodes of high power lithium-ion cells.

Approach

- Apply *in situ* x-ray diffraction (XRD) and x-ray absorption spectroscopy (XAS) on electrodes punched from test cell electrodes to the study phase composition and chemistry of electrodes.
- Supplement x-ray work with electrochemical characterization, including electrochemical impedance spectrometry (EIS).

Accomplishments

- Performed teardown analysis on 25 cells from the cycle life and abuse tests.
- Concluded form polarization and EIS studies that power fade in tested cells is due mainly to changes at the cathode.
- Confirmed the lack of any new bulk amorphous or crystalline phases in cathodes from tested cells by *in situ* XAS and XRD.

Future Directions

- Perform *in situ* XRD studies of anode materials.
- Perform *in situ* XAS and XRD studies of electrode materials from tested Gen 2 cells.
- Perform *in situ* XRD studies at fast rates on X7A using a position sensitive detector (PSD).
- Perform *in situ* XRD/thermal studies on electrode materials and electrolyte/electrode material combinations.
- Perform transmission electron microscopy of electrode materials.
- Study electrolyte effects on power fade.

The primary objective of this work is to determine chemical, structural, and morphological changes in cell components that lead to performance degradation and failure of advanced high-power lithium-ion batteries as they are aged, cycled, and/or abused. The diagnostic results will guide the development of improved cell chemistries. Another objective is to identify diagnostic techniques that may be helpful to PNGV developers. Work during the year included *in situ* high resolution x-ray diffraction (XRD) and x-ray absorption spectroscopy (XAS) on cathodes from fresh cells

obtained from the vendor, and on cathodes from cells used in cycle life and abuse tests at INEEL and SNL. Electrochemical studies were done on electrode samples punched from electrodes from tested cells.

Teardown Analysis of Cells from Cycling and Abuse Tests

A total of 25 cells were disassembled. All the cell packs, including those from the cycle life and abuse tests, were in remarkably good condition. Complete delamination of the anode material from the copper current collector was noted in four of the tested cells. This could not be correlated with any parameter of the testing procedures. All the tested cells showed a slight discoloration of the Celgard separators. The cathodes in all tested cells had lost high rate capability.

XRD Studies

Disc electrodes (2.82 cm^2) were punched from cathodes from disassembled cells and the active material was stripped from one side of the aluminum or copper current collectors. The cathodes were

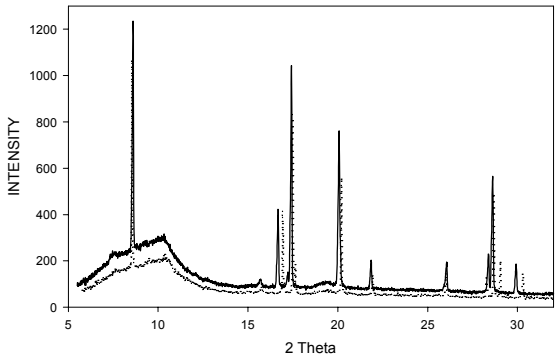

Figure 1. *In situ* XRD patterns for a cathode from a cycled cell in the discharged (-) and charged (···) state. Cell had been cycled at 80% SOC with a 9% ΔSOC at 70°C for 2 weeks.

incorporated into spectroelectrochemical cells with either lithium disc anodes or anodes punched from the anodes from tested cells. The cells had a Celgard separator and electrolyte (1 M $LiPF_6$ in a 1:1 EC:DMC solvent). Most of the XRD measurements were done at Beam Line X7A at the National Synchrotron Light Source (NSLS), using an energy of 17.688 KeV ($\lambda = 0.7009$ '). The Beam Line has a position sensitive detector (PSD) that permits fast data acquisition times. The XRD measurements were done in the transmission mode, so the results reflect the structure of the bulk of the active material. Figure 1 shows XRD patterns for a cathode from a tested cell in the charged and discharged state.

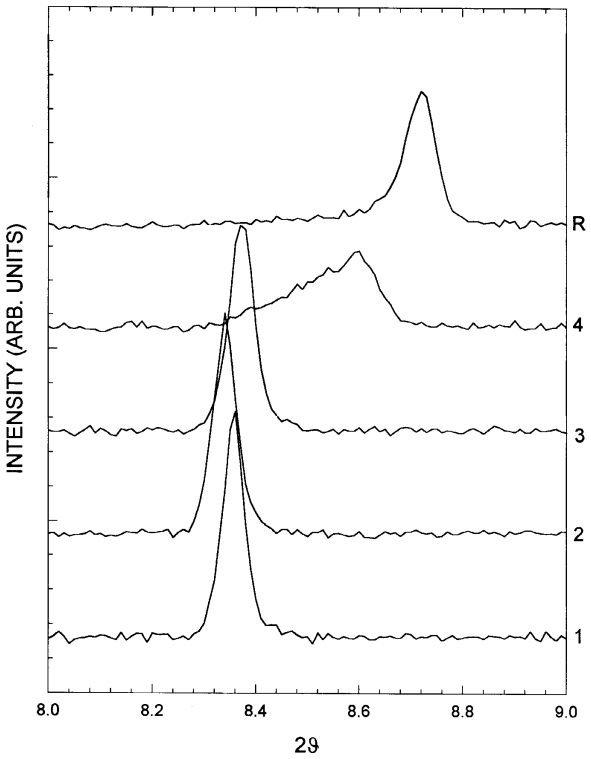

Figure 2. *In situ* XRD, showing (003) peak for a cathode from fresh cell, when charged at C rate from 50% SOC to 4.5 V. Four scans were taken during charge and one scan (R) after the end of charge.

No diffraction peaks for any decomposition products, such as NiO, were found, indicating that no structural changes occur in the bulk of the cathode active material, and no crystalline decomposition products were formed during the cycle testing. This cell had been cycled at 80% state of charge (SOC) with a 9% capacity swing (ΔSOC) at 70°C for two weeks. XRD results for the other cells were substantially the same.

In situ XRD results obtained on electrodes from fresh and tested cells, during charge at the C rate,

were very different. Figure 2 shows the changes in the (003) peak of the XRD pattern for an electrode from a fresh cell, when the cell was charged at the C rate from 50% SOC to a voltage cutoff of 4.5 V. The cell cutoff occurred after 30 minutes of charge. Each complete scan from 6° to 32° took 8 minutes, and the (003) reflection on scan 4 was recorded 1 minute into the scan. Scan R was recorded after completion of the charge. Several scans, recorded after charge, indicated that relaxation processes at the end of charge were minimal. The position of the (003) peak at the beginning of charge indicates that the active material already had been converted to the H2 phase. At the end of charge a considerable amount of the material was converted to the H3 phase.

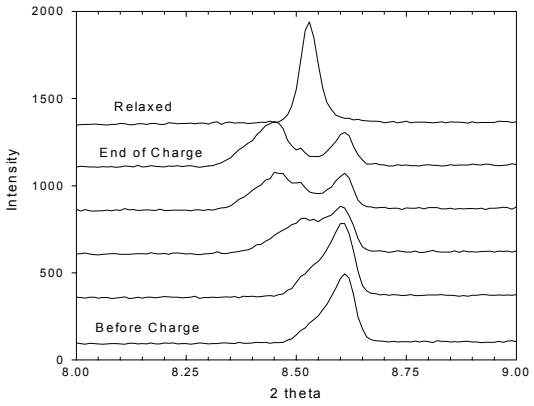

Figure 3. *In situ* XRD, showing (003) peak for a cathode from a tested cell, when charged at C rate. One scan was taken before charge, four during charge and one 30 min after termination of charge. Cell had been cycled at 80% SOC with a 9% ΔSOC at 70°C for 2 weeks.

Figure 3 shows the changes in the (003) peak when an electrode from a discharged cycled cell was charged at the C rate for the first time to a cutoff voltage of 4.7 V. Each of the four complete scans, taken during charge, took 12 minutes and the charge was complete at the end of the 4th scan. The results of the four scans, taken during charge, indicate partial conversion of the initial H1 phase to the H2 phase. There was considerable residual H1 phase present at the end of charge, indicating that some of the H1 phase cannot be converted to the H2 phase at this charge rate before the voltage cutoff. On open circuit, relaxation processes result in the evolution of a single diffraction peak, intermediate to the H1 and H2 peaks. This is due to local cell action between the uncharged H1 and the charged H2 materials. Even though the cutoff voltage is 200 mV higher than that used for the cell with electrodes from the fresh cell, no formation of the H3 phase was observed. Also when the cathodes from any of the tested cells were charged at the C rate, no H3 phase formation was observed. The results indicate that the rate capability of the cathodes from the tested cells is greatly diminished, and that much of the active material can only be accessed at low rates. However, there is no evidence of complete electrical isolation of any of the active material. The evidence suggests some type of resistive pathways in cathodes from tested cells. The fact that the material can be charged and discharged at low rates is consistent with the XRD results that indicate that the structure of the bulk of the cathode material is intact after cycling and calendar life tests.

XAS Studies

The XAS results for discharged cathodes from tested cells were almost identical to those found in a fresh cell. There was a slight shift in the x-ray absorption near edge structure (XANES) to higher

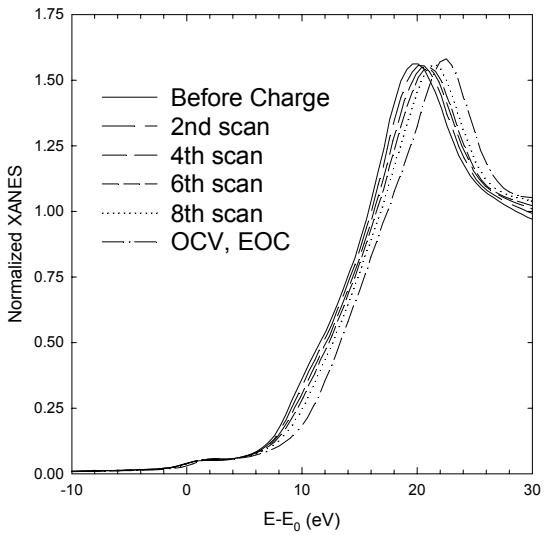

Figure 4. *In situ* Ni K edge XANES for a cathode from a tested cell charged at the C/5 rate to 4.5 V. Cell had been cycled at 80% SOC with a 9% ΔSOC at 70°C for 2 weeks. The last scan (OCV, EOC) was taken on open circuit after the end of charge.

energies, indicating slightly lower lithium content. This can be ascribed to the consumption of lithium in formation of SEI layers at both electrodes and the reaction of anode lithium with acidic decomposition products from the electrolyte. Figure 4 shows the shift in the Ni K edge XANES when an electrode from a tested cell is charged at the C/5 rate to 4.5 V. At this low rate the edge shift is very similar to that seen in electrodes from fresh cells.

Up to the 4.7 V cutoff there is no shift in the Co XANES. This is consistent with our earlier results on fresh material charged to 5.1 V. No shift in the Co XANES was seen until above 4.8 V. The results indicate that up to 4.5 V all charge compensation occurs only on the Ni. The behavior of the Ni EXAFS electrodes from tested cells, during charge, was very similar to that seen in electrodes from fresh cells. Figure 5 shows the Fourier transform of the Co EXAFS for a cathode from a tested cell. The results are essentially identical to that found for electrodes from fresh cells. The results are quite different from those found for $LiCoO_2$ and indicate that there is no phase separation of the Co in the material. The Ni and Co EXAFS results indicate that no significant amount of any new amorphous phases are formed in the tested cells.

XAS results on cathodes from cells with delaminated anodes indicated slight Cu contamination of the cathode. After delamination the Cu foil current collector is no longer cathodically protected, and the Cu can corrode.

Polarization Results

Figure 6 shows a set of polarization charging curves, at the C rate, for spectroelectrochemical cells with electrodes from virgin and selected tested cells. The polarization in the cells with the electrodes from the tested cells is considerably higher. There is considerable scatter in the data. The general trend is increased polarization in electrodes from cells tested at higher states of charge and long times.

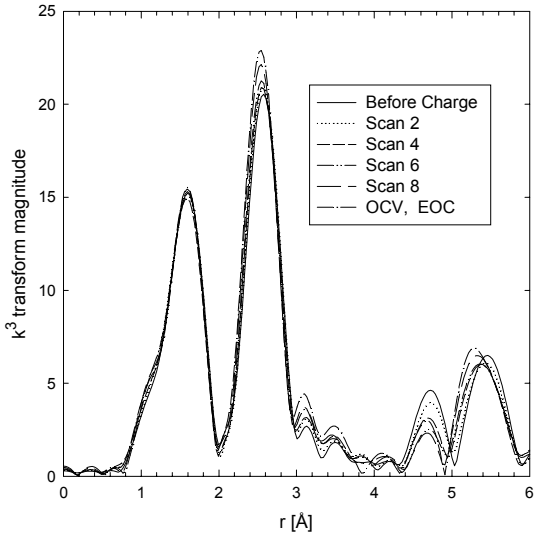

Figure 5. Fourier transform of *in situ* Co EXAFS for a cathode from a tested cell charged at the C/5rate. Cell had been cycled at 80% SOC with a 9% ΔSOC at 70°C for 2 weeks. The last scan (OCV, EOC) was taken on open circuit after the end of charge.

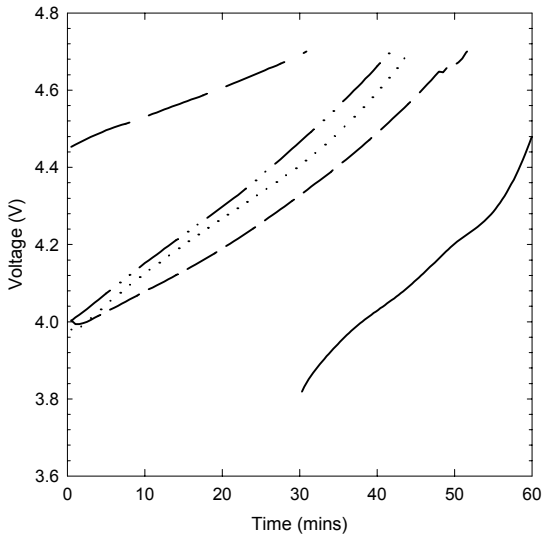

Figure 6. Charging curves for spectroelectrochemical cells with Li foil anodes when charged at the C rate. (a) fresh cell charged from 50% SOC (—), (b) cell at 60% SOC with a 9% ΔSOC at 70°C for 2 weeks (– –), (c) calendar life cell at 60% SOC, 50°C for 8 weeks (····), (d) cell at 60% SOC with a 9% ΔSOC at 70°C for 2 weeks (— ·· —), (e) cell at 80% SOC with a 9% ΔSOC at 60°C for 8 weeks (— —).

The high polarization agrees with the EIS results in three-electrode cells and indicates that the high polarization is associated with the cathode. All of the results are consistent with a resistive coating on either the current collector or on the surface of the active material particles. The power fade is not related to bulk decomposition of the cathode active material.

Publications

1. M. Balasubramanian, X. Sun, X. Q. Yang, and J. McBreen, "*In situ* x-ray diffraction and x-ray absorption studies of high rate lithium-ion batteries," *J. Power Sources*, accepted.

2. M. Balasubramanian, X. Sun, X. Q. Yang, and, J. McBreen, "*In situ* x-ray absorption studies of a high rate $Li_{1-x}Ni_{0.85}Co_{0.15}O_2$ cathode material," *J. Electrochem. Soc.,* accepted.

C. Diagnostic Studies on Gen 1 Cells and Cell Components

Khalil Amine, Jun Liu, Chunhua Chen, Jong Sung-Hung, Jian Shu Luo, and Gary Henriksen
Argonne National Laboratory, Argonne, IL 60439
(630) 252-3838; fax (630) 252-4176; e-mail: amine@cmt.anl.gov

Jai Prakash
Illinois Institute of Technology, Chicago, IL 60694
(312) 567-3639; fax (312) 567-8874; e-mail: prakash@iit.edu

Objectives

- Develop alternative diagnostic techniques for use in identifying and understanding the parameters operative in the Gen 1 cell chemistry that limit calendar life and abuse tolerance.
- Apply these techniques to Gen 1 cells and cell components to identify the most effective techniques for cell performance analysis.
- Correlate results with those from other diagnostic laboratories to establish the mechanisms that limit calendar life and abuse tolerance in the Gen 1 cell chemistry.

Approach

- Perform quantitative and qualitative analyses of gases generated in 18650 Gen 1 cells during formation and accelerated calendar and cycle life testing (accelerated aging tests).
- Perform quantitative and qualitative analyses of electrolyte composition changes during accelerated aging tests.
- Perform reference electrode studies to identify where, and to what extent, the increases in the impedance occur during accelerated aging tests.
- Investigate the effect of current collector corrosion on cell impedance.
- Evaluate the film growth at the surface of the positive and negative electrodes, and correlate the growth with the increases in the electrode impedance.

Accomplishments

- Identified all the gases generated during the formation process and after accelerated calendar life and cycle life testing of Gen 1 cells. CO_2 and CO gases were the only gases generated during the aging of Gen 1 cells, due possibly to a decomposition of the passivation film at the negative electrode at elevated storage temperatures.
- Identified the compositional changes in the Gen 1 electrolyte using HPLC and NMR. No significant changes were observed in the concentration of EC and DEC after accelerated aging tests.
- Identified the product of trans-esterification reaction as diethyl-2,5-dioxan-hexandioate (DEDOHC). The amount of DEDOHC was around 5 wt % in the Gen 1 electrolyte, regardless of cell SOC and test temperature.

- Developed and used a stable micro-reference electrode for identifying the electrode responsible for the impedance rise in aged Gen 1 cells. The positive electrode was found to be responsible for the bulk of the impedance rise in Gen 1 cells.

- Identified the source of impedance rise in the positive electrode, via AC impedance in symmetrical cells. The charge transfer resistance at the electrode interface is the main cause of impedance rise in the positive electrode.

- Evaluated and visualized the film growth at the surface and grain boundaries of the positive active material particles, via HR-TEM.

- Confirmed the presence of aluminum substrate corrosion at the positive electrode current collector and investigated its effect on impedance rise in the cell.

Future Directions

- Continue to develop diagnostic tools that facilitate:
  - A better understanding of the passivation film formation mechanisms operative at the respective electrodes.
  - An understanding of the cause of the impedance rise in the positive electrode during cycling.
  - Understanding and prediction of the behavior of Gen 1 cells during thermal runaway.
  - Isolation of the sources of thermal runaway.

- Apply diagnostic techniques to Gen 2 cell chemistry to understand how and why it performs differently in the critical areas of calendar life and abuse tolerance.

- Provide feedback to the Gen 3 materials development project, to assist in tailoring new materials that solve or mitigate the calendar life and abuse tolerance problems.

Introduction

The goal of the diagnostics project is to develop a thorough understanding of the phenomena that limit the performance, calendar life, and abuse tolerance of the high-power Li-ion cells that employ the Gen 1 baseline cell chemistry. The approach pursued by ANL involves: (1) understanding the electrolyte/electrode surface reactions that generate gases and lead to electrolyte compositional changes, (2) monitoring and isolating the electrode responsible for the cell impedance rise during accelerated aging, (3) identifying the source of the impedance rise within the electrodes, (4) evaluating via HR-TEM any reactions at the surface or grain boundaries of the active particles, (5) identifying the existence of micro-cracks and modulation within the active particles, and (6) identifying the sources of current collector corrosion and studying its effect on cell impedance

Gas Generation and Electrolyte Decomposition

An experimental cell puncture and gas collection fixture was developed by ANL to collect and quantify the gases generated in Gen 1 cells during their formation and accelerated aging tests. The gases collected from the cells after operation were then analyzed qualitatively by GC-MS. It was found that during the formation process, the bulk of the gases (>85%) are generated at the negative electrode, which is associated with electrolyte reduction and formation of the solid-electrolyte interface (SEI) layer. These gases are mainly hydrocarbon gases, such as C_2H_6, CH_4, C_2H_2, C_2H_4 and a very small amount of CO_2. After accelerated calendar and cycle life testing at different temperatures and SOCs, the amount of hydrocarbon gases formed initially remain stable, while the amount of CO_2 and CO increase with the increased aging temperature. Figure 1 compares the gas composition from a control cell, subjected only to

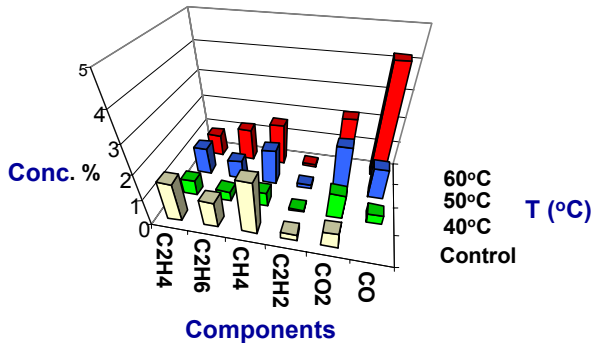

Figure 1: GC-MS analysis data on Gen 1 cell gases obtained from a control cell, subjected to the formation process at 25° C, and a cycle life tested cell (80% SOC) at different temperatures.

the formation process at room temperature and a cycled Gen 1 cell subjected to accelerated cycle life testing at 80% SOC at different temperatures. The amount of CO_2 and CO increased with increasing temperature of testing, but the overall concentration of these gases was less than 4 vol %. The small amount of CO_2 and CO gases could be due to the decomposition of the SEI layer at the negative electrode during elevated temperature testing. This result corroborates the instability of the SEI layer observed at elevated storage temperatures.

Figure 2 shows an example of the changes in Gen 1 electrolyte after accelerated calendar life testing at 60% SOC and different temperatures, using HPLC. The concentration of EC and DEC solvents decreased slightly due to a possible trans-esterification and/or surface reactions with the

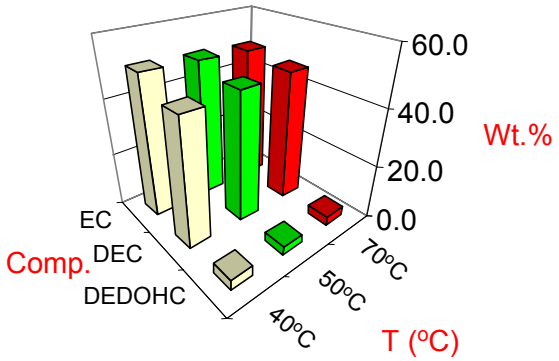

Figure 2. HPLC analysis data on electrolyte samples from Gen 1 cells subjected to accelerated calendar life tests at 60% SOC and different temperatures.

electrodes. The trans-esterification product, which corresponds to diethyl-2,5-dioxan-hexandioate (DEDOHC), was less than 4 vol % regardless of SOC and aging temperature. The overall observed changes in the electrolyte were small, and not likely to be responsible for cell performance degradation during the accelerated aging tests.

Reference Electrode, AC Impedance, and HR-TEM Studies

The micro-reference electrode used in this case was a 25-µm copper wire, insulated by a 3-µm layer of polyurethane enamel. The role of the insulation layer is to prevent any mixed potential along the length of the wire during the study. The insulation layer was stripped from the tip of the wire using a stripping solution, and a tin layer (1-µm thick) was electroplated onto the exposed copper tip. This micro-reference electrode was then placed between two separator membranes to insulate it from both electrodes. After cell assembly, the tin plated wire tip was charged with lithium from the positive electrode, using only a negligible quantity of active lithium (about 200 □A min). Figure 3 compares the area specific impedance (ASI) values obtained on electrodes during the 18s discharge pulses. The cells employed positive and negative electrodes from both fresh and aged cells, where the aged cell was subjected to calendar life testing at 60% SOC and 70° C. The ASI of the cathode and anode were calculated based on the potential change at each electrode, relative to the LiSn reference electrode,

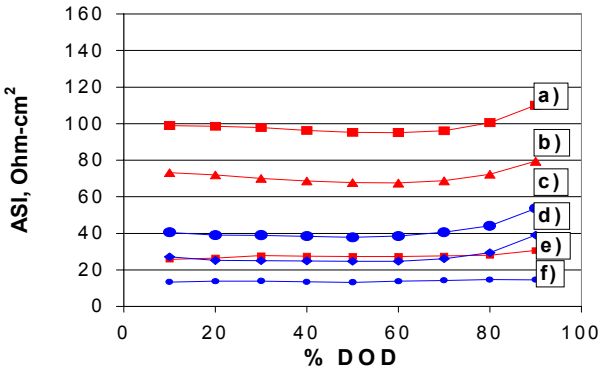

Figure 3. Area specific impedance of: a) aged cell, b) aged positive electrode, c) fresh cell, d) fresh positive electrode, e) aged negative electrode and f) fresh negative electrode.

resulting from the current pulse. The reference electrode was very stable, and its potential didn't drift after repeated HPPC pulse cycling (over 4000 cycles). ASI data from the fresh cell electrodes, subjected only to the room temperature formation process, show that the bulk of the cell impedance resides with the positive electrode (Figure 3d). After being subjected to accelerated calendar life testing for a period of two weeks at 60% SOC and 70° C, the cell ASI increased significantly from 40 ohm-cm^2 in the fresh cell (Figure3c), to 100 ohm-cm^2 in the aged cell (Figure 3a). The bulk of the impedance rise in this case is due mainly to the positive electrode, as clearly indicated from the comparison of the ASIs of the fresh (Figure 3d) and aged (Figure 3b) positive electrodes. The increase in the ASI of the aged negative electrode (Figure 3e) is not significant when compared to the ASI of fresh negative electrode (Figure 3f). To understand the cause of the impedance rise at the positive electrode, we compared the AC impedance of two symmetrical cells, made from two symmetric positive electrodes taken from either fresh or aged cells. The positive electrode symmetrical cells were built by taking positive electrodes from two identical normal cells that has been aged. The two cells were aged at the same 60% SOC and 70°C, disassembled, and then the positive electrodes of both regular cells were reassembled as one symmetrical positive electrode cell. Figure 4 compares the AC impedance of symmetrical positive electrode cells made using fresh electrodes, after one cycle (Figure 4a), and the aged positive electrodes (Figure 4b). The semi circle at medium frequency, which corresponds to lithium transport at the interface between the liquid electrolyte and the positive electrode surface, i.e. a charge transfer resistance, increases significantly after accelerated calendar life testing. Therefore, the impedance rise of the high power 18650 cell is mainly due to the charge transfer resistance at the positive electrode.

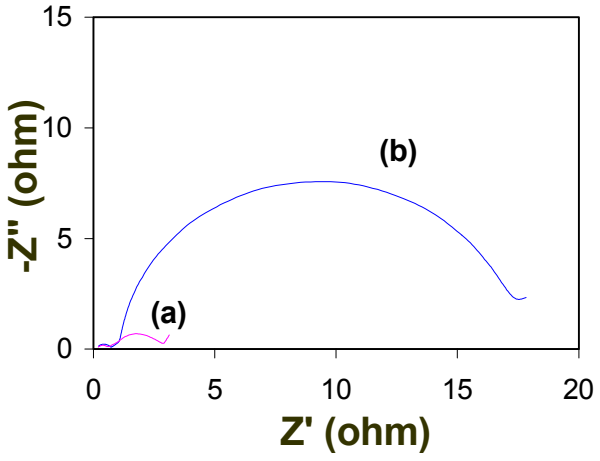

Figure 4. AC impedance spectra of symmetrical positive cells made of (a) fresh electrodes and (b) aged electrodes subjected to calendar life testing at 70° C.

Initial work using High Resolution Transmission Electron Microscopy (HR-TEM) on a cross sectioned positive-electrode particle (Figure 5), indicates the formation of a thick amorphous film at the surface, and at the grain boundaries between primary particles of the active positive material. The presence of this thick film at the surface of these particles could well be responsible for the increase in the interfacial resistance observed at the aged positive electrodes. Also, initial cracking and structural stress were observed in the bulk of the particles themselves.

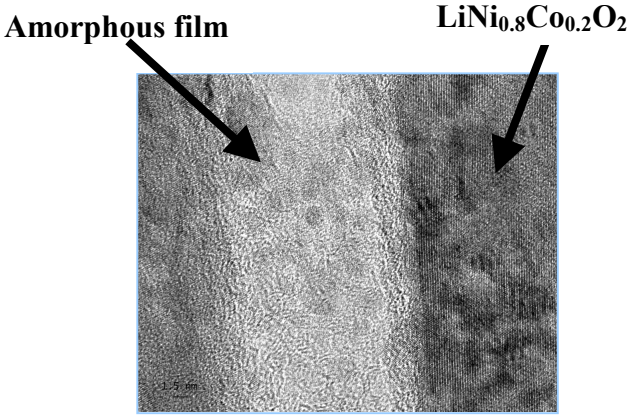

Figure 5: HR-TEM of a calendar life tested positive electrode showing amorphous film formation at the grain boundary of the particles.

Future Work

Diagnostic studies of this type will be continued and expanded to include powerful surface characterization techniques such as XPS, and Auger electron in order to identify and understand the mechanisms that control the calendar life and abuse tolerance of the Gen 1 cell chemistry. When the Gen 2 cells become available, the most useful and informative techniques will be utilized to understand

how and why these cells perform differently from the Gen 1 cells in the critical areas of calendar life and abuse tolerance.

List of Publications

1. K. Amine and J. Liu, "Development of High-Power Lithium Ion Batteries for Hybrid Vehicle Application," *ITE Letters*, **1** (1), B39 (2000).
2. K. Amine, J. Liu, A.N. Jansen, A Newman, D. Simon, and G.L. Henriksen, "Development of High Power Lithium Ion Batteries for Hybrid Vehicle Application," *Intercalation Compounds for Battery Materials Book*, edited by The Electrochemical Society Inc., Vol. 99-24, pp. 389-399 (2000).
3. K. Amine, M.J. Hammond, J. Liu, C. Chen, D.W. Dees, A.N. Jansen, and G. L. Henriksen, "Factors responsible for the Impedance Rise in High Power Lithium Ion Batteries," J. Power sources, (in press 2000).
4. C. H. Chen, J. Liu, and K. Amine, "Symmetric Cell Approach and Impedance Spectroscopy of High Power Lithium Ion Batteries," J. Power Sources, (in press, 2000).
5. C. Chen, J. Liu, and K. Amine, "Symmetric Cell Approach Towards Simplified Study of Cathode and Anode Behavior in Lithium-Ion Batteries," Electrochem. Solid State Lett. (Submitted 2000).

D. Electrochemical Impedance Spectroscopy (EIS)

Ganesan Nagasubramanian
MS 0613 Sandia National Laboratories, Albuquerque, NM 87185
(505) 844-1684; fax (505) 844-6972; e-mail: gnagasu@sandia.gov

Objectives

- Identify cell component(s) that are most likely responsible for cell failure under a variety of conditions.
- Understand which of the electrochemical/transport properties of the cell components limit cell performance.

Approach

- Develop three-electrode in-situ EIS technique, and measure anode and cathode electrode impedances under different conditions.
- Collect cell impedance values at different cell voltages and after various life test environments.

Accomplishments

- Measured cell impedances in two- and three-electrode modes on Gen 1 cells subjected to different temperature conditions. Recorded full frequency impedance spectra for all Gen 1 life test cells at SNL.
- Determined that cell impedance increases as the cell ages - especially at higher temperatures- and the metal oxide cathode is responsible for most of the impedance increase, which in turn leads to premature cell failure.
- Determined that interfacial resistance at the cathode/electrolyte interface is responsible for impedance increase and consequently for power loss; diffusional impedance for Li^+ inside the cathode lattice is virtually absent.
- Observed a "U" shape behavior of low frequency (10 mHz) impedance at different cell voltages. The impedance is lowest between 3.5 and 3.8 V and increases on either side. For a fresh cell the impedance at 4.1V (fully charged) is lower than that at ~3 V (fully discharged).
- Observed that the aged cells also show a "U" shape impedance behavior with cell voltage, and the impedance is generally higher than for the fresh cells. Further, for the aged cells the impedance at 4.1 V is higher than that at ~3 V.
- Found that Ohmic resistance is negligible compared to the interfacial resistance, and does not increase significantly with aging.

Future Directions

- Continue two- and three-electrode impedance studies on Gen 2 cells subjected to calendar and cycle life studies.
- Measure cell impedance at different states-of-charge and at different temperatures.
- Predict – based on the impedance results – the most favorable potential and temperature window in which to operate the cell for power and cycle life.

Impedance Characteristics of Gen 1 18650 Li-ion Cells

We continue to measure cell impedance under a variety of conditions for the ATD program, as part of the diagnostic study on Gen 1 Li-ion cells. The Gen 1 cells contain an MCMB carbon anode, and a $LiNi_{0.85}Co_{0.15}O_2$ cathode (the cathode composition was measured at SNL and is described in the diagnostic section). Standard electrochemical equipment was used to perform impedance measurements. We performed the 3-electrode (the third electrode being a Li reference electrode) impedance measurements to locate more accurately the source of impedance increases, especially at lower temperatures, and to correctly assign the two loops typically seen in the NyQuist plots, to the anode and cathode. The Gen 1 cell was opened to accommodate the Li reference electrode in the mandrel hole that runs along the length of the cell at the center. Both the bottom and the top of the cell were carefully cut open in a glove box with a Dremel tool and tabs were subsequently attached to the anode and cathode for electrical contacts. The construction of the reference electrode is described elsewhere.[1]

Initially, 2-electrode impedance measurements were made at different temperatures and two OCVs. Figure 1 shows a typical NyQuist plot for the Gen 1 cell at 25°C and 3.935 V.

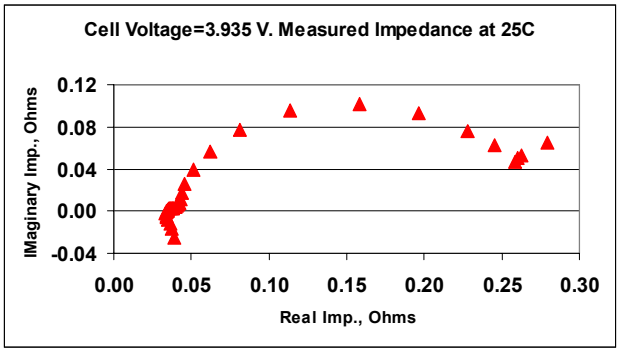

Figure 1. NyQuist Plot of a Fully Charged Gen 1 Li-ion cell at 25°C.

As we have seen before for the Sony cells, the plot exhibits an inductive tail followed by a small loop and a larger loop. The high frequency intercept at the x-axis corresponds to the ohmic cell resistance, and occurs at around 1kHz. Table 1 contains the high and low frequency (10 mHz) resistance values for two of the Gen 1 cells subjected to life test at two temperatures.

Condition	Tested after	~1000 Hz resistance (ohms)	10 mHz resistance (ohms)
Initial		0.027	0.137
70C	1st 2-week	0.033	0.327
70C	2nd 2-week	0.033	0.369
70C	3rd 2-week	0.038	0.329
Initial		0.036	0.126
40C	1st 1-month	0.032	0.198
40C	2nd 1-month	0.032	0.177

Table 1. High and low frequency resistances for Gen 1 cells tested at 6% ΔSOC and two temperatures. Impedance was measured at RT and ~4.1 V.

The life testing at different temperatures did not seem to increase the high frequency resistance of the Gen 1 cells, however, the low frequency resistance increased significantly. Similar results were obtained at 50°C and 60°C and for other ΔSOCs.

Figure 2 shows similar NyQuist plots at 0°C and -10°C. These plots indicate that the ohmic resistance of the cell remains almost constant, while the total cell impedance (low frequency x-axis intercept) has increased considerably.

Although the 2-electrode measurement indicates that the interfacial impedance dominates the cell impedance, especially at lower temperatures, it doesn't tell us whether it is the anode or the cathode electrode/electrolyte interface impedance that is responsible for the increase. To identify which electrode is the cause for the impedance increase, we carried out 3-electrode impedance studies as described in reference 1. Figure 3 shows NyQuist plots for the anode, cathode, and full cell impedance (measured in 2-electrode mode) of the opened cell at room temperature.

The plots clearly show that the impedance of the anode/electrolyte interface is lower than the cathode/electrolyte interface, which dominates the overall cell impedance. Further, both electrodes

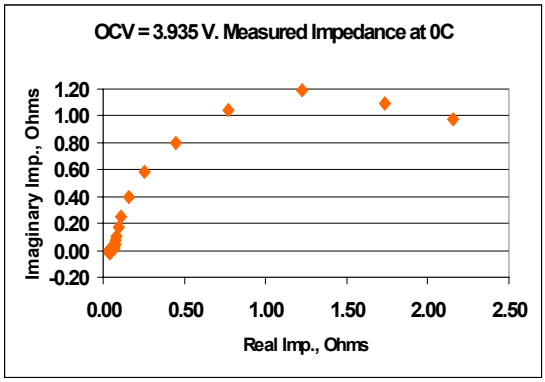

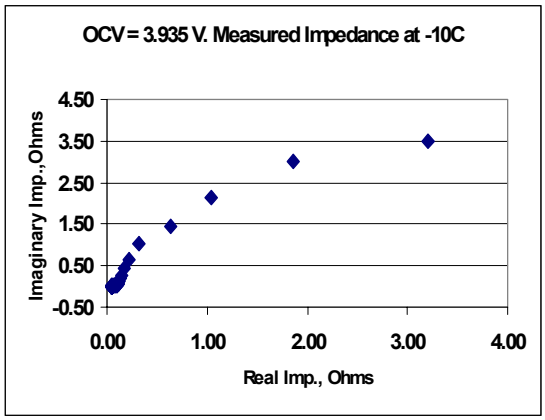

Figure 2. NyQuist Plot of a Gen 1 Li-ion cell at 0°C and -10°C.

contribute to both the loops, with the cathode contributing the most to the second loop. Similar trends in 3-electrode impedance results were obtained on cells opened at ~4.0 V. Our 3-electrode impedance data very clearly indicate that:

1) both the anode and the cathode contribute to the two loops and
2) the cell impedance comes mostly from the cathode/electrolyte interface and not from the anode/electrolyte interface.

This type of behavior was also observed with Sony, Panasonic, A&T, and Moli cells.

To verify if the cathode impedance dominates the cell impedance at other cell voltages we collected impedance data at several cell voltages. It is beyond the scope of this study to cut open several 18650 cells, adjusted to voltage beforehand, to make 3-electrode measurements. So we assumed that the low frequency cell impedance obtained on the unopened (2-terminal) cell was equal to the cathode

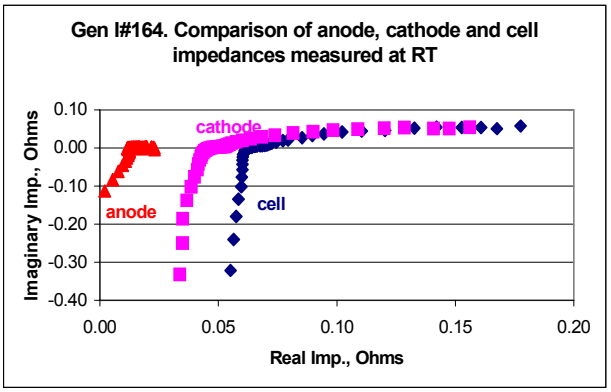

Figure 3. NyQuist Plots of impedances for the anode, cathode and the full cell at RT and 3.3 V.

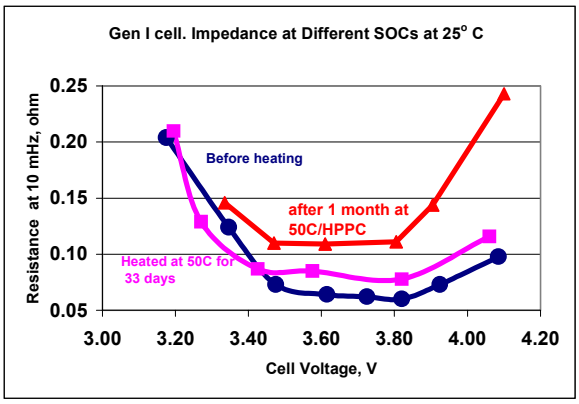

Figure 4. Low Frequency (10 mHz) Impedance at RT for different cell voltages. ●= before heating; ■= after heating at 50°C for 33 days and ▲= after cycle life test at 50°C for one month.

impedance. Figure 4 shows the low frequency (10 mHz) resistance at several cell voltages.

The resistance of the $LiNi_{0.85}Co_{0.15}O_2$ is lowest in the voltage range 3.5 - 3.8 V and increases on either side of this range. The plot suggests that the impedance variation mirrors the variation of one or more of the cathode electrochemical properties. The limiting electrochemical property is accentuated at lower temperatures. Therefore, we performed impedance measurements at sub-ambient temperatures with a view to identify the limiting property. Figures 5, 6, and 7 show NyQuist plots at four temperatures for each of three different cell voltages (3.18 V, 3.50 V, and 3.93 V). In each figure the NyQuist plots in clockwise direction (starting from the upper left) represent impedance plots at 35°C, 25°C, 0°C, and -10°C.

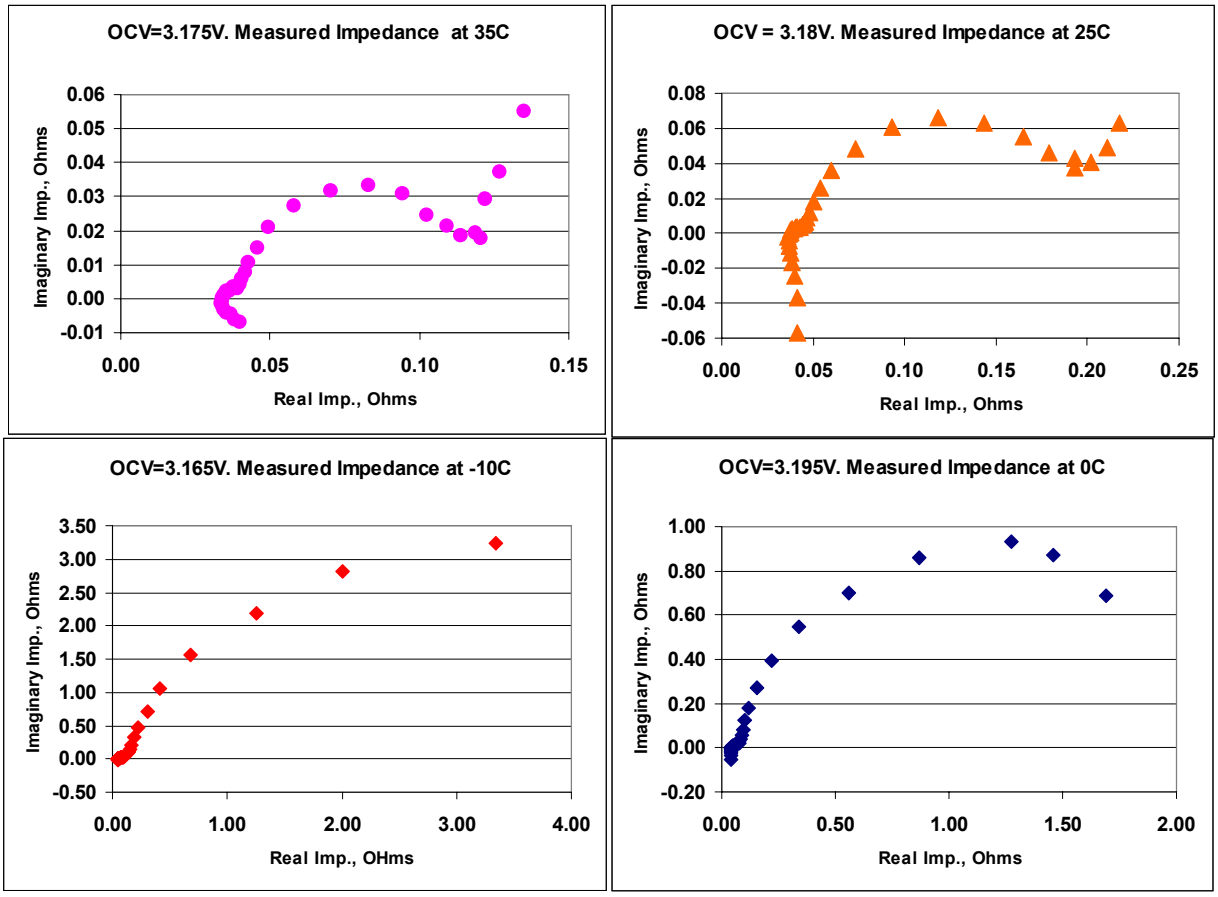

Figure 5. NyQuist plots for Gen 1 cell at 3.18 V as a function of temperature.

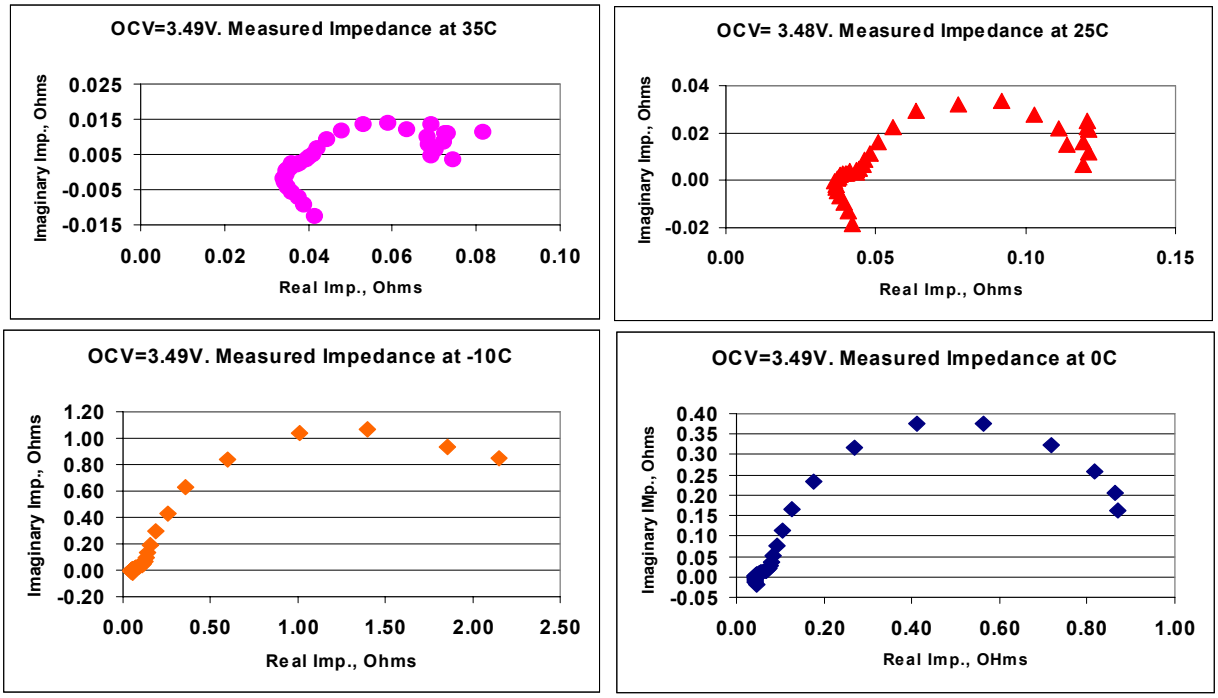

Figure 6. NyQuist plots for Gen 1 cell at 3.5 V as a function of temperature.

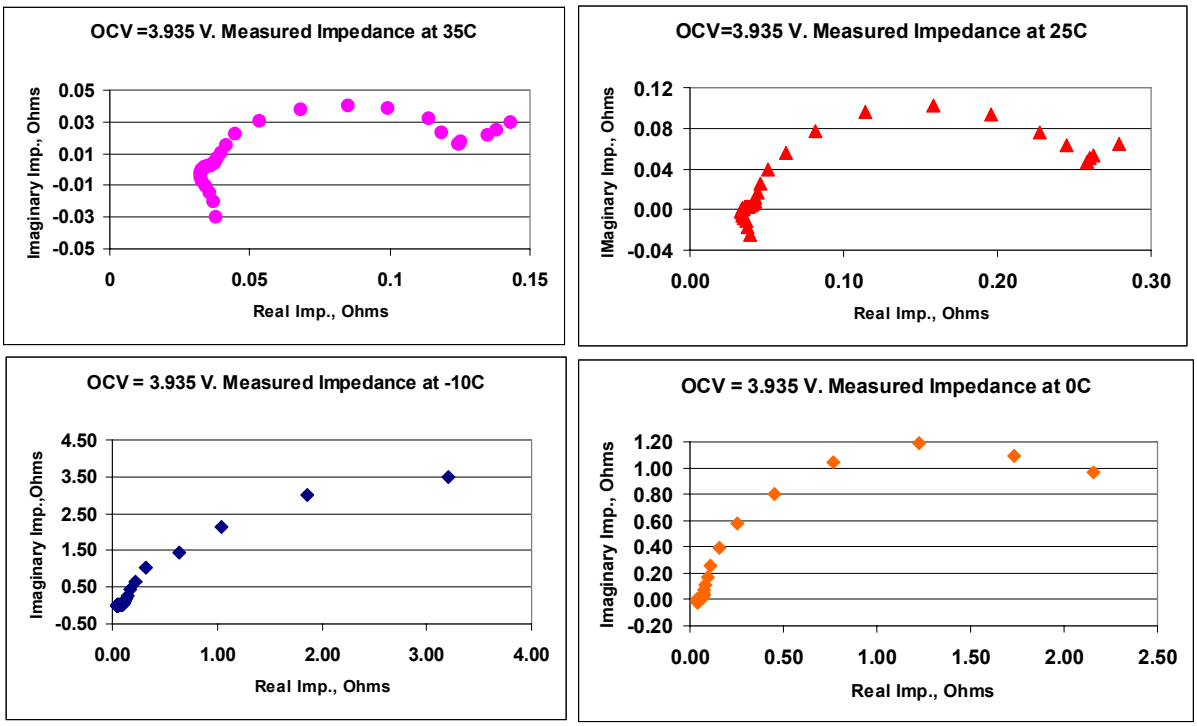

Figure 7. NyQuist plots for Gen 1 cell at 3.93 V as a function of temperature.

Figure 5 shows cell impedance plots at ~3.18 V. The diffusional line at 35°C and 25°C are clearly visible. However, at 0°C and -10°C they are not visible due to the preponderant effect of the interfacial resistance. Figure 6 shows NyQuist plots at 3.5 V. The diffusional lines at all the temperatures are diminished or completely absent. However, the interfacial loop can be seen at all the temperatures. Figure 7 shows similar plots at 3.93 V. The plots show similar behavior to the plots in Figure 5.

The impedance behavior at these three cell voltages can be explained considering the variation of the a- and c-axes at several cell voltages. The variations of the axes, as a function of cell voltage, are shown in Figure 8. While the a-axis decreases continuously, going from low to higher cell voltages, the c-axis goes through a maximum at intermediate cell voltages and rolls off at both ends.

In the voltage regime, where the c-axis is largest, there is apparently no contribution to the cell impedance from Li^+ diffusion inside the cathode lattice, (Figure 6) and where the c-axis is smaller the cell impedance shows contribution from Li^+ diffusion inside the cathode lattice (Figures 5 and 7).

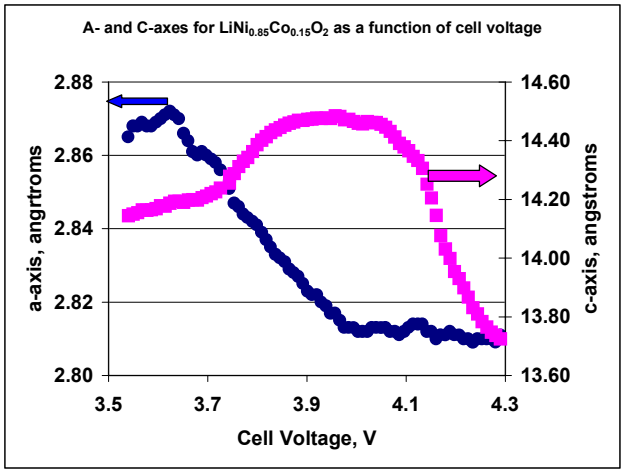

Figure 8. Hexagonal lattice constants, a and c, of $LiNi_{0.85}Co_{0.15}O_2$ as a function of cell voltage vs. Li^+/Li.

However, the cathode interfacial resistance is present at all voltages and temperatures, and dominates the cell impedance.

RPT vs. a-c Impedance Data

Table 2 is the impedance data collected for Gen 1 cell #124 at room temperature before and after each Reference Performance Test (RPT). This cell

was cycled at 70°C and every two weeks the cell was taken off life test to perform RPT and impedance measurements at room temperature.

Condition	~1000 Hz resistance (ohms)	10 mHz resistance (ohms)
Fresh	0.031	0.077
After RPT1	0.036	0.278
After RPT2	0.041	0.289
After RPT3	0.041	0.303
After RPT4	0.065	0.344

Table 2. Real Impedance data for Cell 124 at ~4.1 V.

The high frequency impedance increases only very modestly going from fresh to RPT3 and finally to 0.065 ohms, roughly twice the value at fresh. However, the low frequency impedance increases with each RPT. Further, there is a precipitous increase in impedance between the fresh and RPT1 followed by modest increases at other RPTs. The fully charged cell was subjected to a 7.2 A current pulse for 18 seconds and the cell voltage was monitored to compute the area specific impedance (ASI) which is a time-dependent parameter. The traces show a significant difference in cell performance between the fresh and RPT1 and a modest change after that. The ASI calculated from the RPT measurements are 51 ohm·cm^2, 82 ohm·cm^2, for the fresh and RPT1 respectively and between 90-94 ohm·cm^2 for the rest. This trend is very similar to that observed in the impedance data – a large initial increase in cell impedance followed by a modest impedance increase.

Conclusions

2- and 3-electrode impedance studies were made on Gen 1 cells at different temperatures ranging from 35°C to -10°C. Although the ohmic resistance remains almost constant, the total cell resistance increases by a factor of 10 at -10°C compared to that at 25°C. The increase in cell impedance comes mostly from the cathode/electrolyte interface as shown by our 3-electrode study. Further, the high temperature testing of the cells seems to have a negligible impact on the ohmic resistance and significant impact on the low frequency resistance. This increase in cell resistance leads to power loss and performance degradation. The impedance values obtained from the RPT and a-c impedance studies show a similar trend in impedance values.

Acknowledgments

Sandia National Laboratories is a multiprogram laboratory operated by Sandia Corporation, a Lockheed Martin Company, for the United States Department of Energy under contract DE-AC04-94AL85000.

Reference

1. G. Nagasubramanian, J. Power Sources 87 (2000) 226.

E. Diagnostic Techniques: Gas/Electrolyte/Cell Component Analysis

Rudolph G. Jungst, Ganesan Nagasubramanian, Chris C. Crafts, and Theodore T. Borek
MS 0613 Sandia National Laboratories, P.O. Box 5800, Albuquerque, NM 87185
Contact: R. G. Jungst, (505) 844-1103; fax (505) 844-6972; email: rgjungs@sandia.gov

Objective

- Understand the mechanisms of performance degradation and interactions of cell components under a variety of conditions.

Approach

- Develop a suite of analytical techniques and postmortem analysis methods aimed at identifying the generated gas products, and measuring gas leak rates, electrolyte breakdown products, electrode delamination, binder breakdown products, etc. The following analytical techniques are either being used or will be evaluated for analysis of the reaction products or breakdown of cell components:
  - Gas analyses: GC, GC/MS, helium leak detection, etc.
  - Electrolyte decomposition: IC, GC, GC/MS, LC/MS
  - Cathode or current collector dissolution: ICP-MS
  - Electrode delamination: visual inspection
  - Separator breakdown: flow porometry
  - Binder breakdown: GPC

Accomplishments

- A procedure for measuring leak rates of 18650 Li-ion cells was evaluated on both Sony and Gen 1 product as part of a general seal analysis. The method was refined and then applied to estimate actual leak rates for the Gen 1 cells at both ambient and elevated temperatures. Laser welded seals were recommended for Gen II cells.
- Electrolyte samples were collected from 10 Gen 1 ATD baseline cells and analyses of both the salt and organic solvent were carried out. High $LiPF_6$ concentrations and indications of solvent reaction were found.
- Inductively coupled plasma-mass spectroscopy (ICP-MS) was applied to both electrolyte and electrode samples from Gen 1 cells to look for evidence of cathode dissolution and migration of current collector materials. Initial results show little dissolution after short aging times.
- ICP-MS measurements of lithium content were also made on Gen 1 anodes and cathodes to confirm that the SOC range for cycling had not changed significantly after aging.
- A postmortem procedure for 18650 lithium-ion cells has been successfully applied to Gen 1 samples for observation of the condition of cell components and recovery of electrode and separator samples for analyses.
- Delamination of cathodes from the aluminum current collector, and also anodes from the copper current collector, was observed in some thermally aged Gen 1 cells.

Future Directions

- Leak rate measurements on Gen 2 trial cells will be carried out to confirm seal quality.
- The properties of the binder materials in the Gen 1 cell and possible interactions with the electrolyte or its breakdown products (swelling, specific absorption, etc.) must be investigated.
- Measurements of cathode dissolution and migration will be extended to more highly aged Gen 1 cells.
- Analysis of separator samples for porosity changes after aging will be completed.

- Gel permeation chromatography method development for detection of binder breakdown will be concluded, and Gen 1 samples analyzed.
- Analytical methods will be implemented on the Gen 2 cells, as diagnostic samples become available.
- Studies focused on the SEI layers are being initiated.

Cell Leak Testing and Seal Analysis

Early in the life test experiments, evidence began to accumulate that ATD Gen 1 cells were not hermetic, especially after being exposed to high temperatures. Observations such as discoloration and salt deposits on the cell end caps, solvent odor after cell storage in a closed container, visible accumulation of liquid solvent, and weight loss after high temperature storage were all made at one time or another. However, these manifestations of leakage were seldom observed consistently. Sandia was requested to analyze the seals to see if a cause for the apparent leakage could be determined.

Gen 1 and Sony cells were studied for leak behavior by analysis of disassembled parts and by He ingress tests on whole units. Both Gen 1 and Sony seals are of similar crimp construction. The bulk seal material in both is polypropylene, but the sealing film found by IR differs: Gen 1 uses poly(isobutylene) only while Sony uses a polyamide/rubber mix. Both seal types are affected by temperature.

Earlier oven testing on Sony cells showed a slight change in He ingress within hours, and significant change over several weeks at 70°C. In the later He ingress testing done on new condition Gen 1 cells, cells were exposed to He and directly evaluated at that same temperature. The leak rate of Gen 1 cells changed significantly from 25°C to 50°C, but less so from 50°C to 70°C, in a matter of hours (see Figure 1). Cells exposed at 70°C did not return to the same 25°C rate, but rather a new higher rate. From this work, using a Varian Leak Detector Turbo 959-50, and referring to related He bombing charts, we believe that the actual He leak rate through the Gen 1 seals increases from 1.0 x 10^{-6} std cc/sec to 1.0 x 10^{-5} std cc/sec when the cell goes from 25°C to 70°C.

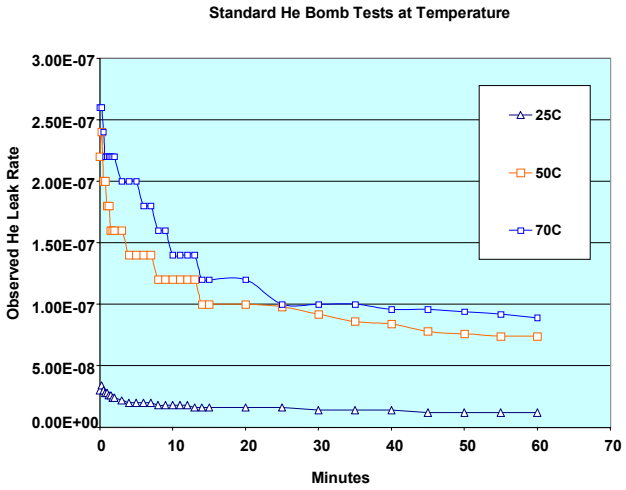

Figure 1. Observed He Leak Rate of a Gen 1 Li-Ion Cell at Different Temperatures

Electrolyte Decomposition

Decomposition of the electrolyte in lithium-ion cells is measured by two primary analytical methods: ion chromatography (IC) for the salt, and gas chromatography (GC) or gas chromatography/mass spectrometry (GC/MS) for the organic solvent. PF_6^- and F^- are quantified using a specialized IC method developed at Sandia for the ATD program, while Li^+ is measured by a standard IC technique. This allows the Li^+/PF_6^- ratio to be checked. The instrumental response for PF_6^- is shown to be linear over a wide range of concentrations. Sensitivity for F^- by this method is also good with a detection limit of as little as 6.6 mM in the undiluted electrolyte.

Electrolyte samples were recovered from a number of Gen 1 life test cells by centrifuging. Cells stored at 40, 50, and 70°C, cycled and uncycled, were sampled, as well as two control cells that had not been heated or cycled. Figure 2 shows the IC results.

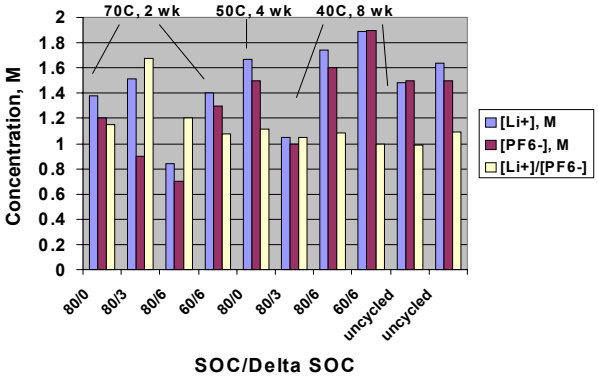

Figure 2. Electrolyte Salt Analysis Results for Gen 1 Li-Ion Cells

The Li^+ and PF_6^- concentrations are nearly the same, as expected, but in most cases the salt concentration is considerably above the nominal 1M at which the cell was built. The only significant discrepancy between the Li^+ and PF_6^- results is for one of the 70°C samples, while the highest overall salt concentrations occurred in 40°C samples. If the increased salt concentrations were due to loss of volatile solvent through leaks, this would be expected to be more noticeable at 70°C than at 40°C. Further evidence that leaks are not responsible for the higher $LiPF_6$ levels is found in the lack of correlation between salt concentration and weight loss, as shown in Figure 3. Small amounts of fluoride (17-89 ppm) were detected in most samples, but there was no consistent trend with the aging conditions.

Companion organic solvent analyses were performed on the same electrolyte samples by GC/FID. This allowed a quantitative analysis of both EC and DEC as well as some of their possible decomposition products. The results of the GC measurements are shown in Figure 4. While the EC/DEC ratio was elevated above 1, especially in the 70°C samples, the DEC response was essentially constant, not what would be expected from a loss through leaks at higher temperatures. Again, there

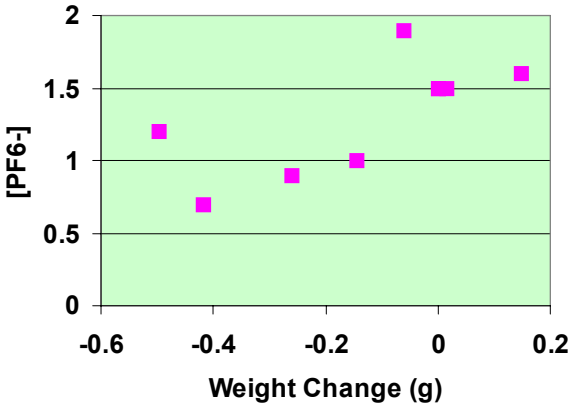

Figure 3. Comparison of PF_6^- Concentration with Cell Weight Change

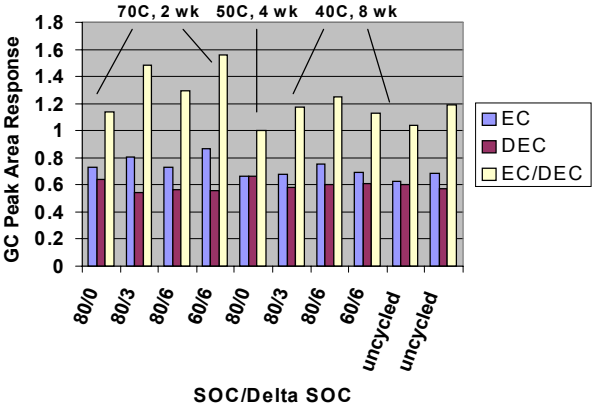

Figure 4. GC Analysis of Organic Solvents in Gen 1 Cell Electrolyte

was no correlation with weight change. Both EC and DEC peak area responses on the GC were significantly below what is observed for a bulk sample of electrolyte.

One possible reason for the observed results could be reaction of the solvents with other materials within the cell. This is supported by the observation of one significant new peak (as yet unidentified) in the gas chromatogram. However, this peak appears under all conditions, even in the control cells. Another explanation could be the selective retention of solvents within the electrode binder. PVDF is known to swell in the presence of battery electrolyte, but this behavior has not yet been studied in the context of the ATD program.

Cathode or Current Collector Dissolution

Analysis of the electrode materials and electrolyte by inductively coupled plasma/mass spectrometry (ICP/MS) enables the composition of these cell components to be tracked after various thermal treatments. The primary species of interest relate to the migration of metals from the cathode active material or from the current collectors to other parts of the cell. It is also possible to determine the lithium content of the cathode and anode materials by using this method.

Figure 5 shows the trace metals analysis of typical samples of anode and cathode material. The arrows indicate species of particular interest, namely Cu in the cathode and Al, Ni, and Co in the anode. The 250 ppm Cu concentration in the cathode is the largest of these. However, the largest impurity overall in the cathode is Fe (nearly 1300 ppm), which is an impurity in the lithium. All other metals present are at very low levels. Our initial conclusion is that metal migration is not significant after short storage times at elevated temperature.

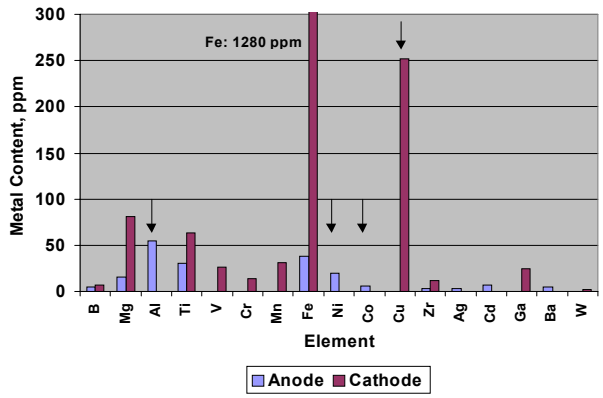

Figure 5. Metals Analysis of Gen 1 Cell Electrodes after Life Test at 70°C for 2 Weeks

A similar analysis was done on the 10 electrolyte samples collected from Gen 1 cells, and the results again showed very low levels of Al, Cu, Ni, and Co. The current collector metals were all less than 2 ppm except for one sample that had an upper limit for aluminum of 3.4 ppm. Nickel ranged from 0.4 to 8.3 ppm and cobalt was less than 0.1 ppm in most samples. These results are consistent with the low values found for the electrodes.

The lithium content of the anodes and cathodes was also determined in the same ICP-MS measurements. A sample of the Sumitomo mixed metal oxide powder was analyzed as a reference point, and was found to have a Ni/Co ratio of 85/15 rather than the nominal 80/20 that was expected. The Ni/Co ratio in Gen 1 cell cathode material was virtually the same as the powder. Figure 6 shows a comparison of the measured lithium content of the cathode with the amount expected for three cells opened at slightly different states-of-charge. The values agree closely for the three cells that were analyzed, although this test cannot distinguish whether all the lithium is capable of being cycled. X-ray diffraction measurements are being made to confirm whether any new phases are present in the positive active material. Preliminary indications are that the lithium content of the cathode has not shifted noticeably after aging.

Opened Cell Voltage	Aging Conditions	Cathode Lithium Content, Li_x	Estimated Li_x of Unaged Cell at Same SOC
3.48	60°C, 56 day	0.73	0.75
3.28	60°C, 4 weeks	0.82	0.81
3.42	70°C, 2 weeks	0.78	0.77

Figure 6. Lithium Content of Aged Gen 1 Cell Cathodes

Electrode Delamination

Visual observations of electrode delamination made during cell postmortems have been recorded. The database is still relatively small at this point, since complete disassembly has only been done on 12 cells. Instances of major delamination have been observed for both the anode and the cathode. Cells not showing delamination were mostly either unaged or stored at 50°C in the life test. Most of the opened cells that were stored at 70°C show major amounts of delamination. Therefore, the preliminary conclusion is that a positive relation exists between delamination and storage temperature. Information on observations of delamination is being collected from the other laboratories working on the ATD program to put together a more comprehensive picture of its occurrence.

Separator and Binder Breakdown

Separator porosity is influenced by elevated temperature, and complete shutdown should occur in the vicinity of 120 – 130°C. Characterization of the pore size of the separator can be done by using flow porometry and a trial measurement has been carried out on a sample of the virgin material to demonstrate this capability. Results are shown in Figure 7. The bubble point pore diameter indicates the largest detected pore and was 0.028 microns for this sample. Separator samples have been obtained from some of the life test cells and porosity measurements for these are in progress.

Breakdown of the polymeric structure of the binder should be detectable by dissolving the PVDF from an electrode and analyzing the material by gel permeation chromatography (GPC). Feasibility trials are still in progress for the GPC technique.

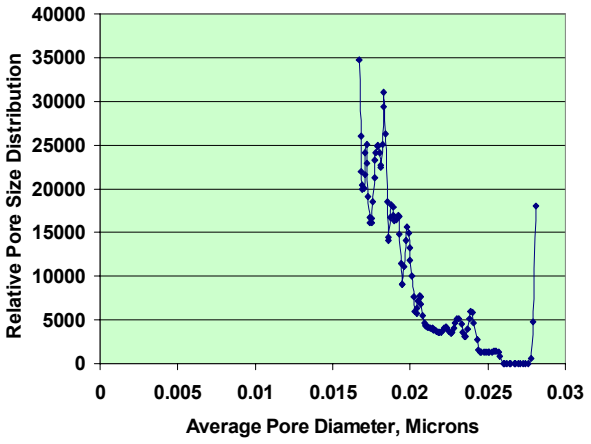

Figure 7. Capillary Flow Analysis of a Virgin Sample of the Gen 1 Separator

Future Work

Diagnostic measurements remain to be completed on the Gen 1 cells. This includes an investigation of the reasons for the high concentration of electrolyte salt found in both Sony and Gen 1 cells. Possible interactions or selective absorption of electrolyte constituents by the binder or other cell components will be studied. Measurements of the migration of current collector or cathode materials within the cell will be extended to samples that have been stored at elevated temperature for longer periods of time. Tests of separator porosity and binder breakdown must also be completed. Leak rate evaluations will be performed on Gen 2 trial cells as requested in order to confirm that the seals are indeed leak tight. The major diagnostics effort in the latter part of the next year will be to apply the developed techniques to analysis of the Gen 2 cells after they have been subjected to life tests.

Acknowledgements

The Sandia Analytical Laboratory supports the ATD program by performing headspace gas sampling and analysis, electrolyte analysis for organic and inorganic constituents, and inorganic analysis of cathode and anode materials. Specialized methods for determining the electrolyte salt concentration were developed by members of the Explosive Materials/Subsystems Department. Postmortems of lithium-ion cells and collection of component samples were done by the Sandia Lithium Battery R&D Department. We are grateful to the following individuals for performing the indicated analyses: T. T. Borek (GC/MS), S. E. Klassen and E. P. Boespflug (IC), J. E. Reich (ICP-MS), M. J. Russell (cell postmortem and leak rate measurements), and H. L. Case (postmortem sample collection and distribution).

Sandia National Laboratories is a multiprogram laboratory operated by Sandia Corporation, a Lockheed Martin Company, for the United States Department of Energy under contract DE-AC04-94AL85000.

4. DIAGNOSTICS
Abuse Tolerance

A. Development of an Abuse Tolerance Test Protocol with Continuous Gas Monitoring

Chris Crafts, Theodore Borek, Rudolph G. Jungst, Daniel H. Doughty, and Curtis Mowry
Mail Stop –0613, Sandia National Laboratories, P.O. Box 5800, Albuquerque, NM 87185
Contact: Chris Crafts (505) 844-5610; fax (505) 844-5924; email: cccraft@sandia.gov

Objective

- Develop comparative methods for studying the tolerance of lithium-ion cells to thermal abuse.

Approach

- Develop techniques to expose 18650 cells to thermal extremes in a controlled manner, and a safe environment. Do this in air while recording video as well as V, I, and T.
- Develop gas chromatographic and mass spectrographic methods to monitor emitted gases as 18650 cells are exposed to thermal extremes.
- Develop the above GC/TCD, GC/FID, and RGA/MS methods as supportive methods, paralleling the ARC, microcalorimetric, and DSC thermal tests done on 18650 cells and parts.

Accomplishments

- Performed thermal abuse tests on Gen 1 cells in air, demonstrating a lower onset of thermal runaway and an increased severity of the event, with increased cell state-of-charge. At a 1°C/min heat rate, these events occurred near and above 200°C.
- Repeated Gen 1 thermal abuse tests as a function of SOC in a safety bomb under a flow of helium gas. Identified CO_2, CO, CH_4, and residual DEC solvent as the major emitted gases during thermal runaway.

Future Directions

- Conduct thermal abuse tests on Gen 2 cells in air to look for improved abuse tolerance.
- Conduct thermal abuse tests on Gen 2 cells under helium to qualify and quantify the continuously emitted gases by GC/TCD, GC/FID, and RGA/MS.
- Identify hazardous gas products and recommend changes to further increase the thermal abuse tolerance of lithium-ion cells.

The primary objective of this project has been to develop and demonstrate experimental methods for studying the thermal abuse tolerance of Li-Ion 18650 cells. This led, in the first year of the program, to the development of a thermal abuse method in which an 18650 cell was placed in a custom-made copper block (Figure 1) and observed while being heated at 1°C/minute in air to 200°C. Both Sony and Gen 1 18650 cells have been tested this way. These remotely observed and recorded results, as visuals, support the other findings on the relative stabilities of Li-ion cells and their parts seen

through Sandia microcalorimetry, Accelerating Rate Calorimetry (ARC), and Differential Scanning Calorimetry (DSC). In this, the second year of the program, DOE has directed the Sandia R&D Team to concentrate more on understanding the basic changes in Li-ion chemistry during thermal abuse.

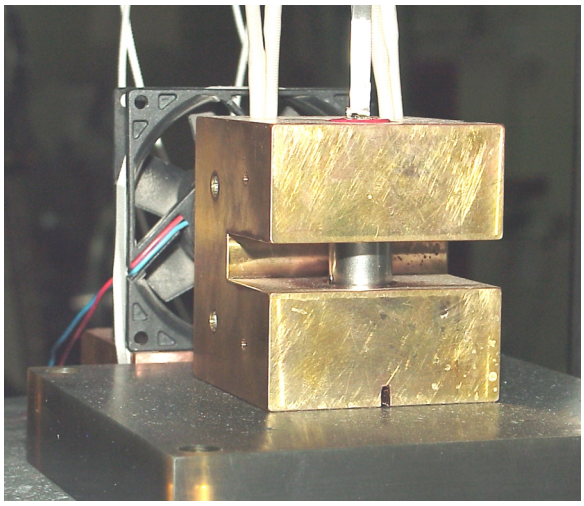

Figure1: Copper block for heating 18650 cells in air.

To support this DOE redirection, an enhanced effort is underway at Sandia. This effort, employing microcalorimetry, ARC, and DSC on whole cells and prospective cell parts, is reported separately in this volume. The remainder of this passage explains the augmentation of the copper block heating test with a test to continuously monitor the gases vented by the 18650 cell during thermal runaway.

Whole-cell ARC testing has shown itself to be an excellent way to monitor self-heating in 18650 cells from room temperature to 200°C. However, introducing a He gas flow through the ARC apparatus changes its heat flow parameters, and makes the results suspect. Using a helium gas flow around a cell is desirable as helium gas is non-reactive, and can be readily taken into a gas chromatograph (GC) or mass spectrometer (MS) to show the nature of vented gases, continuously, as they evolve. By moving a cylindrical copper block apparatus into a sealed Parr bomb, Sandia has been able to monitor an ARC-like heating event, and map the gases evolution.

The overall test setup is depicted in Figure 2. A helium flow of 610 cm^3/min was maintained around Gen 1 Li-ion cells which were heated at 1°C/min from room temperature to 200°C using a cylindrical, resistively-heated block isolated thermally from the bomb. Cell temperature and voltage were monitored as in air tests.

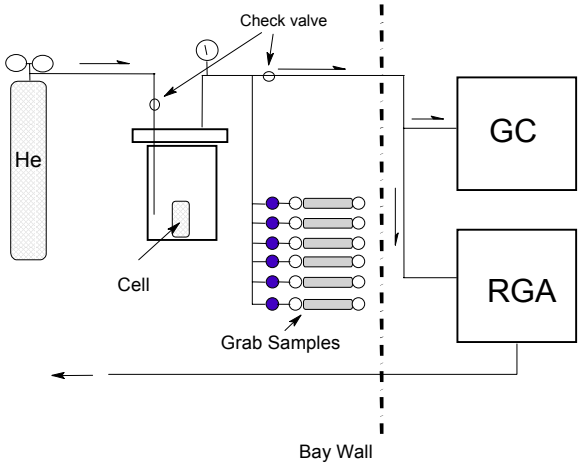

Figure 2: Parr Bomb Test Apparatus for Inert Atmosphere Thermal Abuse Tests.

Inert-atmosphere thermal abuse tests were conducted in a 2-liter Parr bomb (Parr Inst. Co., Moline, IL. MWP 1900). Evolved gases were sampled continuously out of the bomb exhaust loop with a Vacuum Technologies Inc. Aerovac residual gas analyzer (RGA) producing a full spectrum every 1.6 minutes, and every 10 minutes by a Varian 3400 dual column gas chromatograph (GC) equipped with thermal conductivity (TCD) and flame ionization detectors (FID). The TCD is useful for fixed gases and lightweight hydrocarbons while the FID is for general volatile organic species.

Additionally, six remotely actuated, evacuated 150-cc cylinders were positioned in parallel to the bomb exhaust line to capture or "grab" gas samples at different moments in the test for further GC and GC/mass spectrometry analyses.

Results

Thermal abuse tests in air

Thermal abuse testing as a function of SOC is reported here on Gen 1 cells where duplicate tests were run at 20%, 50%, and 80% SOC (Figure 3). For Gen 1 cells, the onset of thermal runaway occurred at a lower temperature and was more severe at higher cell SOC. Cells at lower SOC still fumed and were probably ignitable, but they did not autoignite, and they remained intact. Onset of thermal runaway by this method ranged between 190°C at 80% SOC and 225°C at 20% SOC.

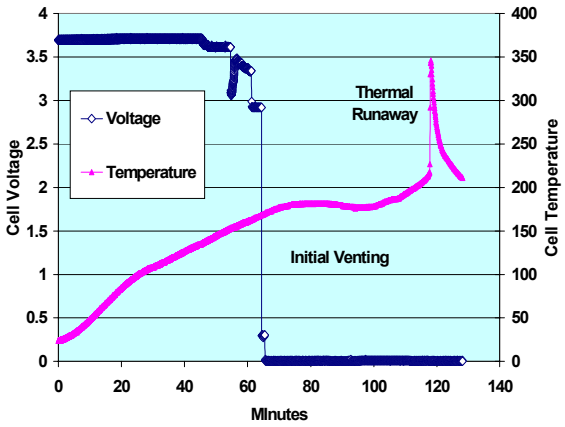

Figure 3: Heat Test on Gen 1 Cell at 20% SOC in air.

Thermal abuse tests under inert atmosphere

The GC and RGA instrument configuration permits real-time observation of gases vented from the cell as a function of temperature. The short duty time of the RGA permits fast evaluation of evolved gases. The GC duty cycle is slower (12 minutes), but will separate and analyze products that have similar mass, e.g., mass 28 species CO, N_2, and C_2H_4. Using this apparatus, it was possible to observe different gas evolution events during heating. A cascade plot of the fixed gas GC(TCD) results on a Gen 1 cell is shown in Figure 4. There was an initial cell-venting event that was observed, followed by major cell venting when thermal runaway occurred. Figure 5 shows a y-scale enlargement of the initial cell venting data. The organic GC(FID) results also showed the initial and major venting occurrences. One organic GC chromatogram is shown in Figure 6. There were many organic gas products, with the principal species observed being methane, ethylene, ethane, and propylene. Higher organic C_4 and C_5 compounds were also observed.

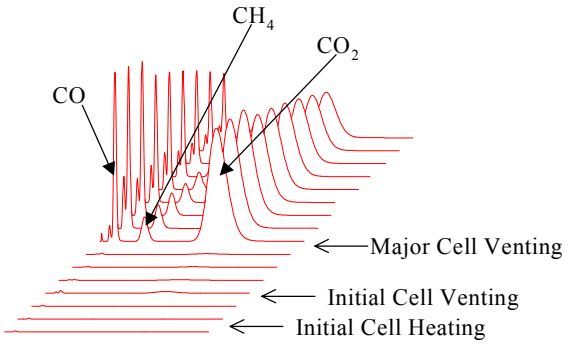

Figure 4: Fixed Gas GC Results. Gen 1 cell at 80% SOC.

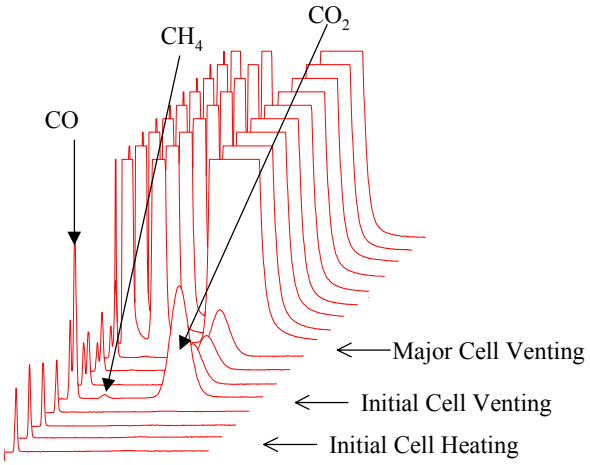

Figure 5: Enlargement of Initial Vent, Fixed Gas GC Results. Gen 1 cell at 80% SOC.

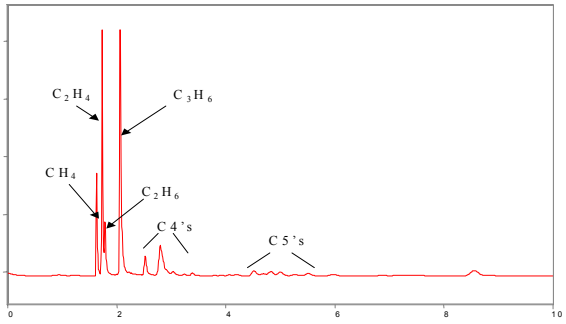

Figure 6: Thermal Abuse Organic Gas Chromatogram, mid-test. Gen 1 cell at 80% SOC. DEC elutes at 12 minutes.

Several mass spectral traces collected during the initial and major vent occurrences are shown in Figure 7. Note the scaling factor for the y-axis of each plot. The increases in magnitude, during venting, of peaks attributable to hydrogen (mass 2), carbon monoxide (mass 28), and carbon dioxide (mass 44) were clearly observed. The grab samples collected during the thermal abuse test were examined separately to complement the real-time gas data. Grab samples collected during the initial venting (Grab 1 through 3) and major venting (Grab 4 through 6) showed dramatically different amounts and inventory of gases, as seen in Figure 8.

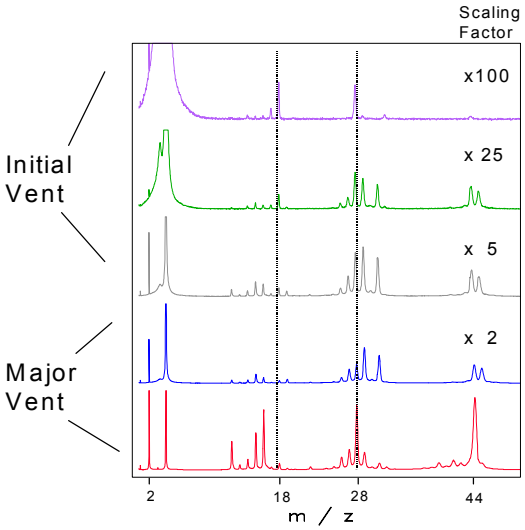

Figure 7: Thermal Abuse MS scans during venting of a Gen 1 cell at 80% SOC.

The grab sample analysis confirms the presence of hydrogen gas during the venting episodes for the cell. Mass spectrometry on the grab samples (not shown) re-affirmed the presence of 7.5% to 8.6% hydrogen in addition to indicating the reported product gases shown in Figure 8.

The balance of the gas in the grab samples was helium from the bomb atmosphere. Fourier transform – mass spectrometry analysis of the grab samples shows a species of mass 39 (F_2H^-) in the negative ion mode; that datum, and the RGA signal at mass 20, suggest the presence of hydrogen fluoride. The presence of this species will be confirmed in later reactive-gas trapping experiments. Figure 8 does not show hydrogen as helium carrier GC with TCD detection does not work for that gas.

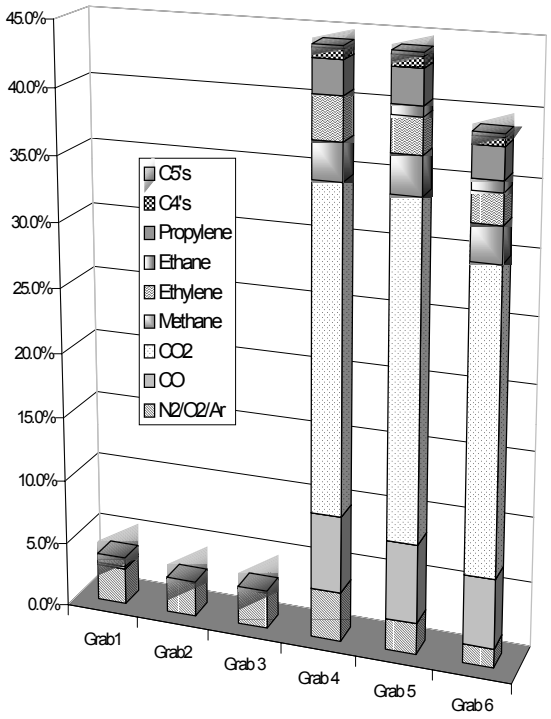

Figure 8: Grab Sample Gas Analysis

Future Directions

The identification of evolved gases by the methods described works well. Full quantification of the identified gases will require the inclusion of mass flow controllers into the experimental set up, and is planned. It is not clear at this time which gases come from the destruction of the SEI layers at the electrodes, and which come from additional reaction of the electrolyte solvents at the time of cell runaway. Joint studies with other ATD labs with solvents outside of built cells, or in half cells, will clarify some of these issues. Since the Gen 2 electrolyte composition is different, there is need for more activity in this area in any case. The important role played by $LiPF_6$ in the maturation of SEI surfaces and in SEI breakup awaits exploration by LC/MS. Reactive gas trapping experiments will be carried out to further investigate the presence of HF.

Acknowledgment

Sandia National Laboratory is a multiprogram laboratory operated by Sandia Corp., a Lockheed-Martin company, for the United States Department of Energy under Contract DE-AC04-94AL85000.

B. Calorimetric Study of Thermal Performance and Abuse Tolerance in Li-Ion Cells

Pete Roth
Mail Stop 0613, Sandia National Laboratory, Albuquerque, NM 87185
(505) 844-3949; fax (505) 844-6972; e-mail: eproth@sandia.gov

Objectives

- Identify chemical mechanisms leading to cell thermal instability and thermal runaway.
- Develop and demonstrate calorimetric methods for the identification of construction factors or chemical constituents leading to reduced thermal tolerance, reduced thermal stability, or reduced operational lifetime in Li-ion cells.
- Determine the effects of aging on cell thermal stability.
- Develop a knowledge base of cell thermal properties leading to improved cell designs.

Approach

- Test whole 18650-size cells using Accelerating Rate Calorimetry (ARC) to determine cell properties leading to cell thermal runaway.
- Test whole 18650-size cells under low to moderate temperature, by Isothermal Microcalorimetry, to measure long-term thermal reaction rates.
- Measure the thermal inter-reactivity of fresh cell solvents, conductive salts, and fresh/aged cell electrodes recovered from disassembled test cells by using Differential Scanning Calorimetry (DSC).
- Determine thermal response of whole cells from measurements of the reactivity and interactions between cell components, which could lead to improved cell designs.

Accomplishments

- Completed ARC measurements of fresh Gen 1 cells from 0% to 100% state-of-charge (SOC) showing that accelerated self-heating only occurs for SOC greater than 50%. Demonstrated the presence of two reaction temperature regimes: a non-accelerating region below 70°C and an accelerating region above 80°C. Both regimes show increased activity with increasing SOC.
- Demonstrated by ARC measurements of aged/cycled Gen 1 cells, that aging/cycling completes low-temperature reactions seen in fresh cells, thus raising the onset temperature for thermal runaway. Showed that reactions that do occur start above 100°C and are abruptly followed by repassivation.
- Demonstrated by isothermal microcalorimetry that the low-temperature, heat generating reactions do not depend on electrical charge/discharge cycling, but are dependent only on temperature, SOC, and time at temperature.
- Performed extensive DSC thermal characterization of Gen 1 cell anodes, cathodes, and electrolyte for disassembled cells that had undergone various aging/cycling tests at different SOCs. Determined reaction and decomposition regions for SEI layers, electrolyte, binder, and active materials.

Future Directions

- Perform gas analysis of decomposition products of individual cell components using simultaneous TGA/FTIR.
- Perform ARC pressurized cell (bomb) tests of individual cell components.
- Perform calorimetric characterization of Gen 2 cells and cell components.

The use of high-power Li-ion cells in hybrid electric vehicles is determined not only by the electrical performance of the cells, but by the inherent safety and stability of the cells under normal and abusive conditions. The thermal response of the cells is determined by the intrinsic thermal reactivity of the cell components and the thermal interactions in the full cell configuration. The purpose of this study is to identify the thermal response of these constituent cell materials, their contribution to the overall cell thermal performance, and the effects of aging on this behavior. Calorimetric techniques were used as a sensitive measure of these thermophysical properties.

ARC Analysis:

ARC allows determination of adiabatic cell response to increasing temperature and thus measures the onset and development of thermal runaway under controlled conditions. ARC runs were performed on Gen 1 cells at several SOCs while monitoring the cell voltages, as shown in Figure 1. The heating rate of the cells showed a strong SOC dependence. The cells with 50% or lower SOC showed no accelerating heating, only transient heating spikes, while the cells with higher SOC showed accelerating heating above 75°C. A low-temperature constant heating rate region was observed whose onset temperature decreased with increasing SOC. This region was separated from the accelerating heat region by about 10°C. Cell voltages dropped abruptly near 130°C with a corresponding dip in the cell heating rate. These results are due to cell venting and also due to separator melt. These Gen 1 cells show greater thermal stability than the commercial Sony cells. This stability may result from differences in mechanical construction rather than intrinsic thermal behavior since the Gen 1 anodes have been shown by DSC to behave similarly to the Sony anodes and the anodes are the initial heat source for thermal runaway.

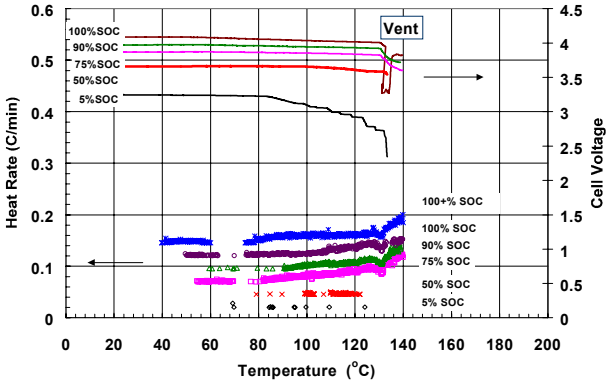

Figure 1. ARC runs of Gen 1 cells at increasing SOC (vertically offset).

Microcalorimetry Analysis:

The low temperature reactions observed during the ARC runs were monitored under more controlled conditions in the isothermal microcalorimeter. Cells were measured at several SOCs at 25°C and 60°C. Previously, we have shown that the cells exhibit strongly increased heat output with increasing temperature consistent with the behavior observed during both DSC and ARC measurements. However, at these lower temperatures Gen 1 cells showed much greater heat output compared to the Sony cells. The heat output decayed following a power-law dependence. Interruption of the microcalorimetry measurements for charge/discharge cycling did not change the thermal output for a given SOC as shown in Figure 2.

The cells were removed, electrically cycled and set to a different SOC. After measurement at the new SOC, the cells were returned to the original value. The cells resumed their thermal decay profile from the time of the interruption.

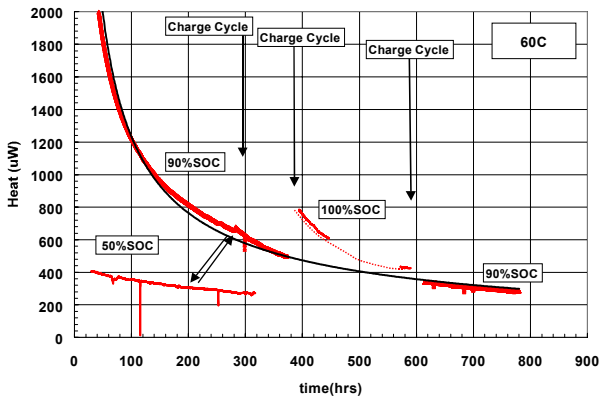

Figure 2. Microcalorimetry of Gen 1 cell at 60°C showing effect of changing SOC.

This behavior shows that the heat output measured in the microcalorimeter is not the result of internal equilibration or residual heat decay from cycling. This heat output most likely results from low-rate decomposition and reformation of the SEI layer that has been previously measured by DSC. Heat output will also result from oxidation and reduction reactions of the electrolyte, which can impact the cell lifetime and capacity. The differences in reactivity between the Sony and Gen 1 cells may result from the different solvents, differences in the morphology of the intercalating carbons and different reactivity of the different metal oxide cathodes. It has been shown that the Gen 1 $LiNi_{0.8}Co_{0.2}O_2$ cathodes are more thermally active than the Sony $LiCoO_2$ cathodes, especially at higher SOCs.

DSC Analysis:

Full cells that had been electrically cycled were disassembled and the electrodes measured up to 400°C in sealed Al pans. The data for the anodes from both Sony and Gen 1 cells (50% SOC), shown in Figure 3, exhibited very similar behavior as expected since they have similar intercalating carbon compositions. A low-temperature region from about 100°C-200°C shows an exothermic reaction that has been found to involve SEI decomposition from a metastable species formed during initial cycling to more stable inorganic reaction products followed by further electrolyte reduction. This reaction has been seen to start as low as 80°C. The exact temperature range of these reactions depends on the particular solvent and salt species used for the electrolyte. The exothermic SEI reactions dominated the low-temperature response and were somewhat higher for the material from the Gen 1 cells.

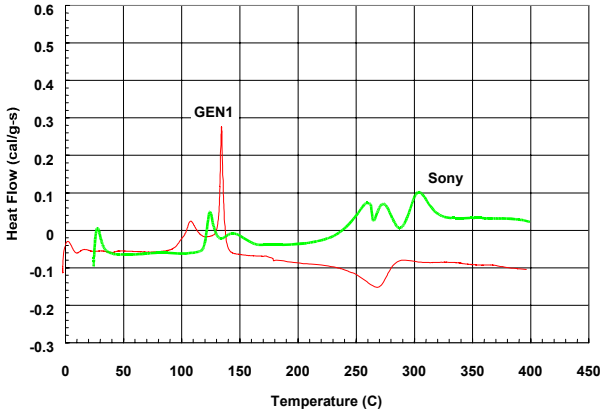

Figure 3. DSC data of Gen 1 and Sony anodes at 50% SOC.

The DSC data for the Gen 1 cathodes (50% SOC) are shown in Figure 4 along with data for the Sony cathodes. The $Li_xNi_{0.8}Co_{0.2}O_2$ cathodes from the GEN 1 cells were markedly more exothermic than the Li_xCoO_2 Sony cathodes at similar SOC and the reactions initiated at slightly lower temperature. Some low-level exothermic reactions were observed in the 100°C-200°C range. These thermal signatures are similar to those seen for the anode SEI but much lower in magnitude. These reactions can possibly result from the reaction of a cathode SEI layer that has been observed by other techniques.

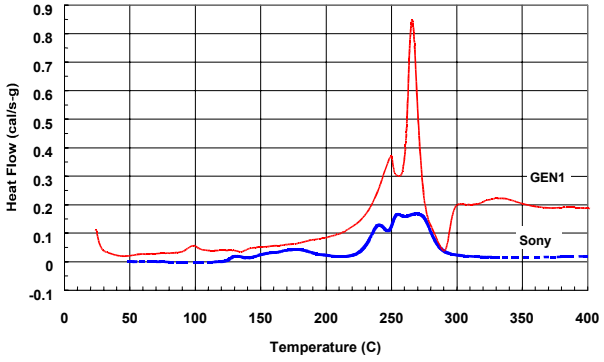

Figure 4. DSC data for Gen 1 and Sony cathodes at 50% SOC.

Cell Aging Effects:

The effects of aging at elevated temperatures were measured by performing ARC runs of thermally aged Sony and Gen 1 cells. Figure 5 shows the results for the Sony cells which had been aged for 6 months at 25°C, 11 days at 60°C and 6 weeks at 70°C. The cells showed less low-temperature reactivity with increased aging. All cells were measured at 100% SOC. The data show that aging resulted in loss of the low-temperature heat output with increasing time and temperature. The onset temperature of sustained heat output increased with increased time/temperature aging. These measurements suggest that the SEI layer is undergoing partial conversion from the metastable species to the stable inorganic species even at these low temperatures. The majority of this conversion takes place relatively quickly (less than two weeks) at 60°C since little further change was noticed for the 70°C/6 week cell. The sudden increase in self-heating in the 100°C-110°C range suggests that the remaining SEI layer undergoes rapid conversion followed by further reaction of the lithiated anode with the electrolyte with increasing temperature. This rapid increase corresponds closely with the onset of the exothermic peak observed by DSC for charged anodes removed from full cells.

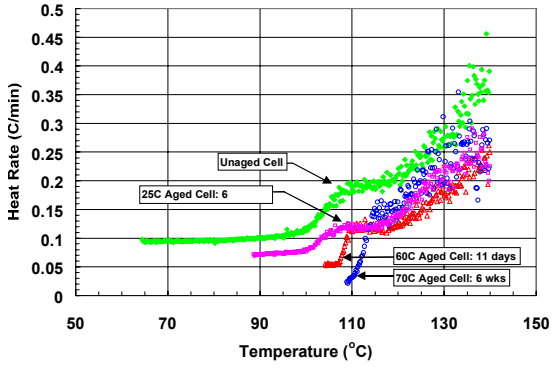

Figure 5. ARC results for aged Sony cells at 100% SOC (vertically offset).

A Gen 1 cell was aged for 4 weeks at 60°C. The ARC run (Figure 6) showed no thermal output below 125°C. Two abrupt increases in heating that quickly decayed below the ARC low-limit threshold were observed above 125°C. These Gen 1 cells apparently form a converted SEI layer at low temperatures which acts like a brittle passivation layer. This layer can break down, exposing the Li-intercalated carbon followed by a rapid reaction process probably involving reduction of the electrolyte to form a new layer. The aged Gen 1 cells thus show greater thermal stability at low temperatures but may exhibit abrupt heating if forced to higher temperatures above 125°C, which can occur under abusive conditions.

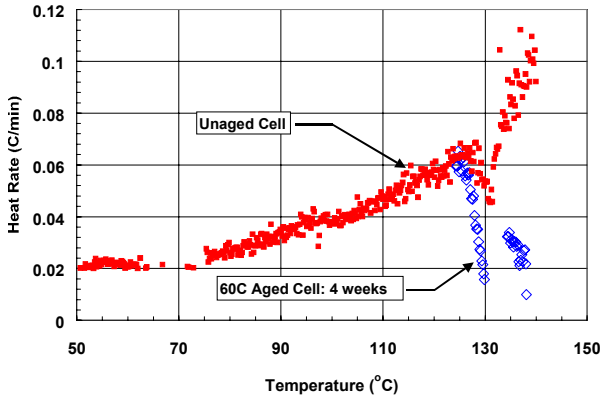

Figure 6. ARC results for aged Gen 1 cell at 100% SOC.

Acknowledgements:

We acknowledge the support of DOE Office of Advanced Automotive Technology through the PNGV Advanced Technology Development (ATD) High-Power Battery Development Program. Sandia National Laboratories is a multiprogram laboratory operated by Sandia Corporation, a Lockheed Martin Company, for the United States Department of Energy under contract DE-AC04-94AL85000.

5. Gen 2: ELECTROCHEMISTRY IMPROVEMENT

A. Second Generation High-Power Cell Chemistry Development

Khalil Amine, Jun Liu, Chenhua Chen, Daniel Simon, and Gary Henriksen
Argonne National Laboratory, Argonne, IL 60439
(630) 252-3838; fax (630) 252-4176; e-mail: amine@cmt.anl.gov

Richard Jow
U. S. Army Research Laboratory, Adelphi, MD 20783
(301) 394-0340; fax (301) 394-0273; e-mail: rjow@arl.mil

Objectives

- Develop a second generation, high-power cell chemistry that exhibits improved low-temperature performance, life, abuse tolerance, and/or cost effectiveness over the Gen 1 baseline cell chemistry.
- Transfer technology to an industrial firm to fabricate ~250 high-power 18650 cells.
- Fabricate (via an industrial firm) ~250 cells and distribute cells to testing and diagnostic laboratories.

Approach

- Obtain advanced electrode, additive, binder, and electrolyte materials from international lithium-ion battery material suppliers and evaluate them relative to Gen 1 materials.
- Develop and evaluate advanced materials relative to Gen 1 materials.
- Select Gen 2 cell materials based on the best combination of performance, stability, safety, and cost.
- Engineer high-power electrodes, and establish cell performance characteristics.
- Transfer materials and processing technology to cell fabricators, and build/evaluate trial cells to verify process scale-up and cell fabrication.
- Contract with industrial firm to fabricate and distribute cells.

Accomplishments

- Completed screening of metal-doped $LiNi_{0.8}Co_{0.2}O_2$ positive electrode, advanced graphite negative electrode, electrode additive, advanced electrolyte, and non-fluorinated binder materials.
- Selected the following materials for use in Gen 2 cells: Fuji $LiNi_{0.8}Co_{0.15}AL_{0.5}O_2$ positive electrode material (with a PVDF binder), Hitachi Chemical MAG-10 synthetic graphite (with an aqueous binder), and 1.2 M $LiPF_6$ in EC:EMC (1:4) electrolyte (as developed jointly with ARL during 1999). Screening test results indicate the following advantages over the Gen 1 cell chemistry: A) enhanced safety with Al-doped positive electrodes without sacrificing capacity density, B) good capacity density, power, and safety with a lower-cost synthetic graphite, and C) significantly improved safety and reduced cost with non-fluorinated binder in the negative electrode.

- Contracted with 3 industrial firms (E-1 Moli, PolyStor, and Quallion) to fabricate 18650 trial cells with these materials, and supplied them with materials. Received 7 trial cells from E-1 Moli in late April and 8 trial cells from Quallion in early May. Developed test plan for the trial cells.

Future Directions

- Evaluate the trial cells and select the industrial firm to build Gen 2 cells.
- Contract with one industrial firm to fabricate and distribute ~250 Gen 2 cells, and supply them with the materials.

Introduction

The Gen 1 cell chemistry exhibited adequate high-power performance for the PNGV fast-response engine requirement at room temperature, but it suffered from poor low-temperature performance, lacked adequate abuse tolerance, and exhibited rapid power fade, which limited its calendar life. The objective of this project is to develop a second generation (Gen 2) cell chemistry that exhibits enhanced life, abuse tolerance, low-temperature performance, and/or cost effectiveness over the Gen 1 cell chemistry. The Army Research Laboratory (ARL) worked with ANL to develop the Gen 2 cell electrolyte, while ANL evaluated a variety of advanced anode, cathode, electrode additive, and binder materials to arrive at the Gen 2 electrode formulations. Candidate electrode, additive, and binder materials were chemically and physically characterized, processed into electrodes, characterized electrochemically (using the PNGV hybrid pulse power characterization [HPPC] test procedures), and evaluated for their reduced chemical reactivity with the Gen 1 electrolyte (1 M $LiPF_6$ in EC:DEC [1:1]) using DSC. The following types of advanced materials were evaluated for use in Gen 2 cells: new natural and synthetic graphites (some of which are surface-treated), doped lithium-nickel-cobalt oxides, soft non-fluorinated binders, electronic additives, and coated current collectors.

Gen 2 Cell Chemistry

Table 1 provides a summary of the materials selected for use in Gen 2 cells. Most of the selected materials were evaluated and identified as promising candidate materials in last year's report. After evaluating 30 different doped positive electrode materials and 14 different advanced graphite negative electrode materials, those shown in Table 1 were selected on the basis of the best combination of performance, safety, and cost.

Component	Composition
Positive Electrode	84 wt % $LiNi_{0.8}Co_{0.15}Al_{0.05}O_2$ (Fuji) 4 wt % SFG-6 (Timical) 4 wt % Carbon Black (Chevron) 8 wt % PVDF Binder (Kureha KF-1100)
Negative Electrode	96 wt % MAG-10 (Hitachi Chemical) 4 wt % Aqueous Binder (Hitachi Mining Corp. H-1004)
Electrolyte	1.2 M $LiPF_6$ in EC:EMC (1:4)

Table 1. Gen 2 Cell Chemistry

In evaluating metal doped $LiNi_{1-x-y}Co_xM_yO_2$ (M = Al, Mg or Ti) advanced positive electrode materials, we sought a material that exhibited power capabilities that were comparable to those of the Gen 1 material, but exhibited reduced chemical activity with the cell electrolyte. The selected Fuji material met these requirements. When compared to the Gen 1 positive electrode material, it exhibited comparable power capabilities and reduced reactivity with the Gen 1 electrolyte (see Figure 1). Based on its performance and availability, the 5-wt % Al doped Fuji material was selected for use in Gen 2 cells. A 10 wt % Al doped Fuji material may actually provide better life and safety, but it currently is not produced in sufficient volume to be used in the Gen 2 cell build.

In terms of the negative electrode, the Hitachi Chemical MAG-10 synthetic graphite was one of 14 different advanced graphites that were evaluated. It is lower cost, possesses variable shape, and it is not necessary to blend the highly

reactive SFG-6 with the MAG-10 to achieve good high-power performance from the Gen 2 negative electrode. Also, its safety characteristics are comparable to the MCMB graphite. The Hitachi H-1004 aqueous binder is one of several non-fluorinated soft binders that ANL evaluated. Its advantages over PVDF binders are: less reactive with lithiated graphite and the electrolyte; lower cost; and works effectively at 4-wt % (vs. 9 wt % for the PVDF binder). Some carbon-coated graphites were studied for use with PC-based electrolytes, but their rate capabilities were too limited due to the thick coatings of carbon on these materials.

In terms of the electrolyte, the Gen 2 electrolyte was developed during the first year of the ATD program, in a collaborative effort between the Army Research Laboratory and ANL. The 1.2 M $LiPF_6$ in EC:EMC (1:4) electrolyte possesses several advantages over the Gen 1 electrolyte. It exhibits superior performance at low temperatures (between -20 and 0°C); it possesses high ionic conductivity (due to the higher salt concentration); and it has a greater voltage stability window than the Gen 1 electrolyte.

Performance characteristics of a 32-cm^2 laboratory cell, employing a 25 xm separator and the Gen 2 cell chemistry, are provided in Figures 2 and 3. These data were obtained in accordance with the hybrid pulse power characterization (HPPC) test procedures provided in the PNGV Test Manual[1]. The area specific impedance (ASI) values, shown in Figure 2, compare favorably with those of cells that employ the Gen 1 cell chemistry. The unit cell power capability of this chemistry, as calculated from the cell ASI values and shown in Figure 3, indicate that this chemistry can exceed the PNGV fast response engine energy storage variable-shaped particles with rounded edges, and has better electronic conductivity than the spherical-shaped MCMB graphite used in the Gen 1 cells. Due to its better conductivity and power targets, as determined using ANL's spreadsheet battery design model.

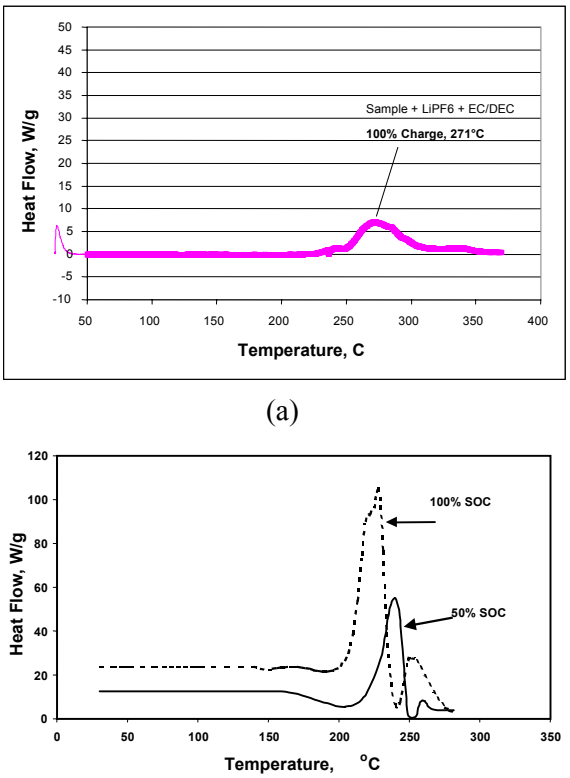

(a)

(b)

Figure 1. Comparative DSC data on Al-doped (a) and non-doped (b) $LiNi_{0.8}Co_{0.2}O_2$ material from Fuji, with the Gen 1 cell electrolyte, showing that the quantity of exothermic heat is significantly reduced and that the exotherm is moved to a higher temperature by addition of the Al dopant.

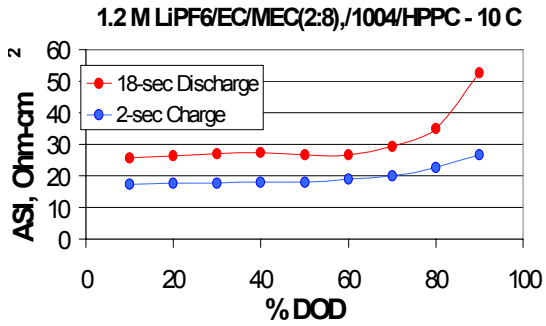

Figure 2. Area specific impedance values obtained during 18-second discharge and 2-second charge pulses at several depths of discharge (DOD). Data were obtained using the Gen 2 cell chemistry and a 25 xm thick PE separator.

Build & Test Gen 2 Trial Cells

The unit cell performance characteristics obtained from these laboratory cells were used to establish engineering specifications for high-power 18650 cells, using ANL's spreadsheet cell model. These specifications were used to procure 18650 trial cells from three industrial fabricators. Two of the industrial firms produced trial cells and these cells are being evaluated at 80 % SOC and 50°C to assess impedance rise rates under these accelerated aging conditions. Some of the cells will be held at 80 % SOC, while others will be cycled to 9 % SOC.

Future Work

Based on the test results from the Gen 2 trial cells, ANL will select the industrial fabricator for the Gen 2 cell build. ANL will implement a contract with the selected industrial cell fabricator to build ~250 Gen cells and to provide one-side coated Gen 2 electrodes for use by the diagnostic laboratories in some specialized cells. ANL will supply the industrial cell fabricator with the materials to use in the fabrication of the electrodes and the cells. The exact quantity of cells will be established on the basis of detailed accelerated life and thermal abuse test plans, that are under development by the test laboratories.

Consideration is being given to building several variants on the Gen 2 baseline cell chemistry. The variants would be used to investigate the effects of minor variations in cell chemistry on the performance, life, and safety characteristics of the Gen 2 cells. The variants under consideration are:

a) Fuji 10 wt % Al doped cathode material
b) PVDF binder in the anode
c) Electrolyte additive (e.g. a flame retardant)
d) Carbon coated aluminum current collectors for the cathode

The Gen 2 baseline and variant cells will be distributed to the test and diagnostic laboratories to conduct the accelerated life and thermal abuse tests and to perform diagnostic studies on new, aged, and abused Gen 2 cells.

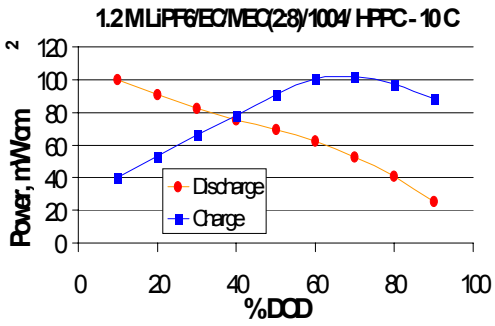

Figure 3. Power per unit area of electrode, as a function of DOD, as calculated using the methodology described in the PNGV Test Manual.

List of Publications

1. K. Amine and J. Liu, "Development of High-Power Lithium Ion Batteries for Hybrid Vehicle Application," *ITE Letters*, **1** (1), B39 (2000).

2. K. Amine, J. Liu, A.N. Jansen, A Newman, D. Simon, and G.L. Henriksen, "Development of High Power Lithium Ion Batteries for Hybrid Vehicle Application," *Intercalation Compounds for Battery Materials Book*, edited by The Electrochemical Society Inc., Vol. 99-24, pp. 389-399 (2000).

3. S. P. Ding, K. Xu, S. S. Zhang, T. R. Jow, K. Amine, and G. L. Henriksen, "Diminution of Supercooling of Electrolyte by Carbon Particles," J. Electrochem. Soc. 146 (11), 3974–4980 (1999).

6. GEN 3: ADVANCED MATERIALS

A. Developing Advanced Materials for Gen 3 High-Power Cells

Khalil Amine, Jaekook Kim, Christopher Johnson, Jun Liu, Chunhua Chen, and Don Vissers
Argonne National Laboratory, Argonne, IL 60439
(630) 252-3838; fax (630) 252-4176; e-mail: amine@cmt.anl.gov

Richard Jow
U. S. Army Research Laboratory, Adelphi, MD 20783
(301) 394-0340; fax (301) 394-0273; e-mail: rjow@arl.mil

Objectives

- Utilize diagnostic results from Gen 1 and Gen 2 cells to develop advanced materials that are tailored to overcome the life and abuse tolerance limitations of the Gen 1 and Gen 2 cell chemistries.
- Develop a high-power Gen 3 cell chemistry based on these materials.
- Transfer the technology to an industrial firm to fabricate ~200 high-power 18650 cells.
- Distribute the ~200 cells to laboratories for testing and diagnostic, as directed by ANL.

Approach

- Develop and thoroughly characterize an optimal multi-doped lithium-nickel-oxide positive electrode material that possesses the desired chemical, physical, and structural properties to survive for 10 years, and exhibits the required performance and safety characteristics—solution-based processes are being investigated to accomplish this.
- Develop and thoroughly characterize low-cost natural graphites and coating processes that form a stable pre-passivation film on the graphite particles.
- Develop and thoroughly characterize a low-cost advanced electrolyte system (preferably propylene carbonate (PC)-based) that possesses enhanced stability to oxidation/reduction reactions at the electrodes, performs well at low temperature, and is less flammable than existing electrolyte systems—electrolyte additives will be studied to limit the oxidation/ reduction reactions and the flammability.
- Develop electrolyte additive, via quantum chemical calculations of redox potential, that could lead to a stable SEI layer at the surface of the electrodes.
- Develop a Gen 3 cell chemistry using these advanced materials, and transfer the processing technology to an industrial cell fabricator.
- Contract with an industrial firm to fabricate and distribute Gen 3 cells.

Accomplishments

- Highly ordered $LiNi_xMg_yAl_zO_2$ materials with suitable compositions were successfully synthesized by the solution combustion, sol-gel, ion exchange, and solid-state reaction processes.

- The effects of Al and Mg doping on the electronic conductivity of $LiNi_xMg_yAl_zO_2$ were established. Although Al doping reduced the electronic conductivity, this effect can be overcome by low levels of Mg doping. By adding less than 10 wt % Mg, the overall conductivity of the multi-doped material was increased by a factor of 5 compared to the non-doped material.

- Amorphous carbon-coated natural graphite was found to intercalate lithium without exfoliation in 70% PC-based electrolytes. The rate performance of the material depends on the thickness of the amorphous carbon coating on the surface of natural graphite.

Future Directions

- Development and characterization of advanced multi-doped nickel oxides will continue.

- Investigate several methods of stabilizing $LiMn_2O_4$ spinel as a low-cost high-rate cathode material.

- Development of low-cost natural graphites, and pre-coating processes will be expanded.

- Development of 2 and 3 component advanced solvent electrolyte systems, with additives, will be continued.

- Fabricate 180 mAh high-power hermetically-sealed prismatic cells, and investigate the effect of the Gen 3 materials on calendar life and safety.

Introduction

The objective of this project is to utilize information from the Diagnostic Evaluation Project to develop new advanced materials that are specifically tailored to overcome the sources of the life and abuse tolerance limitations, while keeping in mind the need for low cost. The project includes: developing advanced materials, engineering the most promising active materials into high-power electrodes, developing a more optimal electrolyte system, and developing a Gen 3 cell chemistry around these advanced materials. The goal is to have a Gen 3 chemistry available for scale up into 18650 Gen 3 cells by November 2001. Work on this project is being performed in a collaborative manner by Argonne National Laboratory (ANL) the Army Research Laboratory (ARL), the Illinois Institute of Technology (IIT), and Quallion LLC (an industrial collaborator).

In the early stages of this project, ANL is focusing on the development of multi-doped lithium-nickel-oxide positive electrode materials. Opportunities exist to enhance the rate capability, as well as to improve the chemical and structural stability of the positive electrode, while reducing its chemical reactivity with the electrolyte via selective low-level multi-doping of lithium nickel oxide.

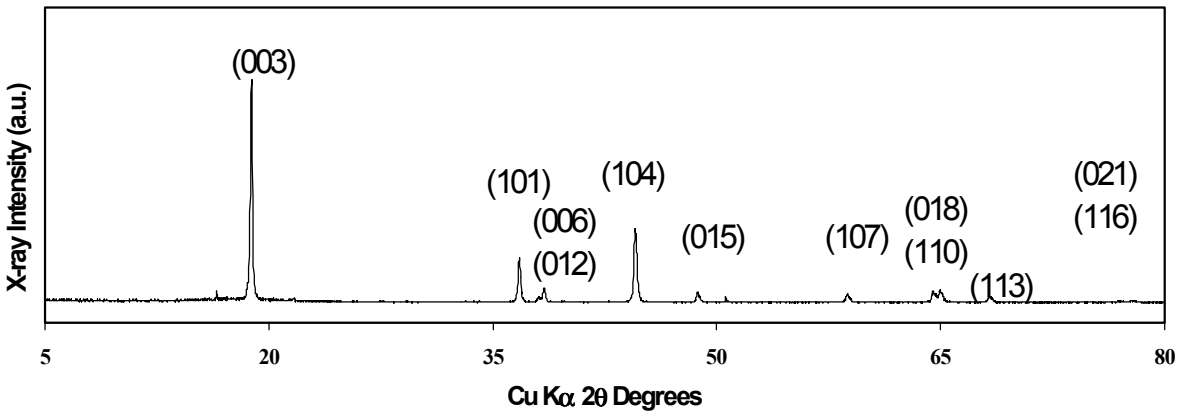

Figure 1. XRD pattern for a layered cathode material, $LiNi_{0.9}Al_{0.05}Mg_{0.05}O_2$, produced via the sol-gel process.

During the last year, ANL investigated four synthesis approaches, co-precipitation/ion-exchange, sol-gel, and solution combustion to identify the best preparation method for producing multi-doped $LiNi_xCo_yMg_zAl_wO_2$ materials that possess the desired product-phase purity, morphology/ particle size, high chemical homogeneity, and a highly property ordered structure. These solution-based homogenous processes were pursued because it is difficult to achieve the required high-level of chemical homogeneity when using high temperature solid-state reaction processes for materials that incorporate Al and Mg dopants.

Additional efforts are being carried out in the areas of pre-coated natural graphites, advanced electrolytes (including PC-based systems), and electrolyte additives that suppress oxidation and reduction reactions at the electrode surfaces. Also, we continue to evaluate the newest advanced materials available from international material suppliers, as well as advanced materials that are developed under other DOE-sponsored projects, e.g. SBIR, STTR, CARAT, and GATE projects. Also, this project is the bridge to DOE's Exploratory Technology Research (ETR) Program, and any promising new materials developed on the ETR Program will be evaluated as candidate materials for Gen 3 cells.

The advanced cathode, anode, and electrolyte materials being developed under this project must be scalable with low-cost high-volume production. To ensure that these materials can be produced in high volume and at low cost, ANL has established working relationships with several industrial firms under the Advanced Process Research project.

Positive Electrode Material Development

This year, we focused our efforts on the sol gel process as a viable low-cost process to obtain pure phase materials with high particle-to-particle chemical homogeneity, since the reaction of the precursors take place at the molecular level. This process is based on dissolving Li, Ni, Al, and Mg based precursors in acetic acid and refluxing the mixture at the boiling point of the acetic acid to form a transparent gel. The gel is then heated to 650°C to obtain a pure $LiNi_xMg_yAl_zO_2$ material. Using this approach, one can readily prepare highly ordered materials that contain no cobalt as a dopant. This results in a cost reduction, since cobalt is 10 times more expensive than nickel metal. Figure 1 shows the X-ray diffraction pattern of the near optimum composition, $LiNi_{0.9}Mg_{0.05}Al_{0.05}O_2$, which exhibits high electrochemical performance. The observed peaks are very sharp with the integrated intensity I(003)/I(104) ratio of 2.95 and with good splitting of the (108) and (110) reflections. This indicates that the structure is highly ordered, the Li occupies only the 3b sites, and the Ni, Mg, and Al occupy the 3a sites. We found that the Al doping plays two roles: 1) it stabilizes the material by reducing the oxygen activity at the fully-charged state, thereby suppressing surface reactions with the electrolyte, and 2) it plays the same role as cobalt in enhancing the covalency of the nickel layer and minimizing the displacement of nickel into the lithium sites, thereby limiting structural transitions that occur during the cycling of pure $LiNiO_2$ materials. The electronic conductivity of the active material was improved by adding a small amount of magnesium to create a mixed valence in the transition metal oxide. The conductivity of the material with (5% Mg) and without Al doping was about (δ=6.395 S/m), which is 2 orders of magnitude higher than that for $LiNiO_2$. However, by adding both 5% Mg and 5% Al doping, the overall conductivity of the multi-doped material was reduced, due to the effect of Al doping, but still remains five times higher that the conductivity of the initial $LiNiO_2$.

Figure 2 shows the charge and discharge behavior of $LiNi_{0.9}Mg_{0.05}Al_{0.05}O_2$. The material

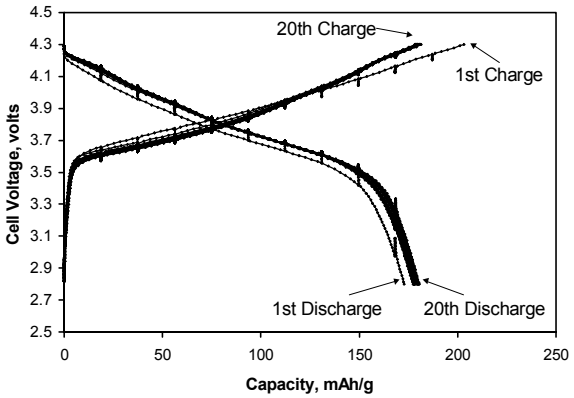

Figure 2. Charge and discharge curves for a cell employing a $LiNi_{0.9}Al_{0.05}Mg_{0.05}O_2$ positive electrode.

shows a high discharge capacity density of 180 mAh/g with excellent cyclability. It should be noted that a 5% Al doped $LiNiO_2$, prepared by the conventional solid-state reaction, usually exhibits capacities lower that 150 mAh/g, with poor cyclability characteristics. The excellent electrochemical behavior of the $LiNi_{0.9}Mg_{0.05}Al_{0.05}O_2$ material is a reflection of the benefit of the Mg doping, as well as the process used in the preparation of this material.

Next year, ANL will continue investigating the effects of dopants on the calendar life and safety of $LiNi_{0.9}Mg_{0.05}Al_{0.05}O_2$ using small hermetically-sealed prismatic cells (180mAh capacity). In addition, ANL will initiate studies that target the stabilization of $LiMn_2O_4$ spinel materials as potential Gen 3 cathode materials. Several approaches will be screened for their viability and the most promising approaches will be studied in depth. This work is being initiated in response to the claims of Shin Kobe, regarding their use of a stable high-rate $LiMn_2O_4$ cathode material in their HEV cell technology.

Negative Electrode Material Development

The objective of this work is to develop high performance graphite materials that cost less and are less reactive with the electrolyte than the existing graphites. To address the cost issue, ANL is focusing on low cost natural graphite as a potential anode material for the Gen 3 cell chemistry. Natural graphites are known to exhibit higher capacities (360mAh/g), lower irreversible capacities, and higher rate capabilities than synthetic graphites, due to their well-ordered laminar structures. However, these materials exfoliate quite readily in the presence of PC based electrolytes. For cost, performance, and stability reasons, our Gen 3 electrolyte development effort is focused on the use of high concentrations of propylene carbonate. Therefore, our effort has concentrated on acquiring modified natural graphite materials that can be used with our PC-based electrolytes. Recent studies coming out of Japan indicate that graphite-based anode materials can be modified so that the material does not exfoliate when cycled in PC-based electrolytes. The technique that is currently being employed involves putting a thin amorphous film of carbon on the surface of the graphite particles, thus avoiding direct contact between the solvated-PC component of the electrolyte and the graphite surface. ANL has obtained pre-coated natural graphites from Mitsui Mining and investigated the effects of the coatings on the stability of the negative electrode, and thus the calendar life of the lithium ion cell. Figure 3 Shows a TEM photograph of a surface view of a cross section of a Mitsui-supplied particle that was cut in half using a microtome. A clear amorphous film can be observed on the surface of the highly ordered

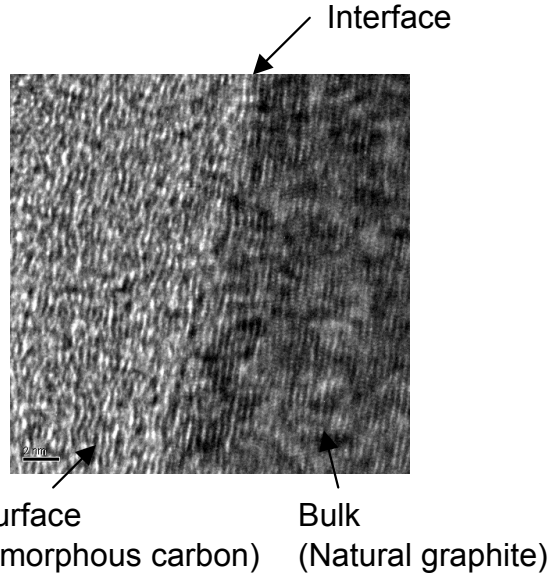

Figure 3. HR-TEM photograph of a cross section of a natural graphite particle coated with amorphous carbon.

layers of bulk natural graphite. We successfully cycled this material in a 50% PC-based electrolyte and obtained a large charge capacity density (340mAh/g) and a low irreversible capacity density [see Figure 4]. Preliminary ASI data, obtained during HPPC 18-s discharge and 2-s charge pulses at various SOCs, on two cells made with $LiNi_{0.8}Co_{0.2}O_2$ cathode material and two types of Mitsui graphite (amorphous carbon coatings of 13 wt. % and 17 wt. %) are shown in Figure 5. The ASIs of the cell made with graphite using the low 13 wt. % carbon coating was 34 ohm-cm^2 for the 18s pulse discharge and 22 ohm-cm^2 for the 2s-regenerative braking charge pulse. These values are slightly lower than the target values calculated from ANL's battery design spreadsheet model for a PNGV battery, which are 35 ohm-cm^2

for an 18-s discharge and 25 ohm-cm^2 for a 2-s charge pulse. The cell employing the thicker (17 wt. %) carbon coating on the graphite exhibited higher ASI values for both the 18-s discharge and 2-s regen charge pulses. These results suggest that the maximum coating level for natural graphite (in order to achieve the PNGV high power requirements) is about 13-wt % of amorphous carbon coating. ANL requested and received additional natural graphite materials from Misui that have lower coating levels and we are currently investigating their power characteristics and their effects on enhancing the calendar life and stability of lithium-ion batteries.

ANL is conducting laboratory scale experiments on several methods for coating natural graphite particles with different types of protective coatings. These approaches will be investigated further to determine if any of them are viable for the HEV high rate application.

Advanced Electrolyte Development

ANL continues to obtain advanced electrolytes from international suppliers and will continue to evaluate these electrolytes. ANL has expanded its collaborative work with the ARL to study advanced electrolytes based on blends of 2 and 3 solvents, which include PC. Salts other than $LiPF_6$ are being investigated, as well as electrolyte additives that limit or suppress the oxidation and reduction reactions of electrolyte at the surfaces of the electrodes.

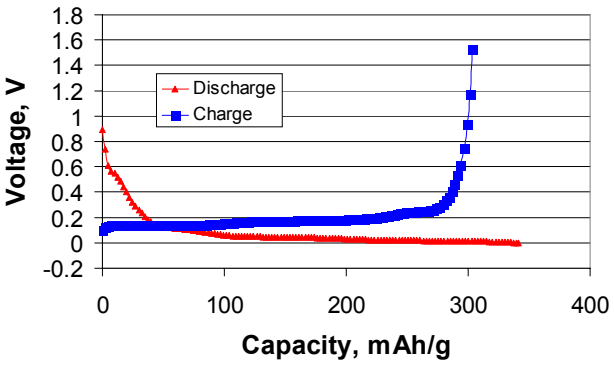

Figure 4. Charge and discharge capacity of natural graphite coated with 13-wt % amorphous carbon in the presence of $LiPF_6$/EC:PC (50:50) electrolyte.

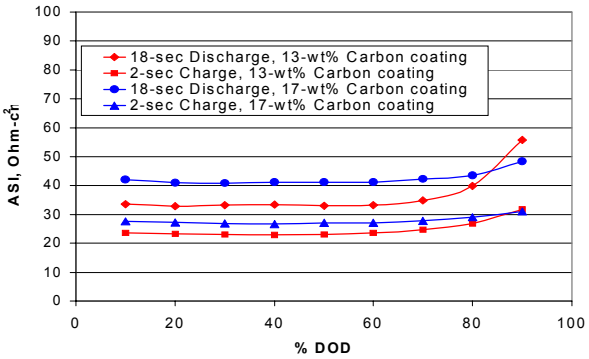

Figure 5. Pulse power ASI as a function of DOD for cells made with $LiNi_{0.8}Co_{0.2}O_2$ positive electrode and natural graphite (coated with 13 wt % and 17 wt % amorphous carbon) using HPPC tests conducted at 10C rate.

Some preliminary work was performed to evaluate candidate electrolyte additives. Early results from these studies indicate the following: 1) polymethyl methacrylate (PMMA), at 1 wt. %, appears to reduce the capacity fade of Li-ion cells during cycling and 2) 2-chloro-p-xylene, at 5 wt. %, appears to prevent lithium deposition during overcharge of the cell, thus improving the safety of the cell chemistry during overcharge.

ANL is investigating new electrolyte additives that decompose at higher voltage (over 1.0 V vs. Li/Li^+) to form stable SEI layers that prevent surface reactions between the electrolyte and the electrode, thus improving the calendar life of the lithium-ion cell system. To develop these additives using this specific approach, ANL will carry out quantum chemical modeling of candidate additives. The modeling will utilize state-of-the-art electronic structure methods to help identify potential additives that decompose to form a protective surface film on the electrode at a potential that is higher than that of the formation of the conventional unstable SEI layers at the electrode surfaces. The electronic structure calculations on possible additives will be done by surveying the ionization potentials and electron affinities of a large number of candidate additives at the molecular level using density functional theory, which is computationally very efficient. These calculations will be done using a total energy difference procedure, which is more accurate than the HOMO and LUMO analyses. This procedure includes orbital relaxation effects

and has an accuracy of about 0.3 eV. This work will provide guidance concerning the electron donor and electron acceptor properties of the electrolytes that are needed to help choose viable additives for experimental evaluation.

Publications

1. J. Kim and K. Amine, "The Effect of Tetravalent Titanium substitution in LiNi1-xTixO2 (0.025<x<0.2) System," Electrochem. Solid State Lett. (Submitted 2000).

7. ADVANCED PROCESS RESEARCH

A. Advanced Process Research of Materials for Gen 3 High-Power Lithium-Ion Cells

Khalil Amine, Jaekook Kim, Christopher Johnson, Arthur Kahaian, Jong-Sung Hong, Jun Liu, Chunhua Chen, Yoo-Eup Hyung, Don Vissers, and Gary Henriksen
Argonne National Laboratory, Argonne, IL 60439
(630) 252-3838; fax (630) 252-4176; e-mail: amine@cmt.anl.gov

Jai Prakash
Illinois Institute of Technology
(312) 567-3639; fax (312) 567-8874; e-mail: Prakash@iit.edu

Objectives

- Select industrial partners to assess and scale up low cost processes for making $LiNi_xMg_yAl_zO_2$ developed under the advanced material development for Gen 3 cells.
- Develop a thin metal coating on natural graphite, and select industrial partners to develop a low cost process for scale up.
- Develop Gen 3 cell electrolyte, and assist industrial partners in the scale up process of the electrolyte materials.
- Develop flame retardant materials, and select industrial partners to scale up the materials preparation.
- Work with industrial partners to develop a cost analysis of all ANL processes used in the development of Gen 3 advanced materials.
- Develop low cost scale up of Gen 3 materials for fabrication of 18650 high power cells.
- Provide large quantities of Gen 3 materials to PNGV industrial partners.

Approach

- Perform industrial cost analyses, with help of FMC Corporation, on the 4 processes used by ANL in the development of $LiNi_xMg_zAl_wO_2$ cathode material for Gen 3 cell. These processes are: 1) solution combustion process, 2) sol gel process, 3) co-precipitation process, and 4) ion exchange process.
- Develop a thin metal coating on natural graphite to enhance stability, and to increase power and safety performance.
- Develop a flame retardant electrolyte additive to improve the abuse tolerance of high power lithium-ion batteries.
- Select U.S. industrial firms that will scale up low-cost Gen 3 cathode, anode, electrolyte, and flame retardant materials.
- Scale up promising Gen 3 materials developed at ANL, via U.S. industrial partners, and use these materials to fabricate 18650 Gen 3 cells.

Accomplishments

- Selected and in the process of implementing contracts with four industrial partners – FMC Corp., INCO Corp., Superior Graphite, and Quallion LLC – to work with ANL in the advanced process research project.
- Developed a low-cost process for the metal coating of natural graphite particles to enhance power, stability, and safety. Superior Graphite is scaling up the metal-coated carbon process using their low-cost natural graphite. Partial thin metal coatings on natural graphite were found to prevent exfoliation of the graphite in the presence of high concentrations of PC based electrolyte (> 70 wt. %).
- Provided detailed laboratory scale experimental procedures on ANL's four proposed processes to FMC for analysis in the scale up of $LiNi_xMg_yAl_zO_2$. FMC is carrying out comparative cost analyses on these four processes to identify the lowest cost process.
- Screened the power and the safety characteristics of some of the more promising FMC cathode materials for potential use in Gen 3 cells. FMC has developed the material for high-power application based on ANL recommendations. Work is underway to reduce the cost of the processing of this material.
- Evaluated a promising flame retardant (developed by IIT under DOE's ETR program) and investigated its effect on both the Gen 1 and Gen 2 cell chemistries.

Future Directions

- Work closely with FMC to complete the cost analysis on the four proposed processes for the scale up of the $LiNi_xMg_yAl_zO_2$ materials.
- Scale up $LiNi_xMg_yAl_zO_2$ with FMC, using the lowest cost process identified in their comparative cost analyses.
- Continue development of low-cost natural graphites and metal pre-coating processes.
- Scale up the flame retardant material developed by IIT.
- Fabricate 180 mAh high-power hermetically sealed prismatic cells and study the effects of the Gen 3 materials on calendar life and safety.

Introduction

The Gen 3 advanced material development project was based on screening advanced anode, binder, and electrolyte materials from industrial material suppliers, while focusing on the development of a multi-doped cathode material to improve calendar life and the safety of the system. Our cathode work has been focused on selecting and optimizing suitable dopants that enhance the electronic conductivity of the material and improve its bulk and surface stability. However, the power performance of this material is also related to the particle homogeneity and the structural order, which are preparation processes dependent.

ANL has developed four solution-based processes to obtain multi-doped materials with suitable morphology and high structural order. These processes are: 1) solution combustion, 2) sol-gel, 3) co-precipitation, and 4) ion exchange. However, without industrial assistance, ANL is unable to identify which of these processes is the most practical for low-cost high-volume production. Additionally, we need to develop larger-scale process capabilities to produce sufficient quantities of the most optimal materials for use in Gen 3 cells. For these reasons, there was an urgent need to create an advanced process research project.

ANL's lithium-ion battery cost analysis for HEV high-power cells has suggested that the cost of the cathode material is 24% of the cell component cost, excluding the containment. Processing cost for this material is high due to the

difficult preparation of doped-lithium nickel oxide materials via the conventional solid-state reaction process. Therefore, a low-cost process will significantly reduce the overall cost of the cathode material.

Furthermore, ANL's work on screening the amorphous carbon coated natural graphite has shown some improvement in the cost of the anode material, since the use of natural graphite is at least 5 times cheaper than the synthetic graphite used presently by the battery industry. The advantage of using amorphous carbon at the surface of natural graphite is that it prevents exfoliation of the graphite in the presence of the PC-based electrolytes. However, amorphous carbon layer at the surface will still form the same unstable SEI, as with the graphite, which could have negative implication on calendar life and safety. Therefore, ANL is investigating a stable thin metal (Ni, Co, Cu, Fe) coating on natural graphite to protect the surface of the graphite and also provide significant improvement to the conductivity and safety of the cell.

ANL is also addressing the safety concerns of the high-power lithium-ion cells by working with IIT on a flame retardant to enhance the inherent abuse tolerance of this cell chemistry.

Development and Process Scale-Up of Positive Electrode Materials

During the last year, ANL investigated (within the Gen 3 advanced material development project) four synthesis approaches – co-precipitative, ion-exchange, sol-gel, and solution combustion – to identify the best preparation method for producing multi-doped $LiNi_xCo_yMg_zAl_wO_2$ materials that possess the desired phase purity, morphology/particle size control, high chemical homogeneity, and most importantly, the proper ordered structure. ANL selected FMC, a major U.S. chemical company, to perform industrial-scale comparative cost analyses on ANL's four lab-scale processes and to scale up the promising compositions developed in our laboratory. We provided detailed laboratory-scale experimental procedures to FMC, who will use this information to develop industrial-scale process flow diagrams and conduct detailed cost analyses on these processes. The results will be used to select and implement the best processes for scaling up the production of the most optimal materials.

We are also thoroughly evaluating a promising oxide material from FMC. This material has a composition of $LiNi_{0.7}Co_{0.15}Mg_{0.05}Ti_{0.05}O_2$. The combined 5% Mg and 5% Ti doping plays the same stabilizing role as the 5% aluminum doping. While the capacity of this material is lower than the Al doped material, because of the combined 10% inactive doping of Mg and Ti, the material shows excellent power and safety characteristics.

Figure 1 illustrates the pulse power capability of the cell made of $LiNi_{0.7}Co_{0.15}Mg_{0.05}Ti_{0.05}O_2$ cathode and the Gen 1 anode. The figure shows the 18-s pulse power discharge capability and 2-s pulse power charge capability at different DODs. The pulse power at each DOD is calculated from the ASI and the cell open circuit voltage. These values are used to determine the total available state-of-charge and energy swing that can be utilized (within the PNGV operating voltage limits) for specified discharge and regen power levels. The pulse power capability for the cell on charge and discharge was found to meet the PNGV power requirements, especially in the "sweet spot" of 30 to 70% DOD. The PNGV power requirement limit calculated from ANL's spreadsheet model is 55 mW/cm^2 for the pulse discharge and 66 mW/cm^2 for the 2-s regen charge, based on a 40-kW battery pack. The cell based on the FMC cathode material shows better power performance than required by the PNGV at

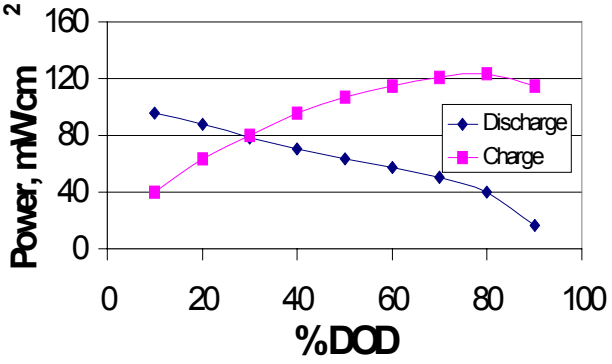

Figure 1. Pulse power as a function of DOD for a cell made of $LiNi_{0.7}Co_{0.15}Mg_{0.05}Ti_{0.05}O_2$ and Gen 1 anode (HPPC test was carried out at 12.5C rate).

12.5C rate, with a "sweet spot" ranging between 20% to 75% DOD.

The FMC cathode material also shows excellent safety performance based on the very low reactivity between the electrolyte and the fully charged cathode material, as illustrated by the DSC data in Figure 2. In this case, the reaction takes place at much higher temperatures (260°C) than Gen 1 "$LiNi_{0.8}Co_{0.2}O_2$" material, which shows a significant reaction at a lower temperature (210°C). The heat flow generated from the reaction between FMC's cathode and the electrolyte is at least an order of magnitude lower than that generated with the Gen 1 cathode and the electrolyte. This result attests to the good stability of FMC's cathode material in the presence of the electrolyte. ANL is carrying out an accelerated calendar life evaluation of the FMC cathode material, charged to 90% SOC and stored at 50°C. Initial results show that after 3 weeks of storage time, the ASI of the cell remains stable. ANL will continue investigating FMC's materials while waiting for the scale up of the multi-doped materials developed under the advanced materials for Gen 3 cell development project.

Development and Process Scale-Up of Negative Electrode Materials

Extensive development work is currently underway in Japan to develop precoated graphite particles for enhanced safety and system stability. Most of these technologies are based on precoating amorphous carbon onto particles of synthetic graphite. The purpose of the coating process is to prevent exfoliation of the crystalline graphite when using PC-based electrolytes. PC is the least expensive solvent, and PC-based electrolytes exhibit the best low temperature performance and stability. However, the amorphous carbon layer at the surface of natural graphite particles still forms the same unstable SEI, as with the graphite, which could have negative impacts on calendar life.

ANL is developing thin coatings of highly conductive metal on natural graphite particles, using a low-cost metal carbonyl decomposition process. The choice of metal compound for the passivation film is dictated by the lithium transport characteristics of the metal. Use of a highly conductive metallic layer on the surface of the graphite particles offers the following advantages: 1) prevents exfoliation of the graphite particles in the presence of PC-based electrolytes, 2) reduces surface reactivity with electrolyte during cycling, thereby enhancing the calendar life of the negative electrode, and 3) enhances the surface electronic conductivity of particles in the graphite-based anode.

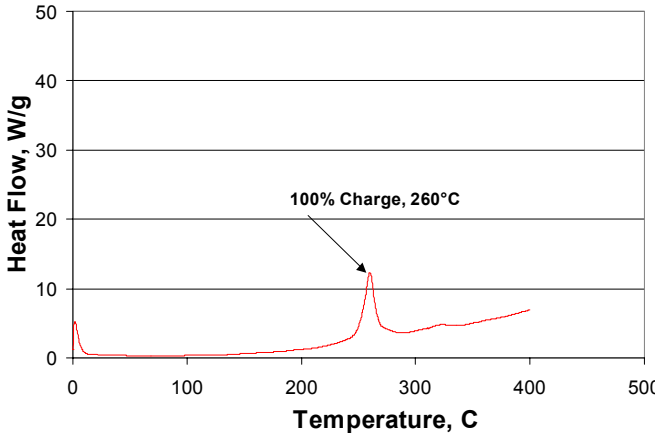

Figure 2. DSC curve showing reaction between fully charged $LiNi_{0.7}Co_{0.15}Mg_{0.05}Ti_{0.05}O_2$ and $LiPF_6$/EC: DEC(1:1).

ANL has contracted with Superior Graphite to develop rounded-edge natural graphite particles, and to work in scaling-up the metal coating process. INCO, a world leader in the metal carbonyl process, has also agreed to work with ANL in the development of nickel-coated natural graphite. Figure 3 shows an SEM photograph of the first sample of nickel-coated graphite supplied by INCO to ANL. The coating was carried out by decomposing nickel carbonyl at the surface of graphite particles at 50°C. The SEM photograph shows that this process can result in over 90% particle coating. The advantage of the nickel coating, in addition to providing a stable SEI layer and improving the conductivity of the negative electrode, is the possibility of the use of more concentrated PC-based electrolyte without exfoliating the natural graphite. Figure 4 shows several discharge cycles of a cell made with a $LiNi_{0.8}Co_{0.2}O_2$ cathode and an INCO nickel coated graphite anode. The cell cycled well in the

presence of $LiPF_6$/EC:PC (50:50) without any sign of graphite exfoliation.

Further studies are underway, in collaboration with both INCO and Superior Graphite, to optimize the thickness of nickel coating on the natural graphite and to investigate the effect of the coating on calendar life and safety of the system. Also, preliminary work in collaboration with IIT on pre-coating graphite particles with Cu and Fe using electroless techniques was initiated.

Development and Scale Up of Flame Retardants

A primary challenge in designing a lithium-ion battery is its safety under abusive, as well as normal, operating conditions. Over-discharge, external or internal short circuiting, crushing, or excessive overcharging could cause Li-ion cells to undergo thermal runaway producing exceedingly high temperatures, smoke, explosion, and/or fire. Also, under certain conditions, the flash point of the electrolyte can be exceeded, and Li-ion cells can be overheated, resulting in a major safety problem. The most important reactions contributing to safety and cell fire are believed to involve thermal decomposition of salts and solvent, and the reaction of cathode and anode with the electrolyte. The initiation temperature and kinetics of these exothermic reactions are interdependent and are affected by the nature and amount of the electrolyte.

One of the low-cost ways of addressing the safety concerns mentioned above is to blend the electrolyte with a small amount of flame retardant. ANL will work in close collaboration with IIT, who developed a new flame retardant called hexamethoxycyclotriphosphazene $[(NP(OCH_3)_2]_3$ under DOE's ETR program. This material was synthesized by reacting sodium methoxide ($NaOCH_3$) and hexachlorocyclotriphosphazene $(NPCl_2)_3$. Cyclic voltammetry studies using both platinum and glassy carbon electrodes confirm the stability of this material in the potential window range of 0 to 5V.

Figure 5 shows the effect of the flame retardant on the onset temperature of a fully-charged Gen 1 anode material. By adding only 5 wt % of $[(NP(OCH_3)_2]_3$ to Gen 1 electrolyte

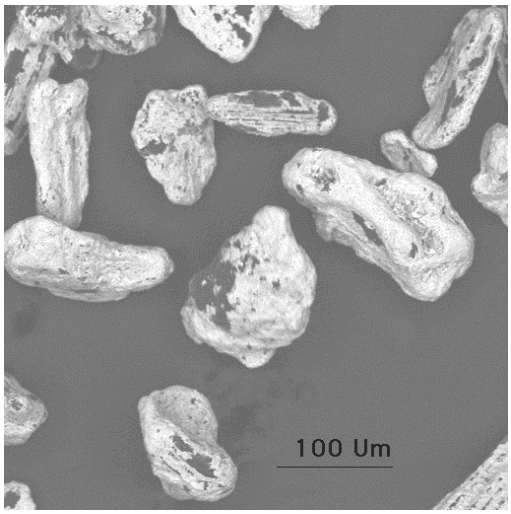

Figure 3. SEM photograph of nickel coated graphite from INCO Corp.

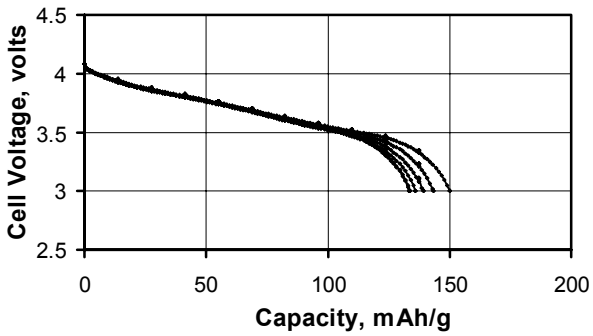

Figure 4. Discharge capacity of a cell made with Gen 1 cathode and nickel-coated graphite from INCO Corp.

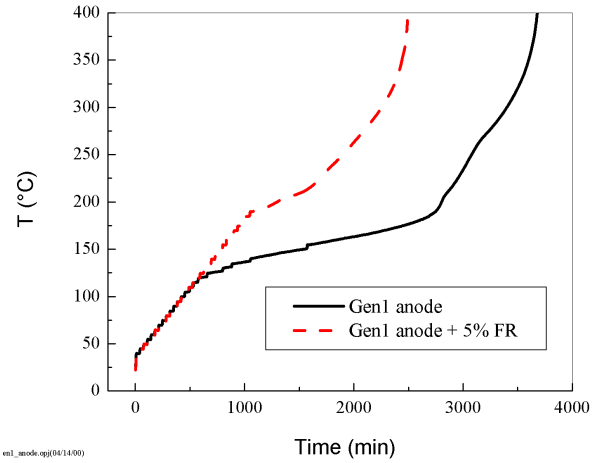

Figure 5. ARC calorimetry data showing the effect of flame retardant (FR) on the Gen 1 cell chemistry onset temperature for thermal runaway.

[$LiPF_6$/EC:DEC(1:1)], the onset temperature for thermal runaway was increased from 125°C without flame retardant additive, to 180°C after adding 5 wt % flame retardant, as observed by Arc-calorimetry. This result shows that the flame retardant suppresses flame generation inside the cell, and allows the shutdown separator to function properly at 130°C.

8. LOW-COST PACKAGING

A. Developing Low-Cost Cell Packaging

Khalil Amine, Aron Newman, Andrew Jansen, Paul Nelson, and Don Vissers
Argonne National Laboratory, Argonne, IL 60439
Contact: Khalil Amine, (630) 252-3838; fax (630) 252-4176; e-mail: amine@cmt.anl.gov

Objective

- Develop novel approaches to reducing the cost of cell packaging for high-power lithium-ion batteries.

Approach

- Develop a flexible cell containment system, based on a laminate, that incorporates barriers for air, moisture, electrolyte, and HF.
- Develop a new flexible pouch design that limits permeation of electrolyte and moisture from the seal edges by means of pattern coating of absorbent near the seal areas

Accomplishments

- Identified the appropriate absorbent for the pattern coating approach in the sealant areas, that selectively absorbs incoming moisture rather than the organic solvent used in the electrolyte.
- Screened and performed permeation tests on candidate polymer films with the assistance of Mocon Controls, Inc.
- Conducted preliminary evaluations of permeation rates, and extrapolated to 10 years for the 10 Ah flexible packaging design.
- Developed several laminate approaches and ink-based pattern coating techniques with the assistance of a flexible packaging consultant and Rollprint Packaging Products, an industrial fabricator of flexible packaging and printing.
- Implemented a contract with Rollprint to manufacture five different laminates.

Future Directions

- Evaluate prototype laminates for chemical resistance, mechanical properties, and barrier resistance to air, moisture, electrolyte, and HF.
- Manufacture absorbent pattern coatings via hot melt extrusion coating and gravure ink-printing.

Introduction

In order to meet the PNGV production cost target of $300/battery (at the 100,000 units/year production rate) in a power-assist hybrid electric vehicle application, analyses indicate that the cost of a 10 Ah cell should be approximately $5.50. Current costs are approximately $30/cell and with design refinements, combined with volume production, the industrial developers are projecting that they can reduce costs to approximately $9/cell. The objective of this project is to develop innovative methods for

reducing cell packaging costs in order to meet the PNGV cost target. Argonne National Laboratory (ANL), in collaboration with 3 industrial partners, is working on low-cost flexible packaging as an alternative to the packaging currently being used for lithium-ion batteries. The goal is to propose innovative packaging approaches, and to develop the air, moisture, electrolyte, and HF barrier layers, for use in a flexible cell containers that have a ten year lifetime.

Low-Cost Flexible Packaging

The ANL low-cost packaging approach consists of developing a low-cost flexible cell container based on plastic laminate technology. The concept is to fabricate a pouch-type container, consisting of a metal alloy foil, which forms the support base for applying polymeric coatings. The layers of the laminate work synergistically to create a cell packaging material that has chemical resistance, heat sealability, and good rupture strength. The required properties of this laminate are as follows:

- A water and moisture barrier, which prevents ambient moisture or water from penetrating into the cell and reacting with electrolyte.
- An electrolyte barrier layer, which prevents electrolyte solvents from leaking out of the cell.
- An HF barrier layer, which prevents any HF present in the electrolyte from attacking the pouch support materials.
- A sealant layer, which provides the seal between the laminates and between the laminates and the current feedthroughs, via a simple and inexpensive hot pressing process. The goal is to develop seals that will yield at the same pressure as the rupture disks in the present metal cans, which are a critical pressure relief safety component of the cells. Therefore, the pouch containment could eliminate the need for this expensive safety vent.

The loss of electrolyte solvent from the flexible cell package is one of the primary concerns for the cell cycle life performance. This phenomenon could lead to cell starvation and performance degradation. The solvent potentially could exit the pouch by three means: (1) across the laminate, (2) through the edges where the two laminates are sealed together, and (3) at the feedthroughs where they seal to the pouch. In addition, the permeation of the solvent across the laminate could lead to the degradation of the adhesive layers that bond the barrier films together resulting in film delamination.

Another concern is the permeation of moisture into the packaging. Potential pathways for entry of the moisture are the same as those mentioned above for solvents exiting the pouch. The moisture permeation could cause degradation of the polymer sealant layer, the formation of HF due to the decomposition of the lithium hexafluorophosphate ($LiPF_6$), and the reaction with the lithium from the electrodes to form hydrogen. The overall result is a degradation of cell life and performance.

The initial approach to laminate construction involved the use of typical aluminum foil and sealant films, with the addition of a second foil layer, to limit moisture permeation. This scheme consists of four layers: a tough polymer exterior barrier; typically oriented polyester; two 9-25 xm thick aluminum foils; and a polyethylene sealant film. These layers are typically joined together using a solvent-based adhesive in which the solvents are driven off and the films joined together under pressure and temperature. The measurement of water transmission through a single 9 xm thick aluminum foil is 0.07 mg-mil/m^2-24 hrs, while water transmission through a laminate of foil/adhesive/foil is 0.02 mg-mil/m^2-24 hrs. The transmission rate reduction by more than 3 times is attributed to a mismatch in pinholes between the two foils. Nevertheless, for a double foil laminate pouch measuring 10 cm by 20 cm, the general dimensions of 10 Ah high-power cell, the calculated quantity of water entering the pouch is 18 grams over a ten year period. Therefore, there is a need for further enhancing the barrier properties. In addition to material selection of laminate layers, absorbents can be used to limit the passage of moisture that enters into the cell. The first location for this absorbent is as an inner liner material made of a blend of polymer and absorbent that serves as the final barrier for water

entering through the laminate (Figure 1). The second location for this absorbent is in between the inner and outer seal region (Figure 2). We are investigating two methods of applying the absorbent and polymer blend to these two regions. Hot melt pattern coating, which depends on material viscosity and its ability to adhere to the substrate, and gravure printing, which is generally used to apply inks and uses a solvent that vaporizes readily and is soluble in the polymer binder. An alternative to the application of a coating in the select region between the seals is to use a polymer/absorbent blend in the form of a ribbon. The advantage of the ribbon is that it permits a greater level of loading of absorbent, but the limitation is that it adds a step to cell fabrication. Another issue in limiting the entrance of water into the pouch is to reduce the thickness of the sealant layer so that there is a very small cross sectional area. This reduction in thickness is limited by the need for a thicker sealant layer for maintaining rupture strength.

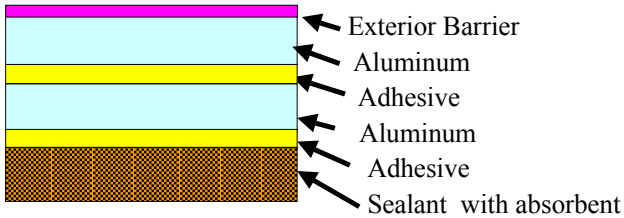

Figure 1. Flexible packaging concept showing the absorbent blended with sealant or inner barrier film material to prevent moisture permeation inside the cell.

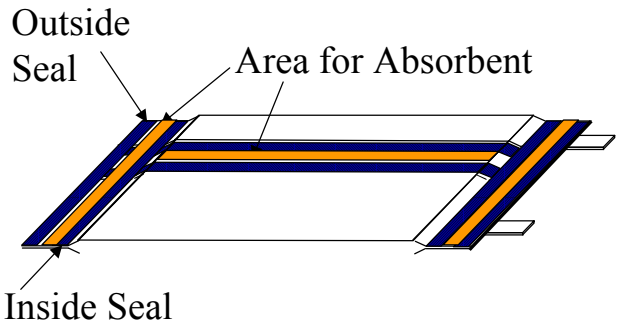

Figure 2. Flexible packaging concept showing absorbent location to prevent moisture permeation.

To select the appropriate absorbent, the absorbent must selectively remove water instead of the organic electrolyte solvents, which would create an electrolyte-starved condition within the cell. Several conventional absorbents, fumed silica, drierite, and molecular sieves, were examined. Fumed silica is traditionally used for rheology control, anti-caking, reinforcement, and free flow of powders. Drierite is calcium sulfate and is an inexpensive desiccant used in the laboratory. Molecular sieves are an alumina-silicate zeolite cage structure with specifically sized channel openings that can capture specific chemical species.

The testing of the effectiveness of the absorbents was performed in a water or diethyl carbonate (DEC) vapor saturated environment. The weight change of the absorbent was measured as a function of time, and upon approaching equilibrium, the absorbents were switched to the alternative environment, i.e. the water-absorbed materials were placed in the DEC environment and vice versa. Our initial observations are that the fumed silica absorbs excessive amounts of DEC, while the molecular sieves absorb water preferentially over the DEC. We continued this investigation by examining several types of molecular sieves. The zeolite type LTA has a nominal hydrated unit cell composition of $\{Na_{12}[Al_{12}Si_{12}O_{48}] \cdot 27\ H_2O\}_8$, known generally as Linde 4A. Potassium exchange with the sodium leads to a smaller cage and is classified as Linde 3A, while calcium exchanging leads to a larger cage and is known as Linde 5A. The other molecular sieve examined is a Linde 13X that has a hydrated unit cell composition of $(Na_2,Ca,Mg)_{29}[Al_{58}Si_{134}O_{384}]$. 240 H_2O. This larger cage size and pore opening permits a larger fraction of water adsorption. The Type 13X adsorbs the largest amount of H_2O; unfortunately it also adsorbs the DEC. The Type 3A and Type 5A adsorb moisture to 25% of their dry weight and DEC to only 3% at room temperature after 19 days, as shown in Figure 3. Drierite is also encouraging, because it absorbs moisture to 42% of its dry weight and DEC to 5%, respectively, at room temperature after 27 days.

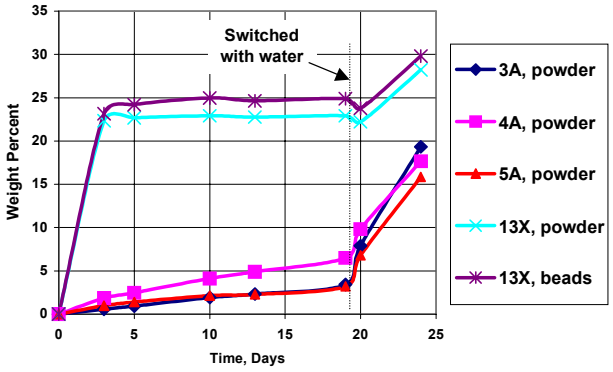

Figure 3. DEC and water uptake by several types of molecular sieve material.

ANL is also screening low-cost polymer films that are resistive to any reaction with electrolyte and which have very low electrolyte solvent permeation. Polymers that are being evaluated are: HDPE [high density poly(ethylene)], PP [poly(propylene)], PET [poly(ethylene terephthalate)], LDPE [low density poly(ethylene)], EVOH [ethyl vinyl alcohol], Surlyn by Dupont (an ionomer), PAN [poly(acrylonitrile)], PVDF [polyvinyldene fluoride], Nylon6 [polyamide], and MDPE [medium density poly(ethylene)]. The other component to cost is the assembly of the laminate and pouch.

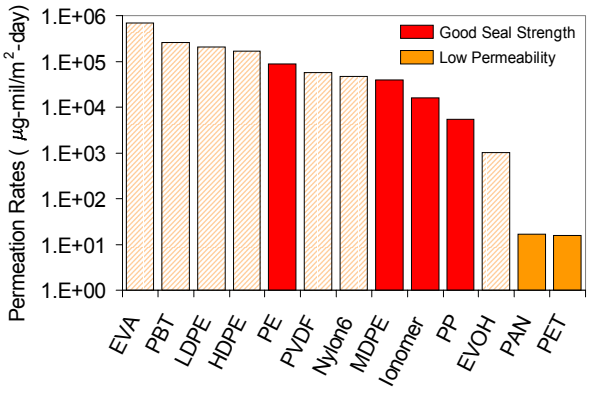

Figure 4. Barrier film permeation rates by mass loss.

An initial screening of polymer films was performed by measuring the weight loss of solvent filled pouches. The films to be investigated were made into pouches by heat sealing two sheets together on three sides, filling with the solvent, and sealing the final side. The pouches were stored at room temperature and their weights were measured as a function of time. Our initial observation (Figure 4) is that the Barex 210 (polyacrylonitrile) and oriented polyethylene terephthalate have the lowest permeation rates with DEC measuring 17 and 16 g-mil/m^2-day, respectively. These results are confirmed by Mocon using film diffusion cell testing at various temperatures that were extrapolated to room temperature. In addition, three sealant films that showed promise: Surlyn (an ioner), polypropylene, and EVOH with permeation rates of 1.58E+4, 5475, and 1025 g-mil/m^2-day, respectively. ANL is working closely with a converter company, Rollprint Packaging Products Inc., to fabricate several lamination schemes using the above-described barriers. The laminates and pouches will be tested by ANL, Rollprint, and Moccon for their mechanical properties, permeation rates, and adhesive strength.

Appendix: ABBREVIATIONS, ACRONYMS, AND INITIALISMS

AC - Alternating Current
ALS - Advanced Light Source
ANL - Argonne National Laboratory
ARC - Accelerating Rate Calorimetry
ARL - U. S. Army Research laboratory
ASI - Area Specific Impedance
ATD - Advanced Technology Development
BNL - Brookhaven National Laboratory
DEC - Diethyl Carbonate
DMC - Di-methyl Carbonate
DOD - Depth-of-Discharge
DSC - Differential Scanning Calorimetry
EC - Ethylene Carbonate
EDAX - Energy Dispersive Analysis by X-ray
EIS - Electrochemical Impedance Spectrometry
EOL - End of Life
EOT - End-of-Test
FTIR - Fourier Transform Infrared Spectroscopy
GC/MS - Gas Chromatography/Mass Spectroscopy
Gen 1 - First Generation High-Power Lithium-Ion Cell
Gen 2 - Second Generation High-Power Lithium-Ion Cell
Gen 3 - Third Generation High-Power Lithium-Ion Cell
GPC - Gel Permeation Chromatography
HEV - Hybrid Electric Vehicle
HPLC - High Pressure Liquid Chromatography
HPPC - Hybrid Pulse Power Characterization
HPPC-M - Hybrid Pulse Power Characterization Test-Medium Current (7.2A)
HRTEM - High-Resolution Transmission Electron Microscopy
IC - Ion Chromatography
ICP/MS - Inductively Coupled Plasma-Mass Spectrometry
IIT - Illinois Institute of Technology
INEEL - Idaho National Engineering and Environmental Laboratory
LBNL - Lawrence Berkeley National Laboratory
MM - Millimolar
NMR - Nuclear Magnetic Resonance
OAAT - Office of Advanced Automotive Technologies
OCV - Open Circuit Voltage
OSPS - Operating Set Point Stability
PC - Propylene Carbonate
PNGV - Partnership for a New Generation of Vehicles
ppm - parts per million
PSD - Position Sensitive Detector
PVDF - polyvinylidene fluoride
R&D - research and development
RPT - Reference Performance Test
SEI - Solid Electrolyte Interface
SEM - Scanning Electron Microscopy
SNL - Sandia National Laboratory
SOC - State-of-Charge
UM - University of Michigan
XAS - X-ray Absortion Spectroscopy
XAFS - X-ray Absorption Fine Structure
XRD - X-ray Diffraction